Feasibility of Making a Lithium Ion Cathode using the Layer-by-Layer Process

By

Binay Prasad

A dissertation submitted in partial fulfillment
of the requirements for the degree of
Doctor or Philosophy
(Materials Science and Engineering)
in the University of Michigan
2013

Doctoral Committee:

Professor John Kieffer, Co-Chairman
Professor Levi T. Thompson, Jr., Co-Chairman
Professor Emeritus Paul G. Rasmussen
Associate Professor Anton Van der Ven

Dedication

Dedicated to my parents, wife and children

Acknowledgements

To all persons who helped me in the entire course of the research. This includes the committee members, who worked very closely with me: Dr. Thompson, Dr. Rasmussen and Dr. Anton. I appreciate some of the graduate students who made useful suggestions and some others who listened to my ideas, as well as the librarians who helped.

Table of Contents

List of Figures

List of Tables

List of Appendices

Chapter 1

Introduction

There has been a renewed interest in secondary lithium ion batteries because of the potential use in various electric and hybrid electric vehicles batteries for automotive applications[1]. These days both high energy and high power density are sought in the same device. Lithium ion batteries are well known for their high energy density. Their power density, however, is relatively low. On the other hand capacitors typically have high power densities but very poor energy densities. It would be ideal to achieve high energy and power densities in the same device. Nano technology could enable the enhancement of both properties in a device.

There has been a great deal of interest in Layer-by-Layer (LbL) entrapped redox active nano particles. From "Electrochemistry of Electroactive surface Immobilized Nanoparticles"[2] Daniel A. Buttry notes:

> "The lure of new physical phenomenon and new patterns of chemical reactivity has driven a tremendous surge in the study of nano scale materials. This activity spans many areas of chemistry. In the specific field of electrochemistry, much of the activity has focused on several areas: (a) electrocatalysis and Nano particles (NPs) of metals supported on various substrates, for example fuel-cell catalysts comprising of Pt or Ag NPs supported on carbon [3,4] (b) fundamental electrochemical behavior of NPs of noble metals, for example the quantized double layer charging of thio-capped Au [5,7] (c) the electrochemical and photochemical behavior of semiconductor NPs [6, 8-10], (d) and biosensor applications of nanoparticles . These topics have received much attention. Considerably less has been done on the fundamental aspect of electrochemical behavior of electroactive NPs that do not fall within these categories. In particular, work is only beginning in the area of the electrochemistry of discrete electroactive Nano particles. Specifically the reduction or oxidation of the metal centers in the electroactive NPs typically is accompanied by ion insertion or expulsion in order to achieve charge compensation."

Our work seeks to exploit LbL films and nano particles to produce high performance materials for lithium ion batteries. The above concepts will be crucial in explaining the working of our battery.

1.1 Motivation

The motivation for this research is to explore the use of LBL methods for the fabrication of lithium ion batteries. Already the battery occupies a dominant position in our world, being present in many electronic devices including electric cars, lap top computers and cellular phones. Batteries are also being developed for nano robots that will drive nano devices in the future. The extension to the nano scale holds promise for a battery and capacitor coexisting in the same device. Figure 1.1 shows pictorially the prevalence of lithium ion batteries.

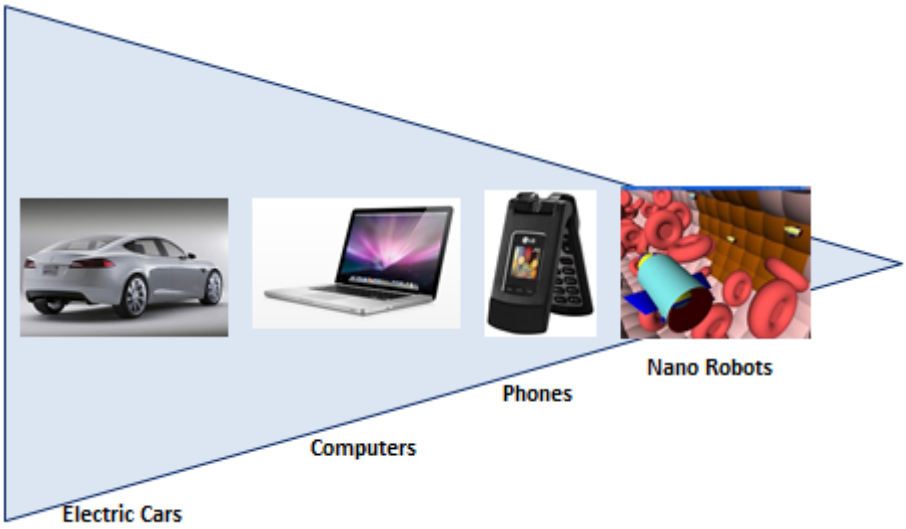

Figure 1.1 Scope of lithium ion battery.

1.2 Goal

The goal of research described in this dissertation was to explore the feasability of using a cathode and an anode made by the LbL process in a rechargeable battery.

1.3 Objective

The main objective was to demonstrate methods to produce a cathode containing $LiCoO_2$ using the LbL method. If this is possible, then we go on to determining specific capacity of the active material.

1.4 Layout of the research of the dissertation

After the introduction chapter we talk about the background information on lithium ion batteries in chapter 2. In chapter 3 we detail the work done on the LbL cathode. There is a little section on polymer pair selection followed by a section on the Layer by Layer process. It details the process used as well as some salient points as described by Decher[11] and Shartori[37]. Then follows the experimental section on cathode making. Also included is the CV work for polymer selection. A section on Impedance Spectroscopy follows this. Then finally we describe the in situ process of the treatment to produce the CoOOH and $LiCoO_2$. Chapter 4 tells why corrosion of the anode occurs and how an alternate lithiated graphite electrode can be substituted for the lithium anode. This change circumvents the corrosion issue. Chapter 5 deals with results and discussions in detail. It describes the battery test results and the appearance of capacitance in the battery. We propose a hypothesis to confirm that capacitance exists in the battery. Finally we explain the excess specific capacity with the help of capacitance. There are two appendices. Appendix A describes in detail the experimental determination of specific capacity and the weight of $LiCoO_2$. Appendix B has the details on statistical analysis that was used.

Chapter 2

The Lithium Ion Battery

The lithium ion battery is a very well researched topic. It has been developed as a commercial battery for high energy density. Because the lithium is a light element it is capable of producing very high energy density per unit weight. However it has poor rate capability when compared to a capacitor. Attempts are being made to produce high power density along with high energy density. We have focused on this aspect in our research.

2.1. Principles of Operation

The energy storage mechanism of lithium ion batteries is quite straightforward. Lithium ion batteries store electrical energy in electrodes made of lithium-intercalation (or insertion) compounds with concomitant oxidation and reduction processes occurring at the two electrodes. A lithium ion battery generally comprises a graphite negative electrode (anode), a non-aqueous liquid electrolyte, and a layered $LiCoO_2$ positive electrode (Cathode). On charging, Li^+ ions are deintercalated from the layered $LiCoO_2$, cathode host, transferred across the electrolyte, and intercalated between the graphite layers in the anode. The discharge reverses this process where the electrons pass around the external circuit to power various systems. The rechargeable lithium ion battery is an ultimate representation of solid state chemistry in action that started with the discovery of intercalation compounds, such as $Li_x MO_2$ (M = Cobalt or Nickel) which were initially proposed by Goodenough and are still widely used today. The discovery of low-voltage lithium, lithium intercalation compounds, carbonaceous materials that are highly reversible, led to the commercialization of Li_xC_6 / Li_{1-x} CoO_2 cells by Sony in 1991 The energy conversion in the so called rocking chair battery is completed via the following reactions:

Cathode: $Li_{1-x}\ CoO_2 + xLi^+ + xe^-$ - > $LiCoO_2$

Anode: Li_xC_6 - > $xLi^+ + xe^- + C_6$

Overall cell reaction

Cell: $LiC_6 + CoO_2$ - > $C_6 + LiCoO_2$ $E^0 = 3.7$ V at 25 ^{0}C

Typical lithium ion cells produce 3.7 volts and demonstrate a capacity and power about 150 Ahr/Kg and over 200 Wh/Kg, respectively. The favorable electrochemical performance in energy/power densities and advancements in system design and manufacturing have made the early lithium ion battery a great success for mobile electronics in spite of the remaining challenges. For a better understanding, a brief historical account of the development of lithium Ion battery technology over the past 30 years is needed. Like most innovations, there were a number of developments that led to mature lithium ion battery technology.

The energy density of the lithium ion battery can be improved through appropriate use of existing or new electrode materials. Optimizing the electrode materials is only the first step in implementing a practical cell. Besides cathode and anode electrodes, the electrolyte which commonly refers to a solution comprising solute and solvents, constitutes the third key component of a battery. The choice of the electrolyte is critical in the design of a battery. The criteria differ, depending on different types – organic liquids, a polymer or an inorganic solid electrolyte. In addition to a large window, there are many other requirements: (1) ionic conductivity and chemical stability over the temperature range of battery operation, (2)electronic conductivity, (3) transference number, (4) low toxicity, (5) low cost, (6) a passivating SEI layer being formed and retained during cycling and (7) nonflammable and non-explosive if short circuited.

While the capacity of the cell is important and relies on the electrodes, cell lifetimes are mainly governed by electrode-electrolyte interface side reactions. Breaking the SEI layer can result in lithium dendrites growth and can short circuit the cell with dangerous consequences.

2.2 Cathode Materials

The most common cathode material is $LiCoO_2$. However a few alternatives have been developed. Among them are layered compounds with hexagonal symmetry based on α-$NaFeO_2$ structure with a space group of $R\bar{3}m$, such as $LiNiO_2$, $LiNi_xCo_yO_2$, $LiMn_xCo_yO_2$, $LiMn_xNi_yO_2$, $LiNi_xCo_yAl_zO_2$, $LiNi_{1/3}Mn_{1/3}Co_{1/3}O_2$ and so on. May different elements can be such as (Co, Mn, Ni, Cr, Al, or Li) can be substituted into the α-$NaFeO_2$ structure and can influence electronic conductivity, ordering of the layer, stability on delithiation and cycling performance.

Lithium iron phosphate ($LiFePO_4$), particularly in nano size, is another very promising positive material. In the late 1990's Padhi et al.[77] proposed olivine structured $LiFePO_4$ with the space group Pnma, which exhibit a lower voltage (3.45V vs. Li+/Li couple) but a higher capacity of 170 mAhs/g. Olivine is a close packed structure , therefore there is need for nano sized particles to be present to facilitate the lithium insertion / extraction . In addition to its low cost and being environmentally benign, the olivine structure is highly stable allowing long cycles of lithium insertion / extraction. Nanostuctured $LiFePO_4$ is the most recent cathode material that has gained commercial success in lithium ion batteries. More research is needed as only a few compositions come close to commercialization.

2.3 Anode Materials

In the late 1980s, graphite developed as an alternative anode material to lithium metal because of its capability to reversibly intercalate/deintercalate lithium ions into/from its lattice. Graphite became the material of choice. It remains as the only anode material practically used in the commercial lithium ion batteries, because of its low redox potential and excellent stability during repetitive cycling. Graphitic carbons have a theoretical capacity of 372 mAh / g and an observed capacity of 280-330 mAh/g , depending on the material.

2.4 Electrolytes

In general, the electrolyte is specially designed for a particular battery system. While an electrolyte can be a liquid, gel or a solid polymer, or an inorganic solid, the majority of lithium ion batteries use liquid electrolyte,

Using an electrolyte containing a lithium salt such as $LiPF_6$, $LiBF_4$, $LiClO_4$, $LiBC_4O_8$(LiBOB) or $Li[PF_3(C_2F_5)_3]$(LiFAP), dissolved in a mixture of organic alkyl carbonate solvents In the presence of flammable organic electrolyte solvents currently in use , there is a risk of heat generation, thermal runaway, and fire. High costs are a deterrent. But additives like vinylene carbonate, to stabilize the electrolyte/electrode interface are being used.

Chapter 3
The Cathode Work

3.1 Polymer Pair Selection

3.1.1 Objective

The LbL process uses a pair of polymers to prepare the films. Generally these polymers are water soluble when present in very high dilutions of around 0.01M. Typically most of these polymers are insulators. To successfully produce an electrode conductivity is require of the polymer pairs. Hence it is logical to start with conductive polymers like PANI (Polyaniline). We therefore started our examination of conducting polymers to find a suitable one. PANI is a modestly good conductor when doped with HCl or Polysufonic acid. This was chosen for the initial cathode work.

3.1.2 Electroactivity of Polyaniline [75]

Polyaniline by itself is electroactive between 2.5 and 4.0 volts vs. Li.
It has been found that electrochemical cells can be prepared having greatly improved capacities and efficiencies. Such cells comprise anode active means, cathode active means and aprotic electrolyte. The cathode consists essentially of active polyaniline species where in each polymer of the polymer chain species is associated with one but only one, hydrogen atom. The electrochemical cells function by reversible oxidation and reduction of the polyaniline species forming the electrode. Thus it is preferred that the polyaniline electrode species be reversibly transformable from an oxidized species having the formula

$$[-(C_6H_4)-N^+(H)=(C_6H_4)=N(H)-] + e$$

To a reducing species having the formula

$$[-(C_6H_4)-N(H)-(C_6H_4)-N(H)-] + A^-$$

Where in A^- is a counter ion, preferably from the electrolyte. Methods for reversible energy storage such as in a secondary battery are comprehended which rely upon the cyclic oxidation and reduction of the foregoing electrodes in aprotic electrolyte. Because we want to use polyaniline merely to provide a conductive background, and not to participate or interfere with the lithium ion battery redox reaction we stopped this approach.

Other Polymer pairs

A large number of polymer pairs were tried. CVs were run to determine window of stability and oxidation reduction characteristic of the polymers individually and the charge discharge was done on two plate tests. Lithium ion and metal hydride cells were made.

List of polymers tried

1. PVA Polyvinyl Alcohol
2. PEO Polyethylene Oxide
3. PAA Polyacrylic Acid
4. PAH Polyallyamine Hydrochloride
5. PAAm Polymethylacrylamide
6. PVP Polyvinylpyrrolidone

Finally the pair selection was done and PEO PAH pair was selected as described in detail in sections 3.5 and 3.5.1.

3.2 Summary of the LbL Process [17-36]

Multilayer films of organic compounds on solid surfaces have been studied for more than 70 years because they allow fabrication of multicomposite molecular assemblies of tailored architectures. Langmuir Blodgett technique and chemisorption from solution can be used only with certain classes of molecules. An alternative approach- fabrication of multilayers by consecutive adsorption of polyanions and polycations – is far more general and has been extended to other materials such as proteins or colloids.

It is desirable to have a simple approach that yields nano architecture films with good positioning of individual layers, but whose fabrication would be largely independent on the nature, size and topology of the substrate. The electrostatic attraction between oppositely charged molecules has the least steric demand of all chemical bonds. The LbL

process uses this. In this process the adsorption of molecules carrying more than one equal charge allows for charge reversal on the surface which has two important consequences: (1) Repulsion of equally charged molecules and thus self- regulation of adsorption and restriction to a single layer, and (2) the ability of an opposite charged molecule to be adsorbed in a second step on top of the first one. Cyclic repetition of both adsorption steps leads to the formation of multiplayer structures. Multilayer structures composed of polyions or other charged molecular or colloidal objects or both are fabricated in a schematic outlined in Figure 3.1.

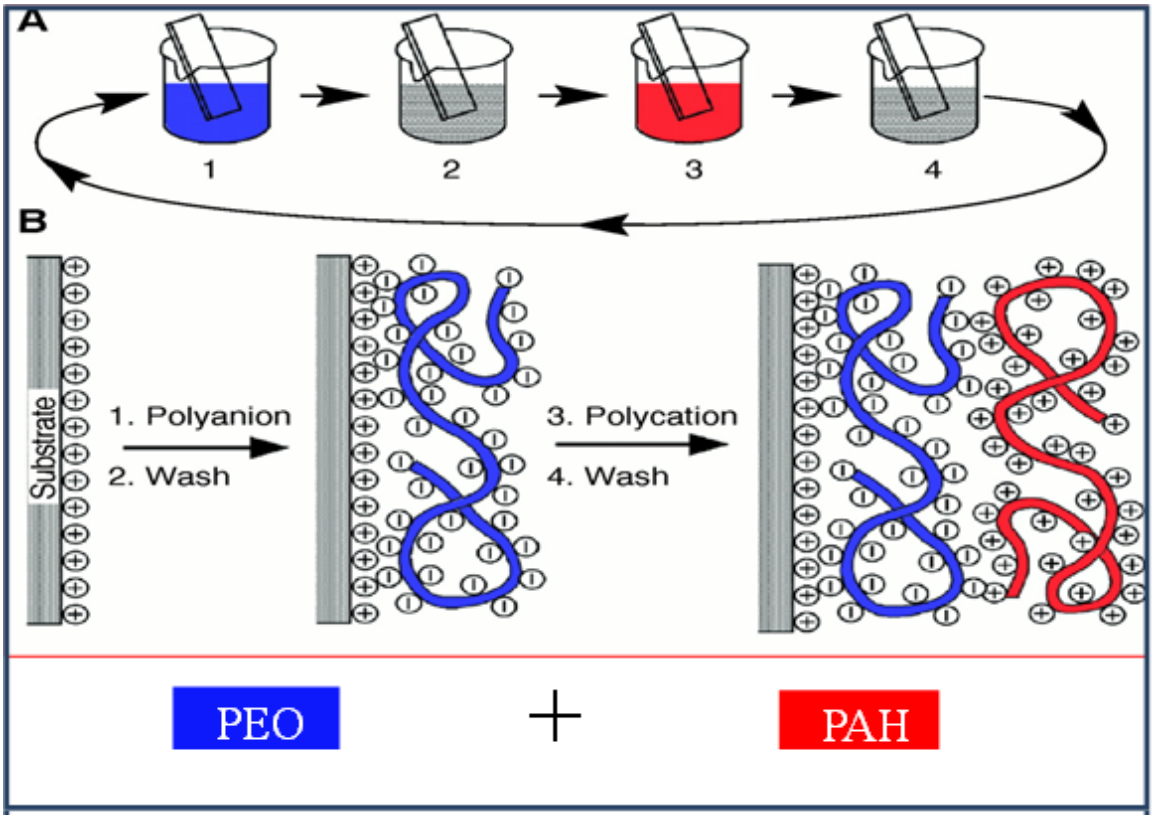

Figure 3.1.(A) Schematic of the film deposition process using slides and beakers. Steps 1 and 3 represent the adsorption of a polyanion and polycation, respectively, and steps 2 and 4 are washing steps. The four steps are the basic buildup sequence for the simplest film architecture, (A/B)n. The construction of more complex film architectures requires only additional beakers and a different deposition sequence. (B) Simplified molecular picture of the first two adsorption steps, depicting film deposition starting with a positively charged substrate. Counterions are omitted for clarity. The polyion conformation and layer interpenetration are an idealization of the surface charge reversal with each adsorption step. (C) Chemical structures of two typical polyions, PEO, polyethylene oxide and PAH , poly(allylamine hydrochloride). [Decher, G. Science 1997,277,1232]

Because the process only involves adsorption from solution, there are in principle no restrictions with respect to substrate size and topology. Film deposition on a glass slide or metal substrate from ordinary beakers can be carried out either manually or by an automated device. A representation of the buildup of a multiplayer film at the molecular level shows a positively charged substrate absorbing a polyanion and a polycation consecutively. In this example the counter ions have been omitted. The stoichiometry of charged groups between polyions and between the substrate and polyions is arbitrary. The use of polyelectrolytes rather than small molecules is advantageous mainly because good adhesion of a layer to the underlying substrate or film requires a certain number of ionic bonds. Therefore the overcompensation of the surface charge by the incoming layer is more a property of the polymer than that of the surface. This is because polymers can simply bridge over underlying defects. Their conformation at the surface (and thus also at the newly created film surface) is mostly dependent on the chosen polyelectrolytes and adsorption conditions and much less dependent on the on the substrate or the substrate charge density [26, 36]. The linear increase of film thickness with the number of deposited layers is often similar even if different substrates are used, which makes the film properties rather independent of the substrate. In cases where substrate charge densities are very small, the first layer binds to the surface with only a few groups and exposes a larger number of oppositely charged groups to the solution. This effective “multiplication of surface functionality” often continues over a few layers before a linear deposition regime is reached.

Similar to this self -regulation of thickness increments per layer, there is a tendency towards a certain value of the interfacial overlap between a polyanion layer and a polycation layer and a certain roughness at the film-air interface. These attributes are probably a property of the polyanion- polycation pair rather than a property of the substrate. Polyelectrolyte multilayers have a similar surface roughness, regardless of the roughness of the underlying substrate. One possible explanation for this is that the surface roughness of rough polyelectrolyte films can be ”annealed” to smaller values by continuously dipping in solutions of salt and pure water. Presumably in this post preparation treatment of the films, the salt breaks some of the anion - cation bonds, and

its removal by washing in pure water leads to their reformation in a more equilibrated confirmation of the polymer chains.

Films are typically deposited from adsorbate concentrations of several milligrams per milliliters. These concentrations are much greater than that required to reach the plateau of the adsorption isotherm, but this excess ensures that the solutions do not become depleted during the fabrication of films composed of several hundred layers. One or more washing steps are generally used after the adsorption of each layer to avoid contamination of the next adsorbing solution by liquid adhering to the substrate from the previous adsorption step. The washing steps also help to stabilize weakly adsorbed polymer layers. Typical adsorption times per layer range from minutes in the case of polyelectrolytes to hours in case of gold colloids, depending on the molar masses, concentrations and agitations of the solutions.

Presumably, in the post-preparation treatment of the films, the salt breaks some of the anion-cation bonds, and its removal by washing in pure water leads to their reformation in a more equilibrated conformation of the polymer chains. Films are typically deposited from adsorbate concentrations of several milligrams per milliliter. These concentrations are much greater than that required to reach the plateau of the adsorption isotherm, but this excess ensures that the solutions do not become depleted during the fabrication of films composed of several hundred layers. One or more washing steps are usually used after the adsorption of each layer to avoid contamination of the next adsorption solution by liquid adhering to the substrate from the previous adsorption step. The washing step also helps to stabilize weakly adsorbed polymer layers [28]. Sections 3.2.1 to 3.2.4 show some important aspects of the LbL process.

3.2.1 **The LbL Process Highlights: Why LbL Process [18-22]**

Multi layers of organic compounds on solid surfaces allow fabrication of multicomposite molecular assemblies of tailored architectures. An alternative approach is the fabrication of multilayers by consecutive adsorption of polyanions and polycations is far more general and extended to proteins and colloids. Resulting superlattice architectures are non- crystalline that proves beneficial for many potential applications. But both the

Chemisorption and Langmuir- Blodgett (LB) techniques are limited to only a certain class of molecules.

3.2.2 **Comparison with LB Process: Drawbacks of Lb Process** [23-26]

The Langmuir- Blodgett (LB) method, which is the fore runner of the LbL process, requires special equipment It has limitations with respect to substrate size and topology. Film quality and stability are suspect. Problems are most likely caused by the high steric demand of covalent chemistry and the severely limited number of reactions with 100% yields, which is a prerequisite for the preservation of functional group density in each layer. In the LbL process the films can be deposited consecutively on- solid surfaces. Nano scale arrangements of organic molecules can be controlled in one direction. The electrostatic attraction between oppositely charged molecules has the least steric demand of all chemical bond in a one direction arrangement.

3.2.3 **Functioning of LbL Process**

The process involves absorption from solution. Typically adsorbate concentrations are several milligrams per milliliters. These concentrations are much greater than that required to reach the plateau of the adsorption isotherm. Excess ensures that depletion during 100s of layers formation does not occur. Washing between each layer ensures that contamination does not occur one layer to the next. It also stabilizes weakly adsorbed polymer layers. Adsorption time per layer varies from minutes as in polyelectrolytes to hours as in the gold colloids. Self- regulation of thickness occurs by change of charge density and roughness. There is also a tendency towards interfacial overlap due to a certain roughness at the film-air interface.

3.2.4 **Versatility in Application of LbL Process**

Electrostatically driven assembly of multilayered structures allow for a wealth of incorporation of different materials. Biological materials layering of biotin and avadin leads to the formation of streptavidin and biotinylated poly(L-lysine). The LbL method is used for the electrochemical sensing of glucose. Also it is used to form bridges using hydrogen bonds. Polymer pairs with side groups carbazole and dinitrophenyl units form charge transfer complexes. Covalent chemistry can also be successfully used in multilayer fabrication. Ionic interactions are attractive as they use water. The use of

charged biopolymers such as DNA, proteins and many other charged or chargeable materials is possible. Multilayer microcapsules in biomedical applications and multilayered films on colloids in photovoltaics applications are easy to do. It is convenient in the use of multilayers as gas separation membranes. This method is used for the fabrication of light emitting diodes

The Shiratori Process is an extension of the Decher process for the making of LbL film. Essentially films from dilute solutions of polyelectrolytes can be made in several different ways. The first is the pure electrostatic attraction between oppositely charged polyelectrolytes. This was employed in earlier processes as in PSS/PAH . Hydrogen bonding is another way of forming bonds. This produces weaker bonds between polymers involved. However one of the simplest methods uses weak polyelectrolytes. These work by creating bonds using control of charge on the polymer by varying the pH of the polyelectrolyte solutions used. The process developed by Shiratori et al is described below.

3.3 The Shiratori Process of Film Making [37-46]

An elaborate study [33] of the role that solution pH plays in the layer-by-layer processing of the weak polyelectrolytes poly(acrylic acid) and poly(allylamine hydrochloride) was carried out. It was found that drastically different polymer adsorption behavior is observed as one systematically increases (or decreases) the charge density of a weak polyelectrolyte including transitions from very thick adsorbed layers (ca. 80 Å) to very thin adsorbed layers (ca. 4 Å) over a very narrow pH range. By controlling pH, it is possible to vary the thickness of an adsorbed polycation or polyanion layer from 5 to 80 Å. In addition, control over the bulk and surface composition of the resultant multilayer thin films is readily achieved via simple pH adjustments. These studies have provided new insights into the polyelectrolyte sequential adsorption process. We found this method very suitable for our work.

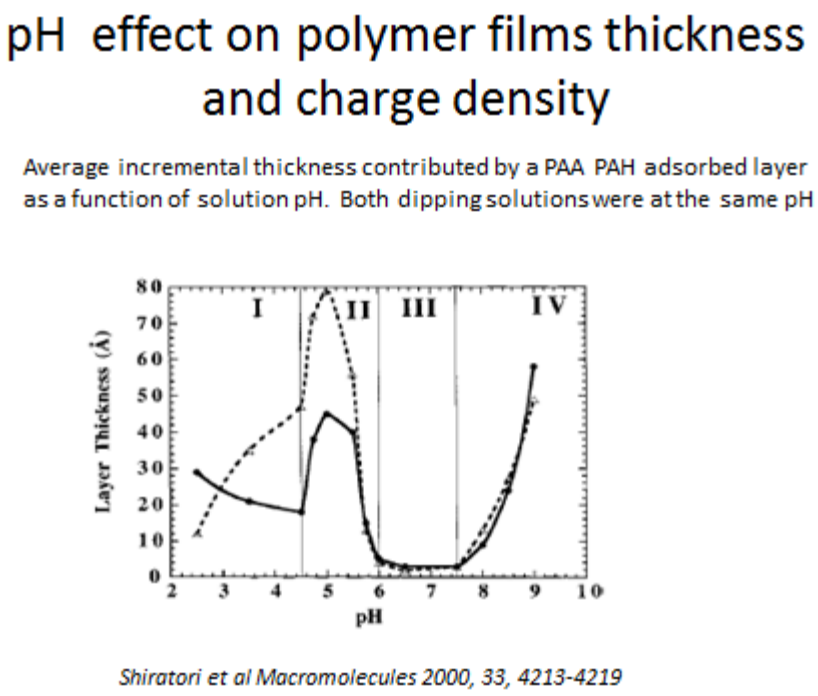

Figure 3.2 pH effect of polymer on thickness and charge density

We used the above Figure 3.2. to guide our selection of pH region for our polymer pairs. The pH was kept in the region II.

3.4 Experimental

The set- up of Figure 3.3. has been used to produce 20 layers of LbL film within which $Co(OH)_2$ has been introduced in each layer. This is done by putting a $Co(OH)_2$ solution in between the polymer solutions . The principle used to make the films is shown in the Figure 3.3. A variation of pH of the polymer solution changes the charge density of the polymer. The best situation is to have a fully charged polymer combining with a nearly fully charged polymer.

3.4.1 **Electrode Preparation (Experimental)**

The layer by layer process of thin film making developed by Decher [11] has been used to make a lithium ion cathode. Dilute solutions of polyethylene (PEO) polyallylhydrochloride(PAH) and $Co(OH)_2$ (cobalt hydroxides) are prepared. All solutions are made in water. An aluminum substrate is alternately dipped in them to form

20 blocks of the repeat unit PEO/$Co(OH)_2$ /PAH. All excess chemicals are rinsed away in intermediate steps.

The Layer by Layer process has been pioneered by Greco Decher [11] and has been extensively used in a large number of applications. This produces nano sized very stable films using dilute solution of polymers. Materials can be incorporated within the layers. By successfully incorporating battery active materials within films, suitable cathodes and anodes can be produced. In addition to incorporating active materials directly, materials can be introduced within films which can be subsequently converted to desired materials. We have incorporated $Co(OH)_2$ within films. Later this material is converted to $LiCoO_2$ and CoOOH by an electrochemical process. Thus the resulting cathode contains active material, $LiCoO_2$ and the electronic conductor, CoOOH.

This electrode is later taken in a glove box. Here under argon cover an electrochemical treatment to produce $LiCoO_2$, the active material is done. A three volt discharge is carried out for two hours as shown in Figure 3.3. below:

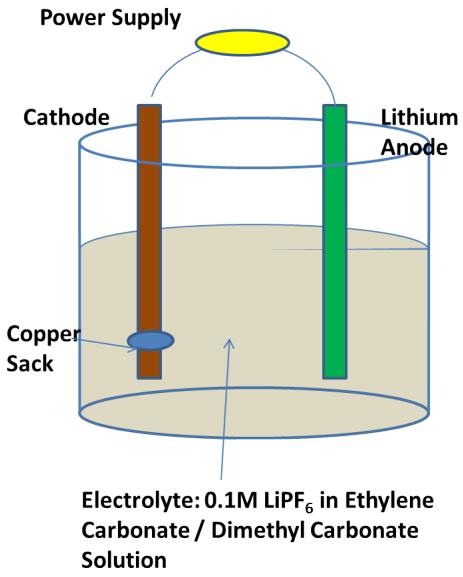

Figure 3.3 Treatment set up inside the argon filled glove box

Comment on LbL films made by weak polyelectrolytes[4]

This is a comparatively new approach to making multilayer thin films. Most researchers have utilized strong polyacids and polybases to construct multilayer thin films. With such materials, adding salt to the polyelectrolyte dipping solutions best controls the thickness of an adsorbed layer. The use of weak polyelectrolytes such as polyacrylic acid (PEO) and polyallylamine hydrochloride (PAH) whereby control over the layer thickness and molecular organization of an adsorbed polymer chain can be achieved by simple adjustments of pH of the dipping solutions. In this case, pH controls the linear charge density of an adsorbing polymer as well as the charge density of the previously adsorbed polymer layer. It presents unprecedented ability to control the blending of a polycation and polyanion at the molecular level. Dramatic changes in thickness of an adsorbed layer can be induced by very small changes in the pH of the dipping solutions. An understanding of the molecular origin of these thickness transitions is expected to provide new insights into basic polymer physics of the sequential adsorption process as well as to provide new possibilities for their technological applications.

3.5 Cyclic Voltammetry Experimental Work

CVs were run on many polymers and on plates loaded with films. Solution of polymers were made in acetonitrile . The working, counter and reference electrodes were Pt. The scan rates used varied on the low side from 1 mv to 500 mv. Both aqueous and non-aqueous media were employed. The stability window was examined from -2V to 2V and 0 to 4 Volts. The non-aqueous work was done in the glove box filled with argon. 1M $LiPF_6$ salt was added in the acetonitrile, with and without the typical solvent 50% EC / DMC . The aqueous electrolyte had 7 M KCl. The CV was run outside , not in the glove box.

Magnitude of the currents are larger than the polymer free condition. Polymers can be contributing to current produced.

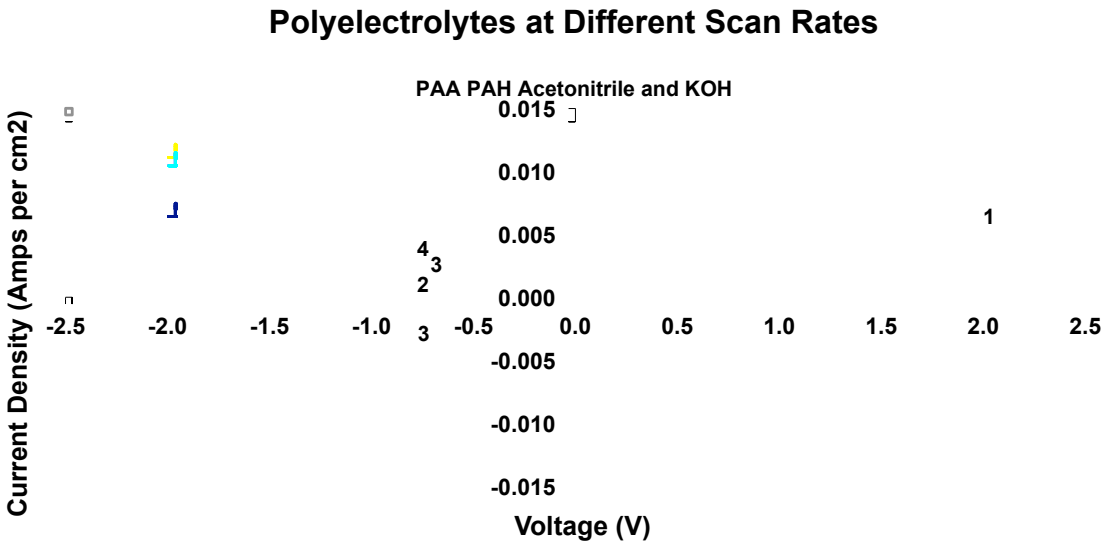

Figure 3.4 CV of polyelectrolytes in a Metal Hydride environment

This plot Figure 3.4 is for an aqueous condition. A metal counter electrode has been used. From the figure it is easy to see reversible peaks of K^+ occurs at -0.75V vs. Pt. The LbL process is usable and does not cause PAA / PAH to degrade.

There were several other scans that were done on non- aqueous solutions. The one shown in Figure 3.5 is of just the acetonitrile solution. As expected the scan from -2 to + 2 volts is stable. No oxidation or reduction peaks are visible.

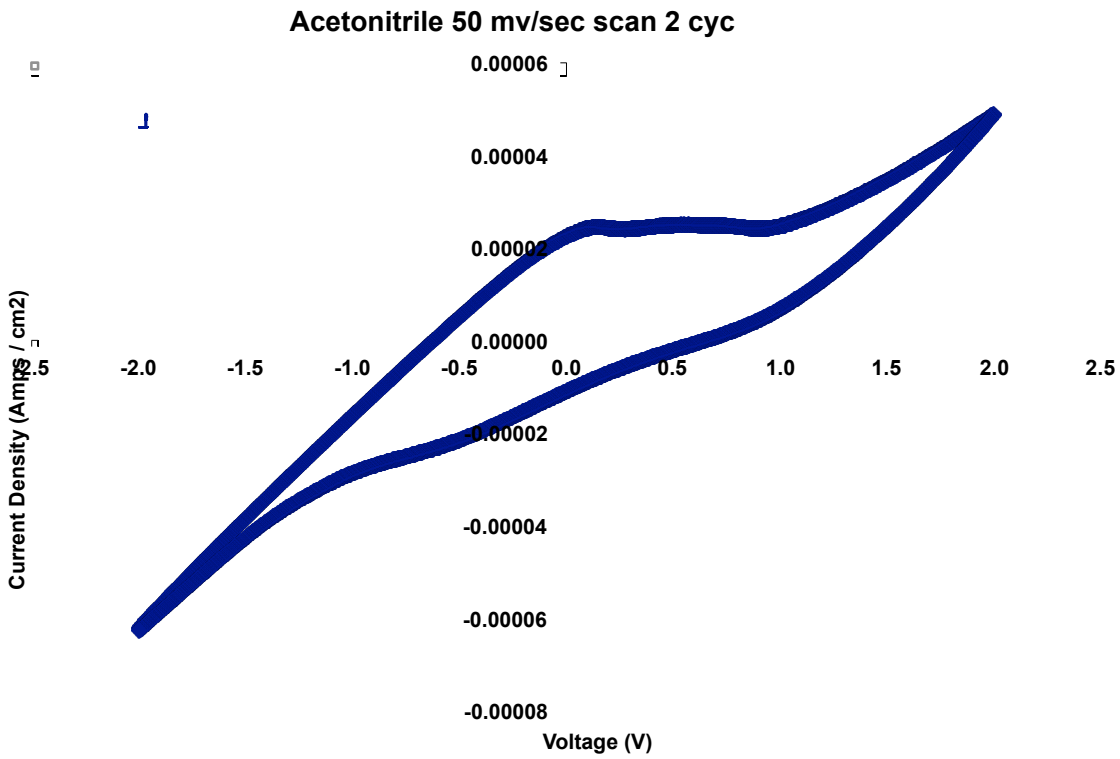

Figure 3.5 Acetonitrile 50 mv/sec 2nd scan

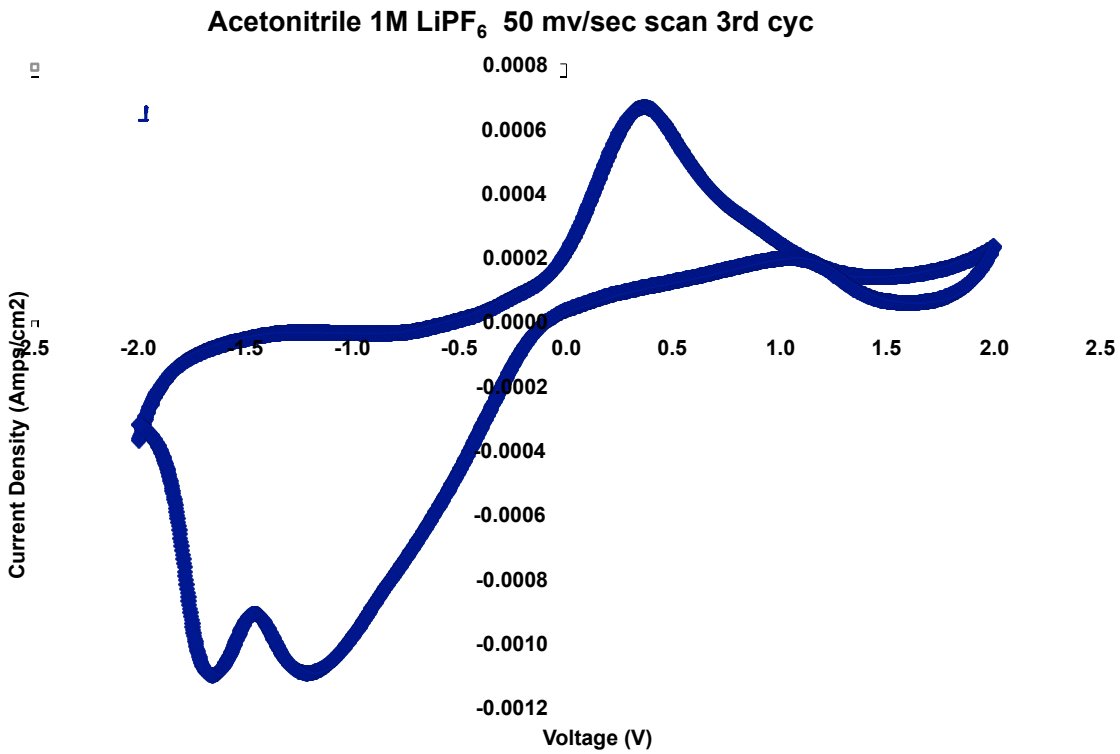

Figure 3.6 Acetonitrile 1M $LiPF_6$ 50 mv/sec 3rd scan

From this Figure 3.6 we see oxidation and reduction peaks because of the presence of $LiPF_6$. As expected acetonitrile only does not have oxidation and reduction peaks. There is no ionic species to show redox behavior. But addition of $LiPF_6$ causes major change and shows clearly oxidation and reduction peaks. These are not of the same height.

In the Figure 3.7 below, PEO is also added to acetonitrile and $LiPF_6$. This CV has been run from -4 to 0 Volts. The acetonitrile still is stable

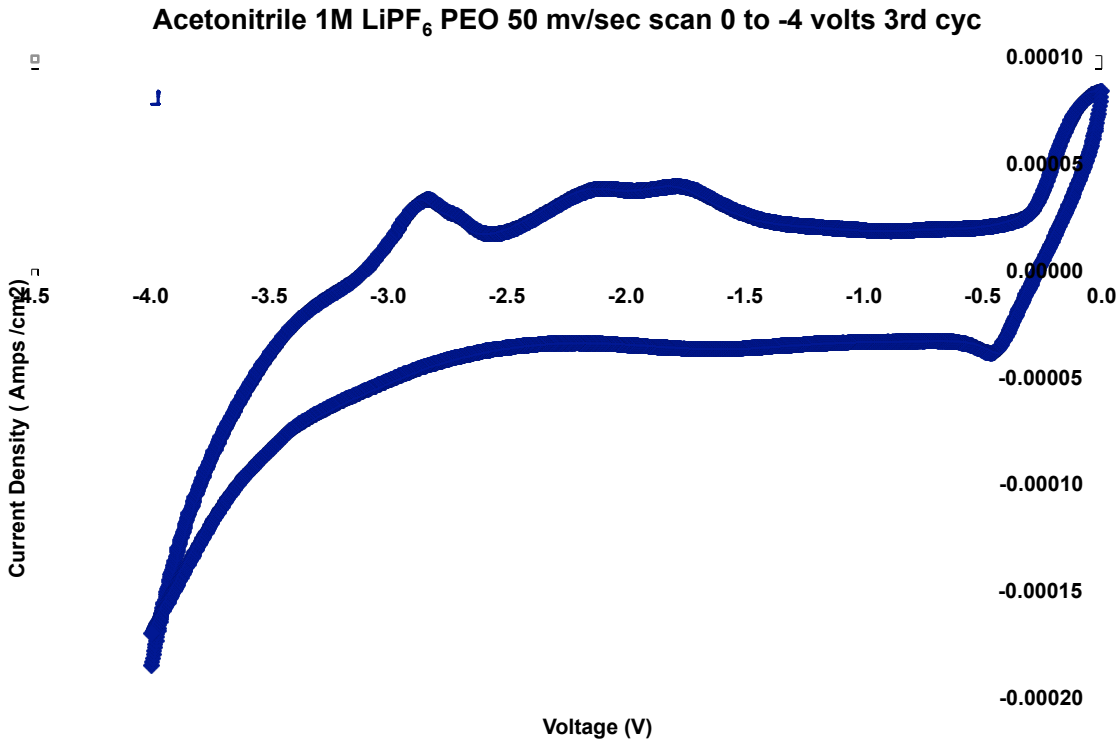

Figure 3.7 Acetonitrile 1M $LiPF_6$ PEO 50 mv/sec scan 0 to -4 volts 3rd scan

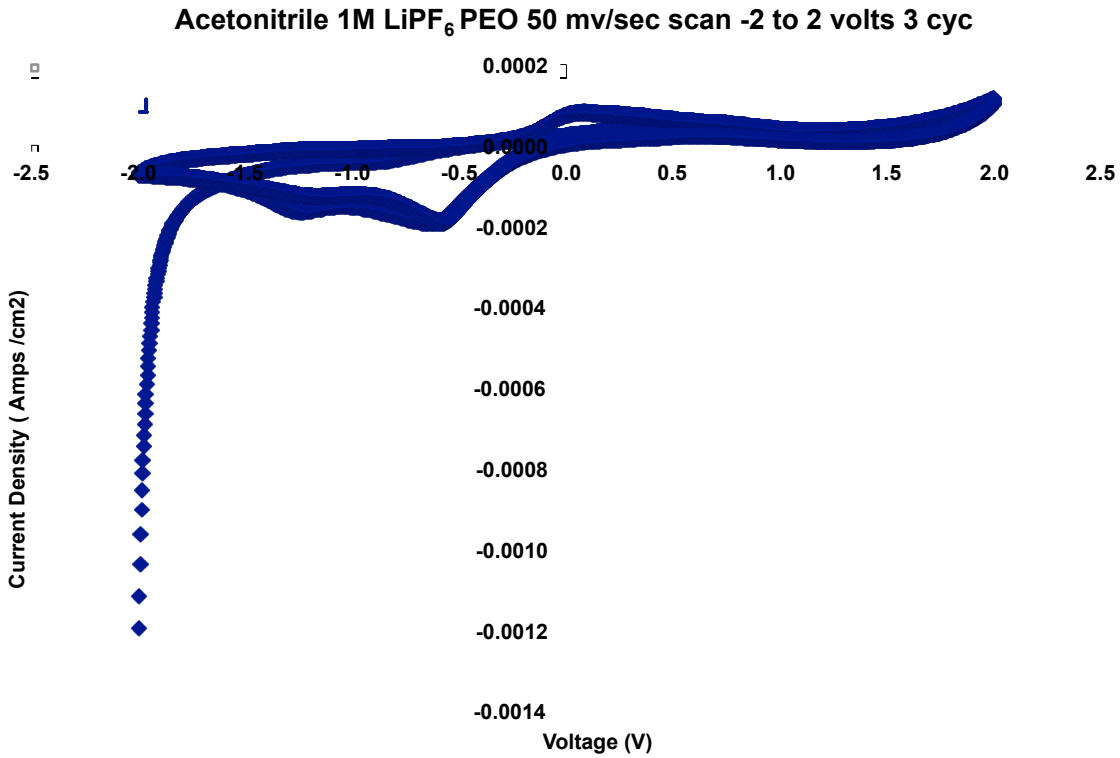

Figure 3.8 Acetonitrile 1M $LiPF_6$ PEO 50 mv/sec scan -2 to 2 volts 3rd scan

In this Figure 3.8 the scan from -2.0 to 2.0 V looks normal. It suggests that the addition of the polymer PEO does not alter the voltage on the cv but affects the current and reduces it compared to the situation without the polymer.

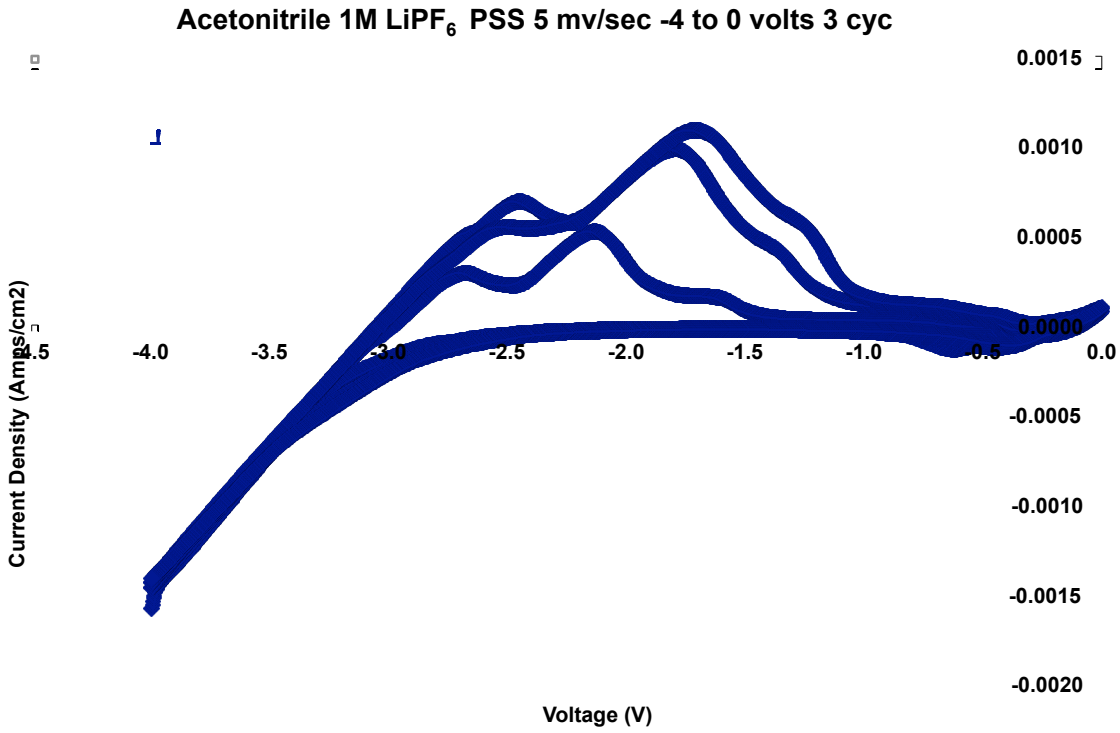

Figure 3.9 Acetonitrile 1M $LiPF_6$ PSS 5 mv/sec -4 to 0 volts 3rd scan

Figure 3.9 has PSS along with acetonitrile and $LiPF_6$. Irreversible reactions occur from -2.5 to -1.5 Volts.

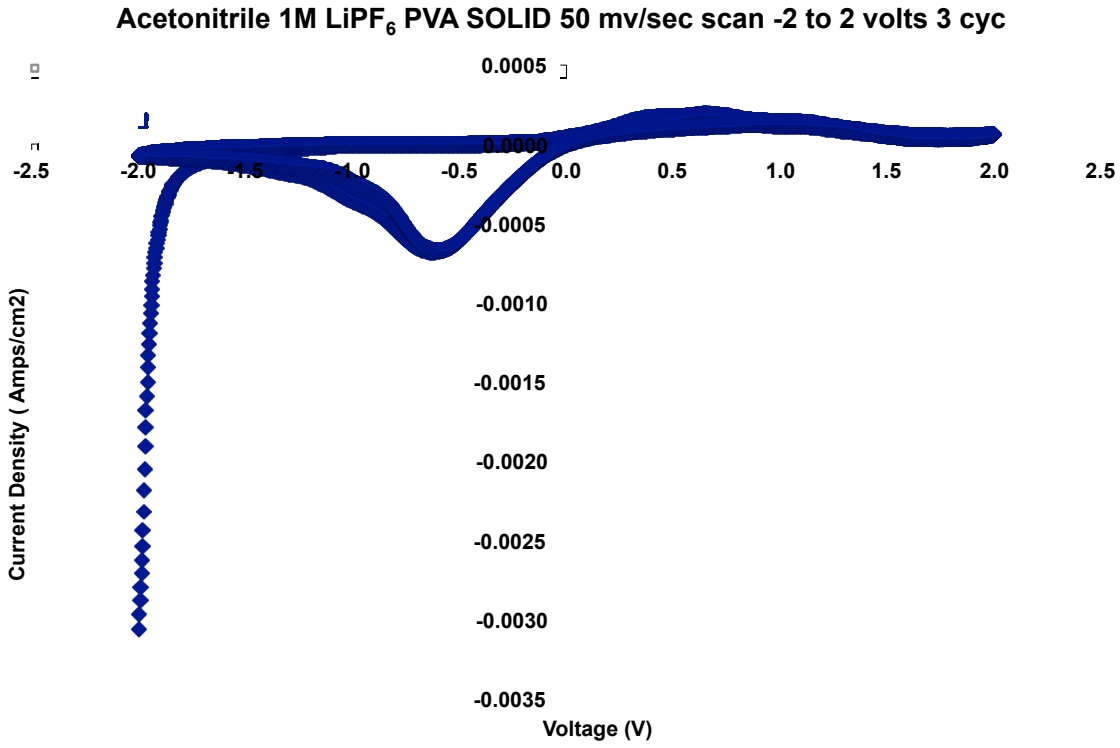

Figure 3.10 Acetonitrile 1M $LiPF_6$ PVA SOLID 50 mv/sec scan -2 to 2 volts 3rd scan

Figure 3.10 shows the polymer PVA shifts the oxidation and reduction peaks significantly without affecting the magnitude of the current, suggesting a mild reaction between PVA and the solution .

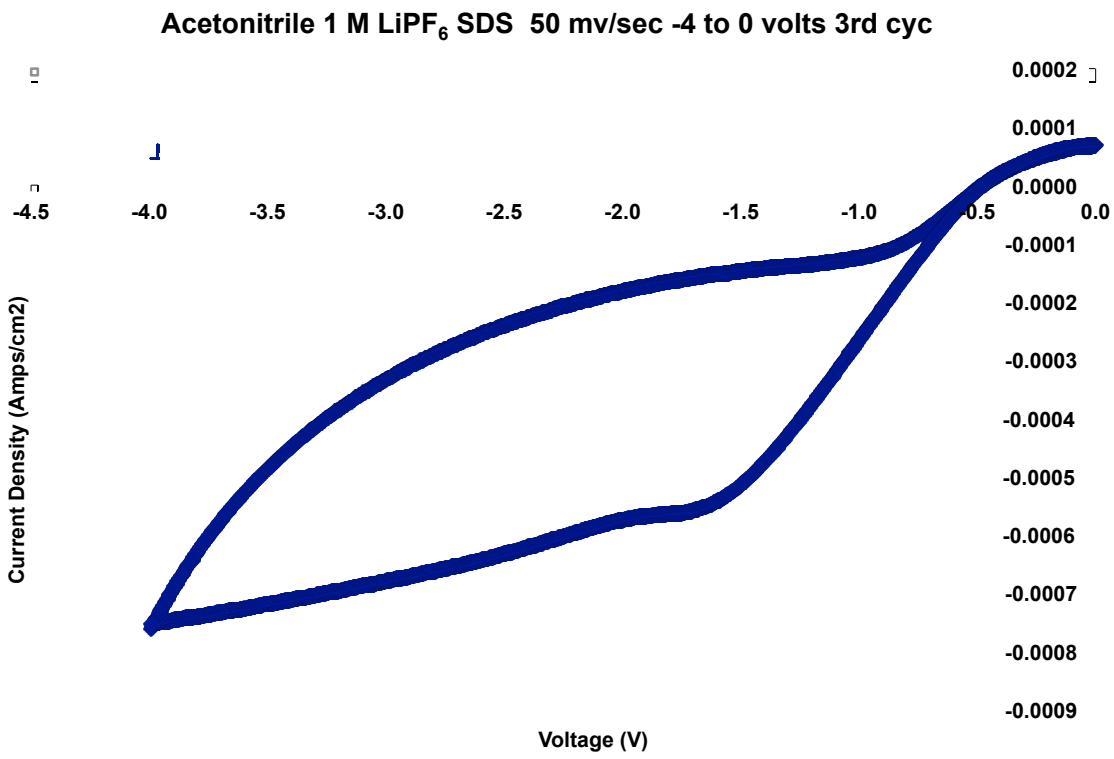

Figure 3.11 Acetonitrile 1 M $LiPF_6$ SDS 50 mv/sec -4 to 0 volts 3rd scan

Figure 3.11 shows that SDS really does not affect the CV. There are no additional peaks. SDS was used as a surfactant to float $LiCoO_2$.

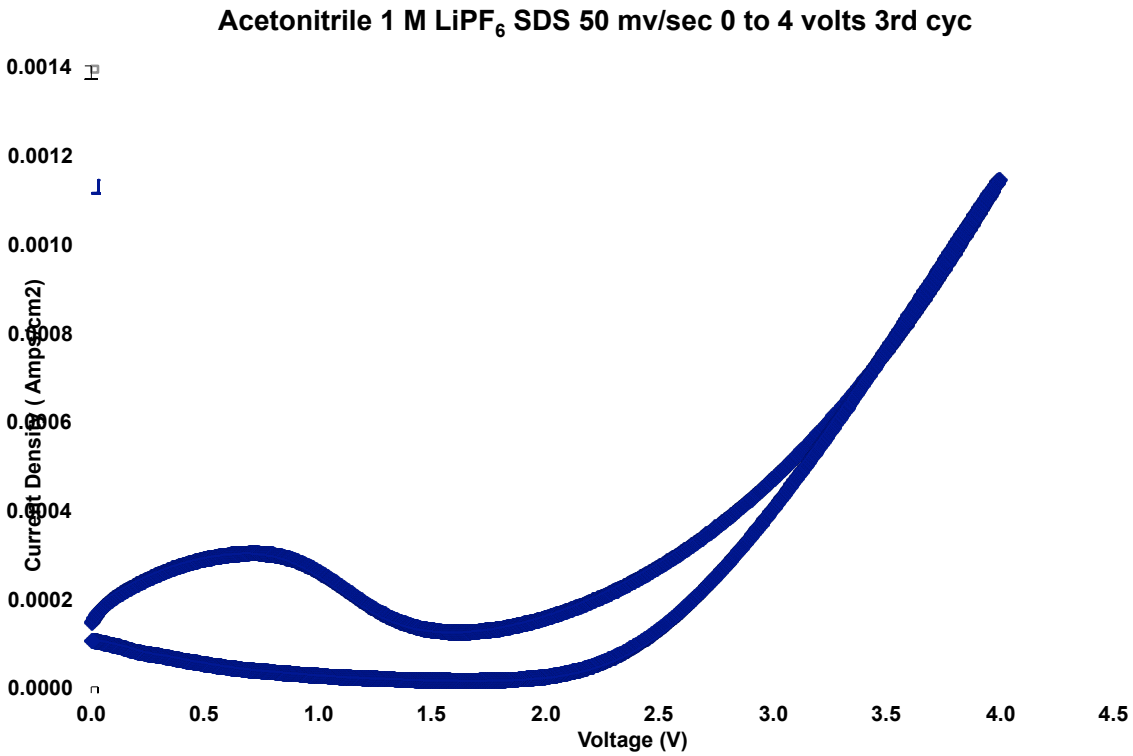

Figure 3.12 Acetonitrile 1 M $LiPF_6$ SDS 50 mv/sec 0 to 4 volts 3rd scan

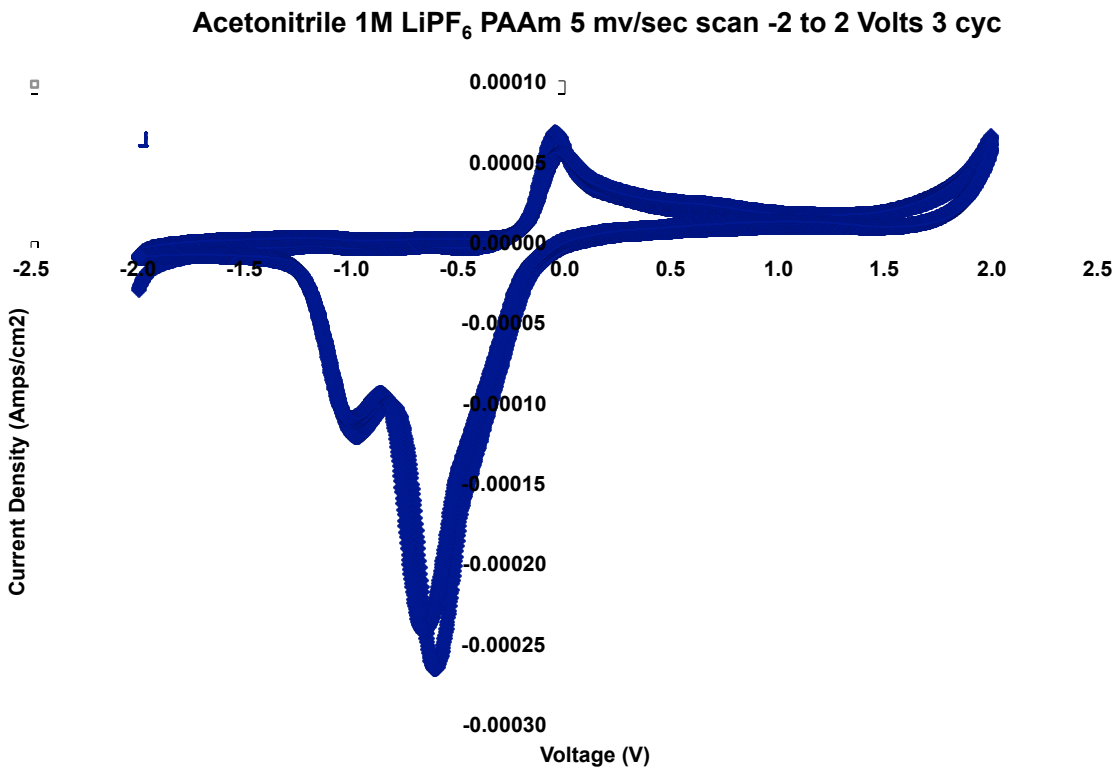

Figure 3.13 Acetonitrile 1M $LiPF_6$ PAAm 5 mv/sec scan -2 to 2 Volts 3rd scan

Here in Figure 3.13, voltages shift slightly to the left and the magnitude of the peak currents are reduced. The response looks to be partially reversible.

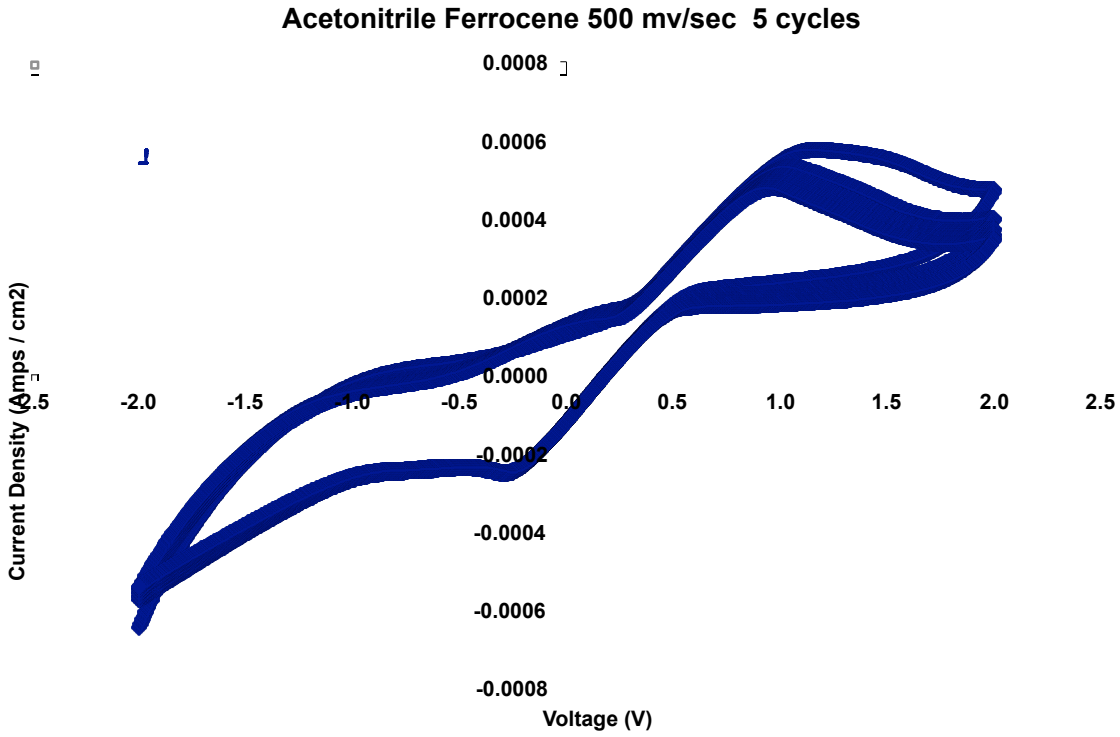

Figure 3.14 Acetonitrile Ferrocene 500 mv/sec 5 scans

The above CV is for ferrocene and shows sharp oxidation and reduction peaks when a very high scan rate is adopted. The charge transfer is very fastreaction, that is the kinetic rates are very high. It was used to establish a pseudo reference point for the platinum electrodes used in cyclic voltammetry.

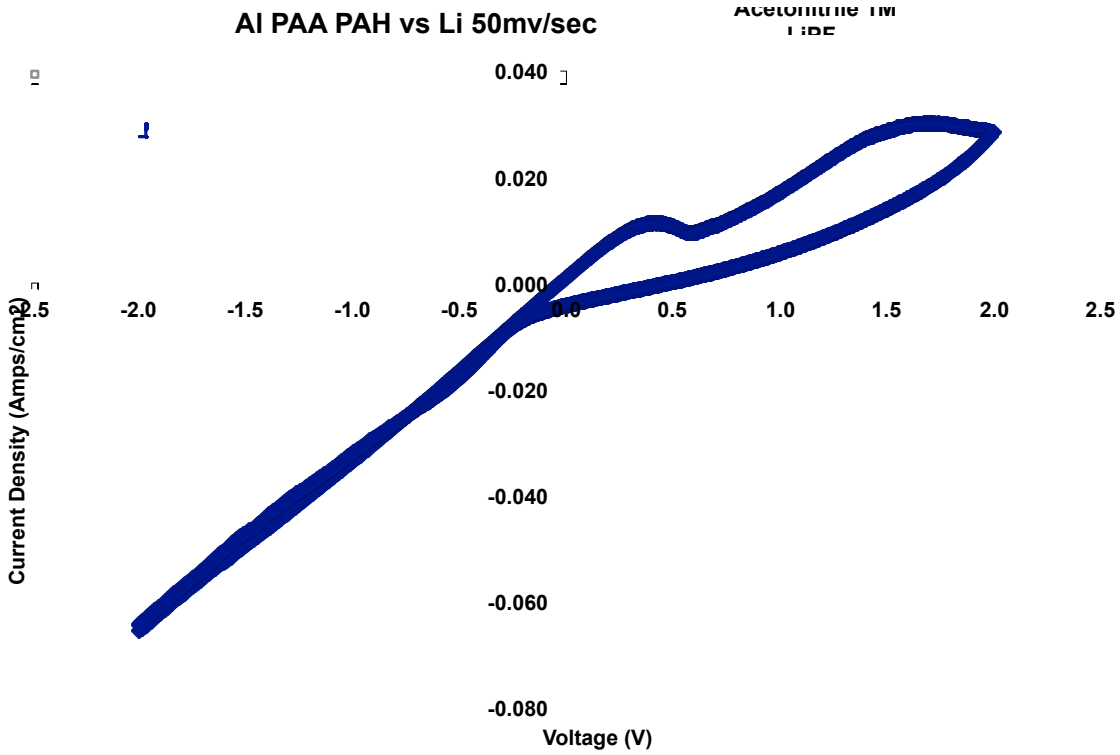

Figure 3.15 Al PAA PAH vs. Li 50mv/sec

The figure above, Figure 3.15 shows that in the -2 to 2 Volt range PAA PAH pair are stable. Accordingly we used this pair initially in our work.

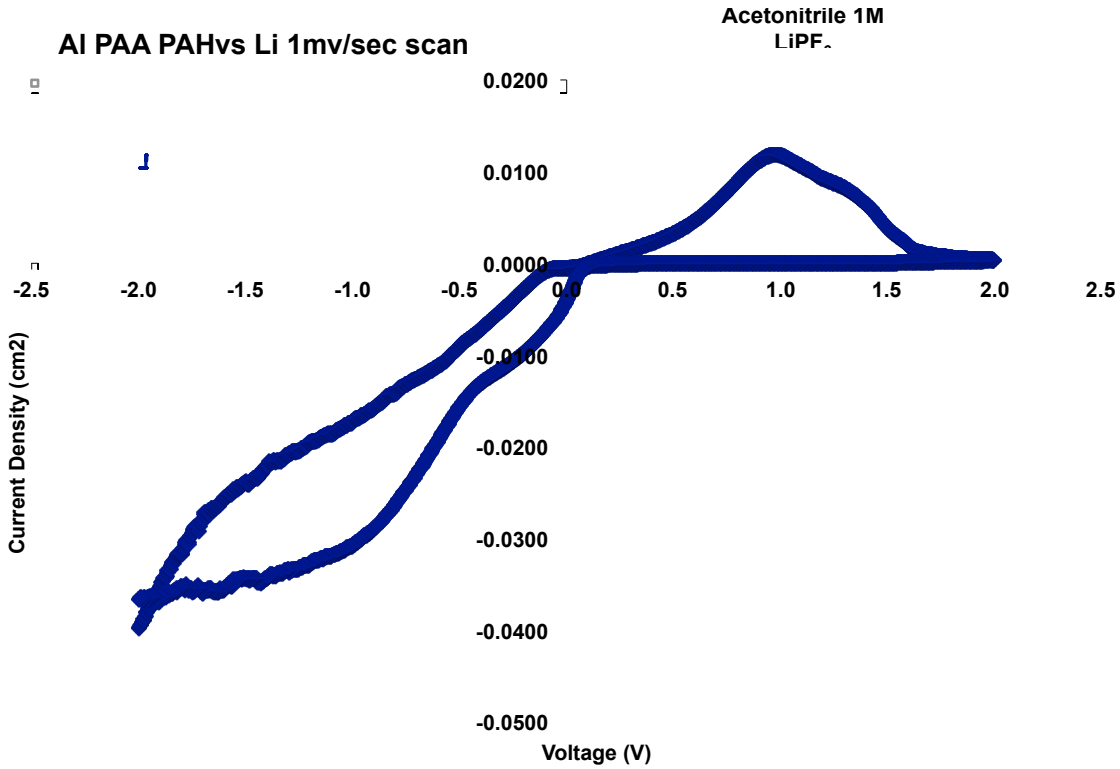

Figure 3.16 Al PAA PAH vs. Li 1mv/sec scan IN 1M acetonitrile

Figure 3.16 above shows that the introduction of aluminum causes an irreversible reaction. Aluminum is corroded by lithium irreversibly.

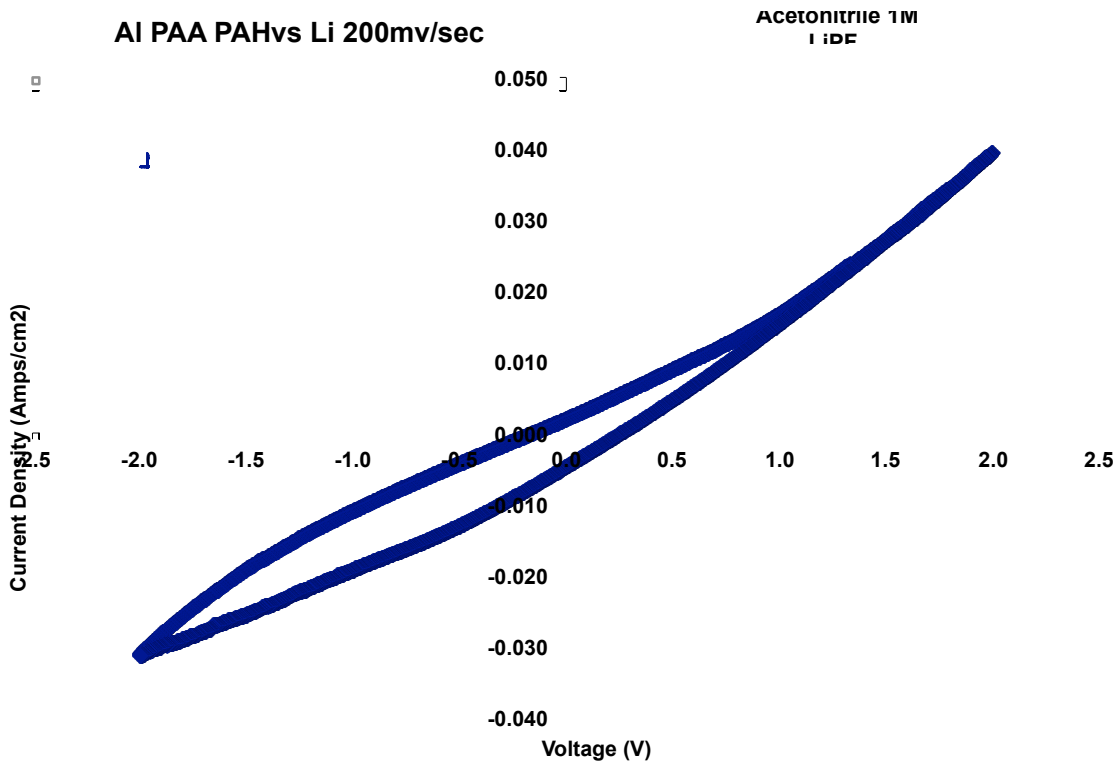

Figure 3.17 Al PAA PAH vs. Li 200mv/sec in 1M acetonitrile

The two figures above for a non aqueous situation show how scan rate affect the oxidation and reduction of lithium. A small rate accomodating diffusion shows charge transfer but when scan rate is increased the charge transfer reaction is suppressed. The charge transfer reaction is sluggish.

We see from the above figures that when acetonitrile is examined alone it does not show any redox response as expected. However when mixed with small quantities of the electrolyte $LiFF_6$ the redox activity of the Li+ and PF_6^- is clear. On further addition of different polymers to the mix we see their responses in the voltamograms. The polymer pair selected PEO PAH, rather than PAA PAH appears useable as shown in Figure 3.7 and Figure 3.15. Hence we learn from the CV that the choice made is right. No electrochemical contribution is expected when these selected polymers are used as electrodes. Other polymers like PVA, PSS, SDS, PAAm do show electrochemical activity.

3.5.1 **Final Selection of Polymer Pair**

We selected two polymer pairs: PAH/PAA and PEO/PAH based largely on the Shiratori criteria. At the same time cyclic voltammetry experiments were performed to ascertain their suitability of usage. Even though small changes in magnitude of peak currents occur and peak shifts occur, by and large no polymer degradation effect is discernible as repeated cycling is being sustained. Because of current produced by PAA/PAH pair and also this pair faces corrosive attack by alkali [$Co(OH)_2$] we have finally fixed PEO/PAH pair to be used. The PAA is acidic and reacts with $Co(OH)_2$ which is alkaline. Processing is done with $Co(OH)_2$ to load and enhance the conductivity of the electrode.

3.6 Impedance Spectroscopy

3.6.1 **Background Information of Impedance Spectroscopy**

Lithium Ion rechargeable batteries of various types have been moving rapidly towards commercialization. High practical specific energies up to 130 Wh/Kg and over a thousand cycles have been achieved by Sony type lithium ion cells [47]. New materials are being developed for the next generation of lithium ion batteries- nano lithium manganese, lithium iron phosphate as cathode and lithium titanate as anode. Choosing among various chemistries and optimizing the battery's design can be costly and time consuming. Mathematical modeling and computer simulations can be helpful in understanding the processes occurring inside the battery [48-51].

EIS has been used in battery research and for several decades. More recently, study of Lithium Ion cells have proliferated, motivated by the desire to measure kinetic and transport properties and to characterize structural degradation leading to losses in capacity [52-58]. One limitation of EIS study is the difficulty of interpreting the impedance data. Battery impedance data are impacted by a complicated set of processes including porous electrode effects, the superposition of the separator and two electrode impedance responses, transient and nonlinear responses and the additional artifacts of the battery current collectors, terminal and other peripherals [59-60]. All these phenomena make interpreting full battery impedance data a difficult task. The approach taken in the past

has nearly been to fit data to an equivalent circuit composed of passive and frequency dependent circuit elements. Both simple and lumped parameter circuits and more complex finite transmission line circuits have been used [61-63]. One disadvantage of this approach is the difficulty in interpreting the equivalent circuit parameters in terms of fundamental properties [64-65].

Impedance spectroscopy experiment involves using a source of sinusoidal voltage with a small amplitude say 10 millivolts imposed on a cell like lithium Ion held at a given voltage, say 3.6Volts. The frequency of the voltage is varied over a considerable range. It can be from 10^{-4} to 10^{6} Hertz. The graph of resulting impedance change called Nyquist plot, gives a pictorial view of impedance. Because the voltage varies with time, the response current also varies with time. It generally lags the applied voltage by an angle called the phase difference. The general impedance situation at two extremes- at very high to very low frequency- enables us to derive kinetic and diffusion information.

3.6.2 **Variation of Total Impedance**

The EIS approach, which is largely based on similar methods used to analyze circuits in electrical engineering practice, was developed by Sluyters and coworkers [67] and later extended by others [69-71]. It deals with the variation of total impedance in the complex plane (as represented by Nyquist plots). The measured total impedance of the cell Z is expressed as a series combination of R_B and C_B. These two elements provide the real and imaginary components of Z, that is $Z_{Re} = R_B$ and $Z_{Im} = 1/\omega c_B$. The electrochemical system is described theoretically in terms of an equivalent circuit such as that in Fig 3.18.

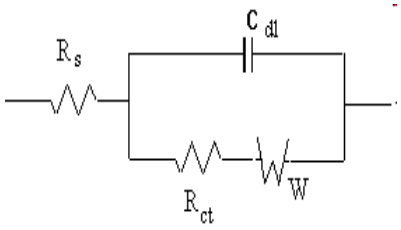

Figure 3.18 Randles' Circuit

The real part, which must equal the measured Z_{Re}, is

$$Z_{Re} = R_B = R_\Omega + R_S / A^2 + B^2$$

$A = (C_d / C_s) + 1$ and $B = \omega R_S C_d$

$$Z_{Im} = 1/\omega C_B = (B^2/\omega C_d + A/\omega C_s)/A^2 + B^2$$

On substituting for R_S, C_S provides

$$Z_{Re} = R_\Omega + (R_{ct} + \sigma \omega^{-1/2}) / (C_d \sigma \omega^{1/2} + 1)^2 + (\omega C_d)^2 (R_{ct} + \sigma \omega^{-1/2})^2$$

$$Z_{Im} = [\omega C_d (R_{ct} + \sigma \omega^{-1/2})^2 + \sigma \omega^{-1/2} (C_d \sigma \omega^{1/2} + 1)] / (C_d \sigma \omega^{1/2} + 1)^2 + (\omega C_d)^2 (R_{ct} + \sigma \omega^{-1/2})^2$$

Where $\sigma = [1/nFA][2^{0.5}][\square_O/D_O^{1/2} - \square_R/D_R^{1/2}]$

Chemical information can be extracted by plotting Z_{Im} vs. Z_{Re} for different ω. For simplicity let us first consider the limiting behavior at high and low ω.

3.6.2.1 Low Frequency Limit

As ω approaches zero the above equations approach their limiting forms:

$$Z_{Re} = R_\Omega + R_{ct} + \sigma \omega^{-1/2}$$

$$Z_{Im} = \sigma \omega^{-1/2} + 2 \sigma^2 C_d$$

Elimination of ω between these two gives

$$Z_{Im} = Z_{Re} - R_\Omega - R_{ct} + 2 \sigma^2 C_d$$

Thus the plot of Z_{Im} vs. Z_{Re} should be linear and have unit slope. The frequency dependence in this regime comes only from Warburg impedance terms. The linear correlation of Z_{Re} and Z_{Im} is characteristic of a diffusion controlled process.

3.6.2.2 High Frequency limit

At very high frequencies the Warburg impedance becomes unimportant in relation to R_{Ct}

$$Z = R_\Omega - j[R_{Ct}/(\omega R_{ct} C_d - j)]$$

$$Z_{Re} = R_\Omega + R_{ct} /1 + (\omega R_{ct} C)^2$$

$$Z_{Im} = \omega_t C_d R^2_{ct} / 1 + (\omega R_{ct} C)^2$$

Elimination of ω from above yields

$$[Z_{Re} - R_\Omega - R_{ct}/2]^2 + (Z_{Im})^2 = (R_{ct}/2)2$$

Hence Z_{Im} vs. Z_{Re} should give a circular plot centered at $Z_{Re} = R_\Omega + R_{ct}/2$ and $Z_{Im} = 0$ and having a radius of $R_{ct}/2$.

At very high frequencies the impedance is represented by an equation as follows:

$$[Z_{Re} - R_\Omega - R_{ct}/2]^2 + (Z_{Im})^2 = (R_{ct}/2)2$$

$$X^2 + Y^2 = C^2$$

This is the equation of a circle. This shows the charge transfer situation. A semicircle whose diameter coincides with the Y=0 line gives many valuable parameters.

At very low frequencies a straight line is obtained inclined at 45 degrees. A typical plot is shown below. The data obtained represents the Randles Circuit shown.

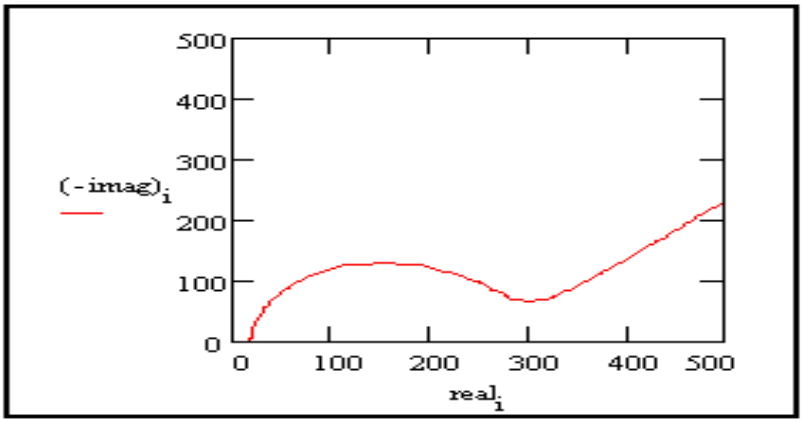

Figure 3.19 Ideal Behavior

Figure 3.19 shows two distinct regions and the ideal behavior. The semicircle is the charge transfer region and the straight line represents the diffusion region.

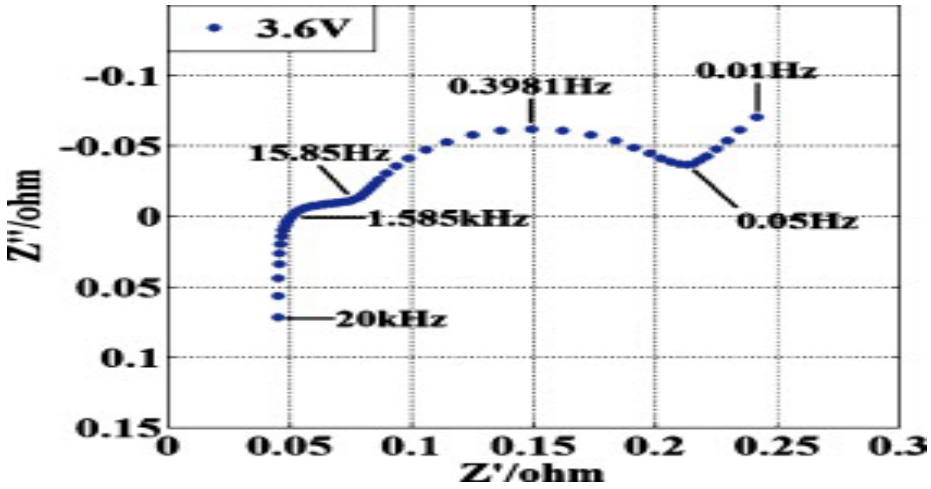

Figure 3.20 Typical Nyquist plot for new Lithium Ion cell perform at OCV of 3.6 V.

The Figure 3.20 above represents an experimental cell which follows the ideal behavior

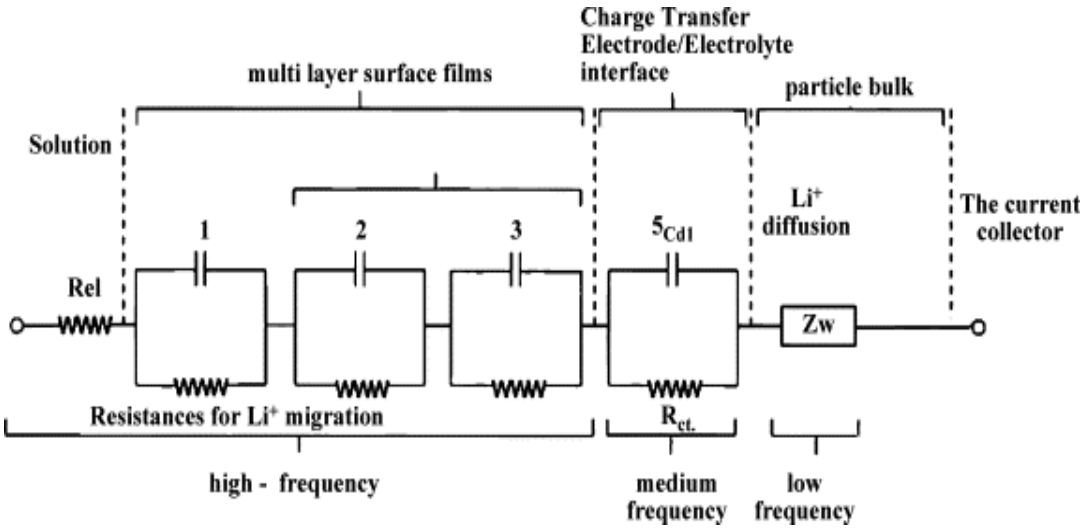

Figure 3.21 Equivalent Circuit: Lithium Ion Cell

The Figure 3.21 above shows the equivalent circuit of a lithium ion cell. Going from high to low frequency different regions are visible. There are many capacitances in the multilayer films. The charge transfer region has the double layer capacitance.

3.6.3 **Analysis of Single Impedance Arcs** [76]

Analysis of experimental data that yield a full semicircular arc in the complex plane can provide estimates of parameters R and C and hence lead to quantitative estimates of conductivity, faradaic reaction rates, relaxation times, and interfacial capacitance . In practice, however, experimental data are only rarely found to yield a full semicircle with its center on the real axis of the complex plane. There are three common perturbations which may still lead to at least part of a semicircular arc in the complex plane:

1. The arc does not pass through the origin, either because there are other arcs appearing at higher frequencies and or $R_\infty \rightarrow 0$
2. The center of an experimental arc is frequently displaced below the real axis because of the presence of disturbing elements in the material- electrode system. Similar displacements may also be observed in any of the other complex planes plots (Y, M, or ϵ). The relaxation time is not single- valued but is distributed continuously or discretely around a mean value $\tau_m = \omega_m^{-1}$. The angle by which such a semicircular arc is depressed below the real axis is related to the width of the relaxation time distribution and such is an important parameter.

3. Arcs can be substantially distorted by other relaxations whose mean time constants are within two orders of magnitude or less of that for the arc under consideration. Many instances of overlapping arcs are found in the real world.

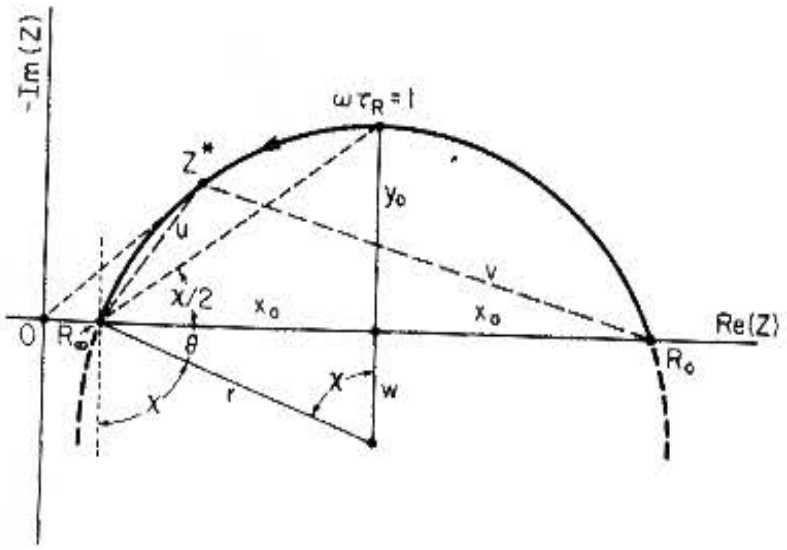

Figure 3.22 Geometrical Construction

This Figure 3.22 has arc depressed below real axis. A full semicircle has to be constructed geometrically taking the arc as a starting point. The diameter of this semicircle is the charge transfer resistance when the faradaic reaction occurs. Due to various similar reasons, the arc can also be above the real axis so much that the semicircle fitted to it is above the real axis rather than be on it.

Given below are some fitted experimental curves. Figure 3.23 shows the impedance of a commercial cell compared to that of an LbL Cathode. The impedance values are sharply different. In the Figure 3.24 more curves are shown. These are for all LbL cell and LbL anode. Notice that the values for the cathode and anode are very close to each other. This indicates that the films present similar behavior whether we have anode or cathode.

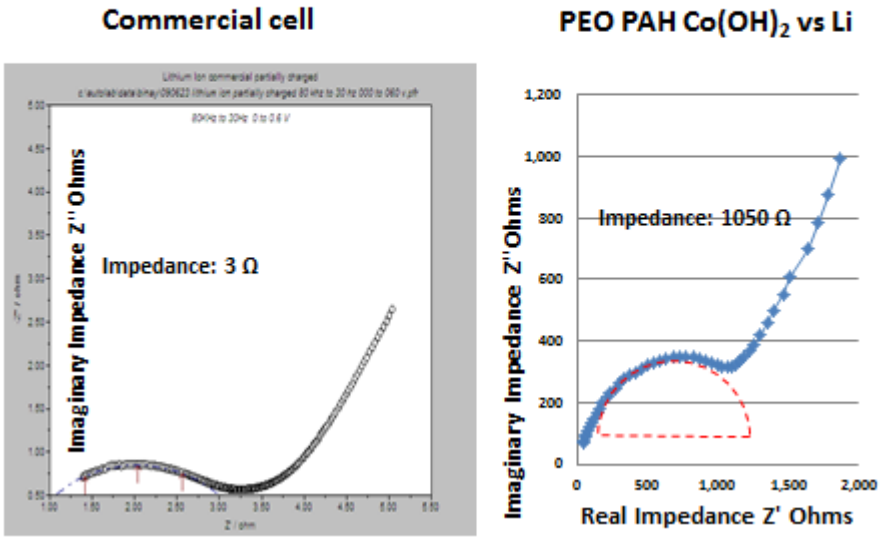

Figure 3.23 Commercial vs. LbL electrode impedance

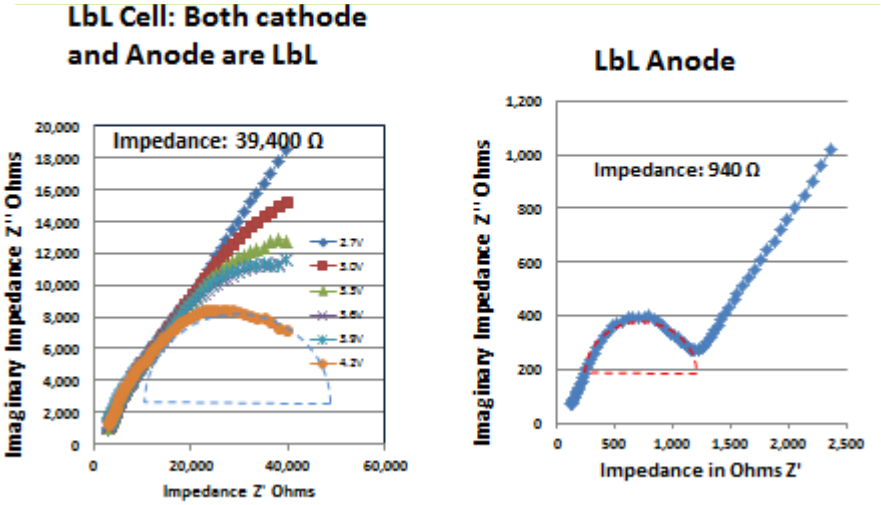

Figure 3.24 All LbL Cell vs. LbL anode

The plots above are typical for batteries and they all show a semicircle from which charge tranfer resistance can be obtained. The commercial cell shows 2 to 3 Ohms, LbL cathode 800 Ohms, LbL anode 1000 Ohms and an all LbL cell shows 20,000 Ohms. These values are obtained from high frequency regions. At low frequency they all show a straight line at 45 degrees typical of diffusion controlled phenomena.

3.7 Conductivity Measurements

Using impedance spectroscopy we see that the LbL cathodes have significantly high values, of impedance, to the order of $10^{4 \text{ to } 5}$ Ω. Commercial lithium ion batteries measure 1 to 10 Ω. Typically carbon is used to enhance conductivities of electrodes in batteries. These batteries are made with electrodes having active materials that have large particle sizes. They are more appropriately called batteries using bulk powders. In such cases significant improvements are made in the electrode conductivities by using carbon.

Our LbL cathode is made of layers by a layering process. It produces 20 pairs of layers. Each pair of polymer film is only a couple nanometers thick. Within each film pair $Co(OH)_2$ is deposited and electrochemically converted to CoOOH and $LiCoO_2$. The particle size of these materials is in the nanometer range. Introducing carbon in any form, say even nano carbon, is a daunting proposition. Carbon also must be able to be deposited in each layer of the film. We tried cells with nano carbon introduced during the layer by layer process. These showed no significant improvement in conductivity. Because of this a drastic new step had to be taken. An electrochemical method was employed to produce this electronic material in situ within the films. The electronically conducting material is cobalt oxyhydroxide (CoOOH) . Really this material is a common additive in the nickel electrode of NiMH or NiCd batteries. These are aqueous batteries. And there cobalt hydroxide is converted to cobalt oxyhydroxide during the charging of the battery. If the battery is not discharged below 1.0 V vs. cadmium the cobalt hydroxide is maintained. It keeps its conducting character.

In the lithium ion battery, the electrolyte is non- aqueous. We used 1M $LiPF_6$ in a 50-50 mix of ethylene carbonate and dimethyl carbonate**.** In the organic solvent there is no prior case of CoOOH existing in its electronically active form. Therefore when attempting this in the Li ion battery there was no certainty that the conducting phase would be produced and maintain its electronic conductivity. However, the treatment was successful as confirmed by X-Ray analysis and conductivity measurements. In fact this works not only in the LbL environment but also in a mixture condition. The defining conditions are given below.

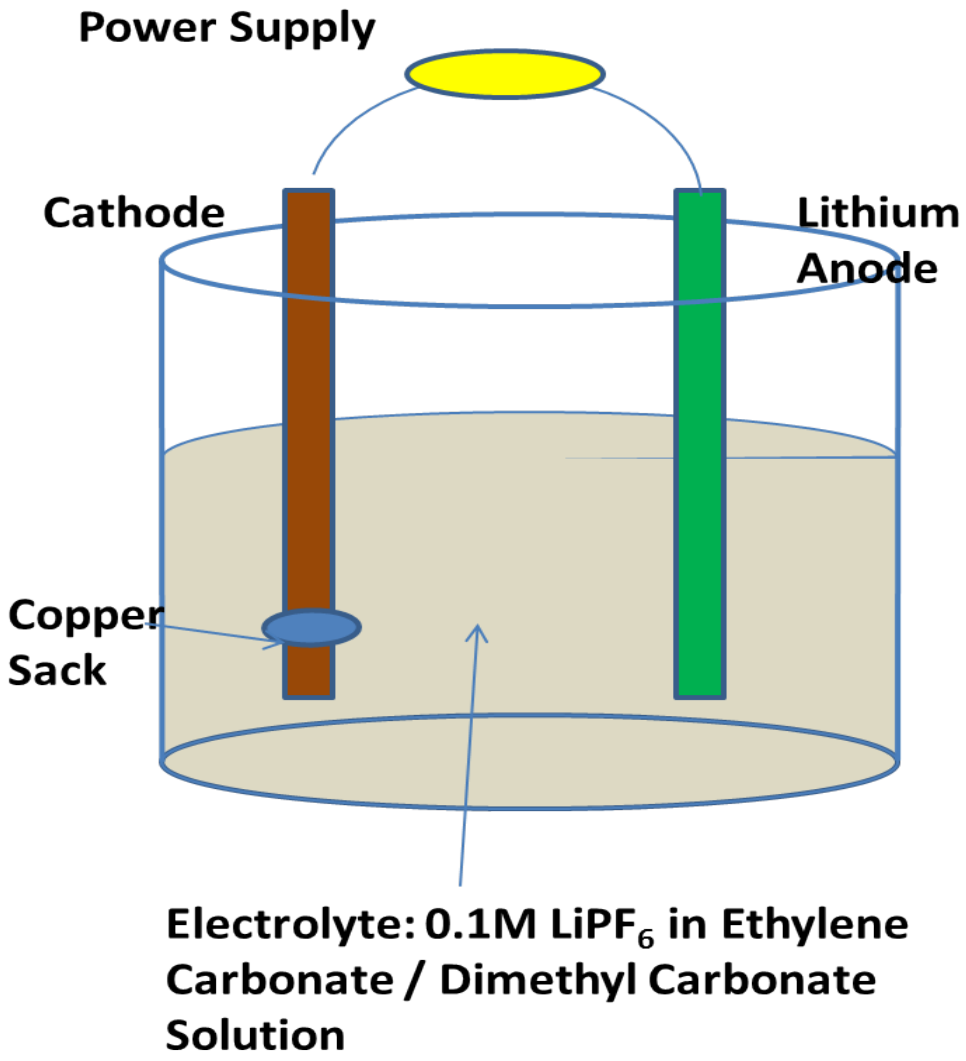

Figure 3.25 The set up for the treatment

Figure 3.25 is the apparatus used in the treatment. Essentially it is an electrochemical cell. While discharging it produces $LiCoO_2$ and while charging CoOOH.

These are the important aspects of the treatment:

1) The $LiCoO_2$ is produced during discharge of the above electrochemical cell
2) The reaction is : $xLi^+ xe^- + CoO_2$ - > Li_xCoO_2 at 3.0 Volts
3) On charge cycle or external oxidation in air CoOOH is formed from $Co(OH)_2$
4) The electrochemical oxidation is a solid state reaction producing the nonstoichiometric phase $Co_x^{4+}Co_{(1-x)}^{3+}OOH$
5) This phase is formed when the rate of charge exceed the C/5 rate with respect to the cobalt hydroxide
6) The conductivity of the nonstoichiometric phase Co^{4+} is 10^{-2} S/cm

The above experimental set up is used and the cell is put under a constant voltage discharge for 2 hours. A charge step may or may not be done before the start of discharge. This method produces both CoOOH and $LiCoO_2$. Confirmation is obtained by X-Ray Diffraction. Shown below is the XRD picture of Figure 3.26.

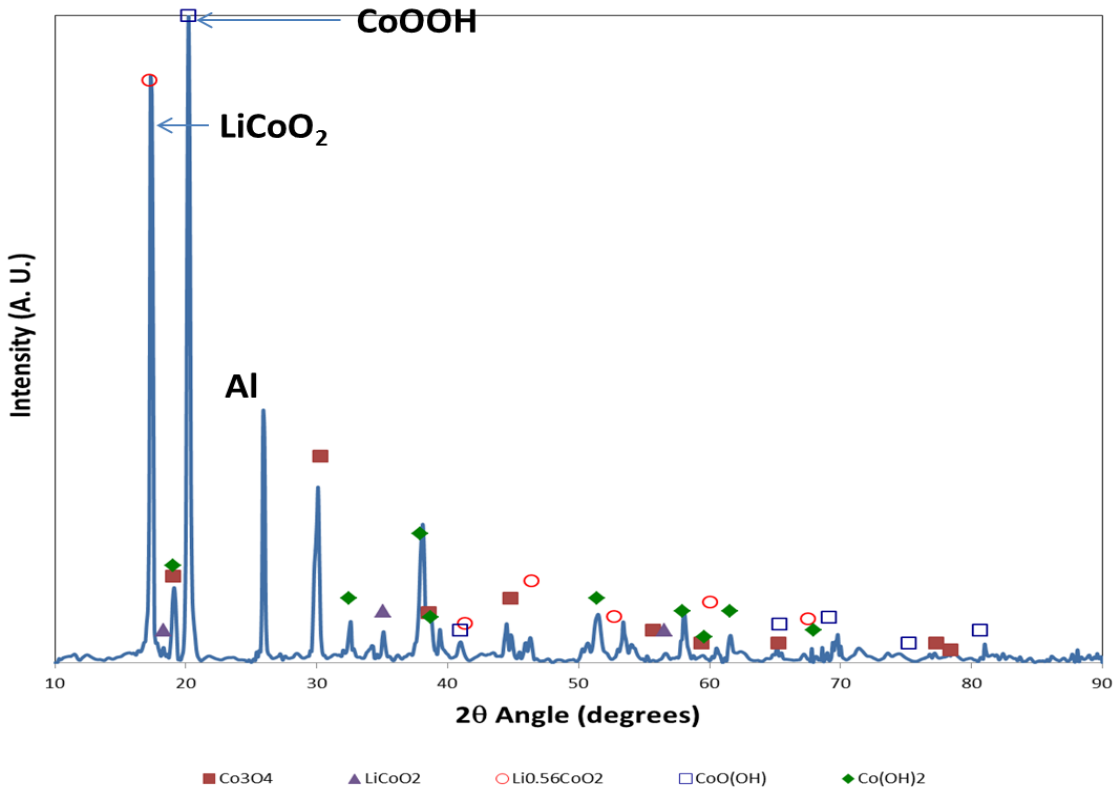

Figure 3.26 Diffraction pattern of the LbL electrode

Significant conductivity improvement was achieved. Thus we abandoned the attempt to add nano carbon to the electrode. All cells were made with only CoOOH acting as the electronic conductor.

3.8 In Situ Active Material Preparation

We see that with the same treatment during discharge, $LiCoO_2$ is formed. The above test experimental set up is used and the cell is discharged at 3 volts for 2 hours inside a glove box with argon atmosphere. This attempt is also new and not reported in literature as yet. Hundreds of electrodes have been successfully made by the above method. The treatment conditions have to be kept tightly in control and drifts in the discharge voltage are very detrimental to the outcome.

After successfully producing CoOOH and $LiCoO_2$ within the PEO / PAH pair the cathode produced makes a very promising battery vs. lithium. If conditions are kept tightly in control very high level of repeatability is achieved.

Chapter 4

The Counter Electrode (Anode)

Once the cathode had been produced it was important to concentrate on the anode as counter electrode for testing. Lithium metal is the typical choice for the counter electrode. The lithium metal is so virile in an organic solution containing Li^+ ions that it attacks all metal substrates on which the electrodes are made.

4.1 Corrosion

There is a corrosion effect seen with lithium anode when the battery is discharged at low rates ($3.5x10^{-7}$ Amps) below 1.0 Volts. A corrosion couple is set up between the aluminum substrate and the lithium anode. This effect is minimal when the anode is changed to lithiated graphite. On changing the cathode substrate to stainless steel the corrosion is minimized further. Even commercial batteries show the corrosion effects. To mitigate or nearly eliminate this effect, use lithiated graphite anode and make the cathode on stainless steel substrate. Given below are some graphs that show corrosion. Typically where corrosion occurs the discharge goes on for a great length of time. Figure 4.4 show the long on going corrosion effect. Literature reports corrosion of the lithium metal[14].

4.1.1.1 Aluminum vs. Lithium

Aluminum corrosion curves are shown in the Figures 4.1, 4.2 and 4.3. In Fig 4.1 the discharge current is 10^{-6} Amps. The voltage falls only to near 2 Volts but at a six times higher current $6x10^{-6}$ Amps this voltage drops drastically to 0.2 Volts. But at an even higher current (10^{-4} Amps) the cell voltage drops to zero (Fig 4.3) instantly. **Corrosion is set up at lower currents. At higher discharge voltages, say 2 Volts, it is not present. It sets in only at around 1.0 Volt[14] or below.** Inside the LbL battery, such corrosion will take place as well. Unless discharge rates are high, the cell will continue to

discharge continuously. Such phenomena were encountered during the course of the research. Figure 4.4 is a typical curve.

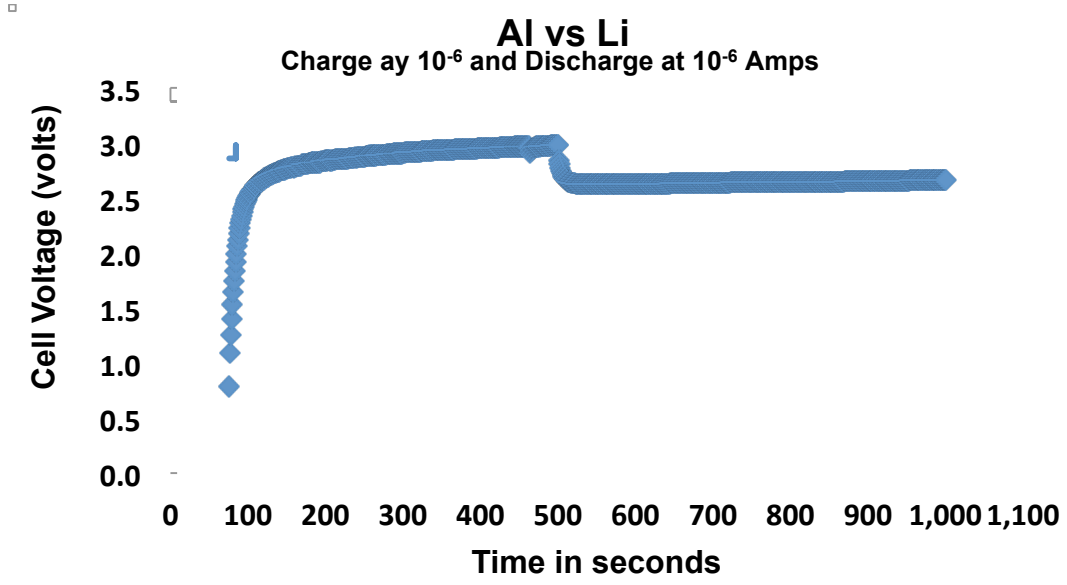

Figure 4.1 Charge and discharge at 10^{-6} Amps

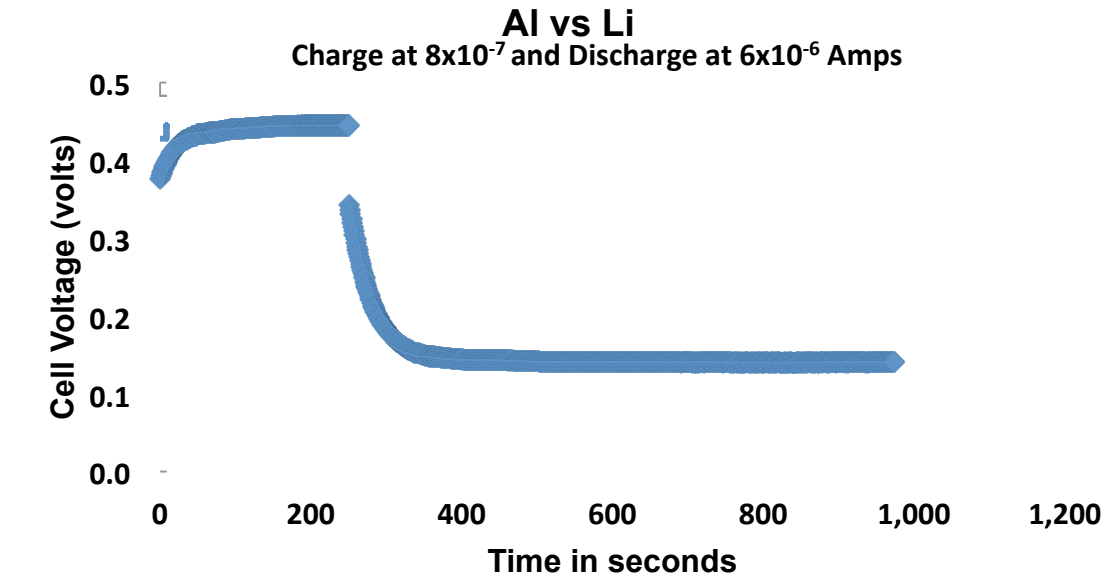

Figure 4.2 Charge at 10^{-6} approx. and discharge at $6x10^{-6}$ Amps approx..

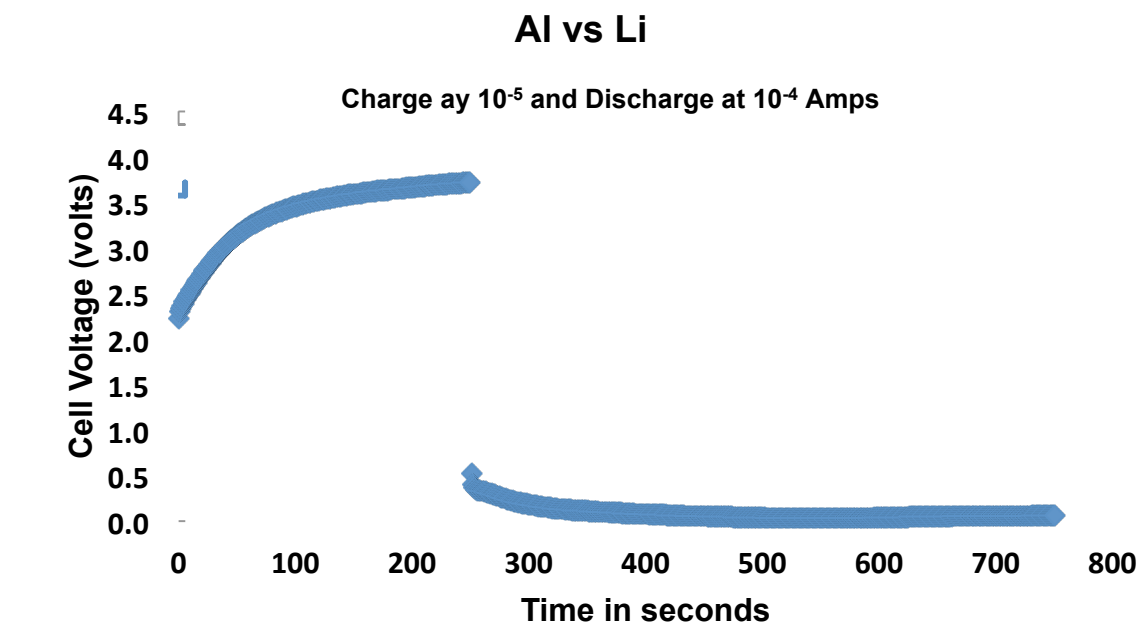

Figure 4.3 High rate discharge (10^{-4} Amps)

At a higher discharge current of 10^{-4} Amps the voltage falls rapidly to 0.5 Volts.

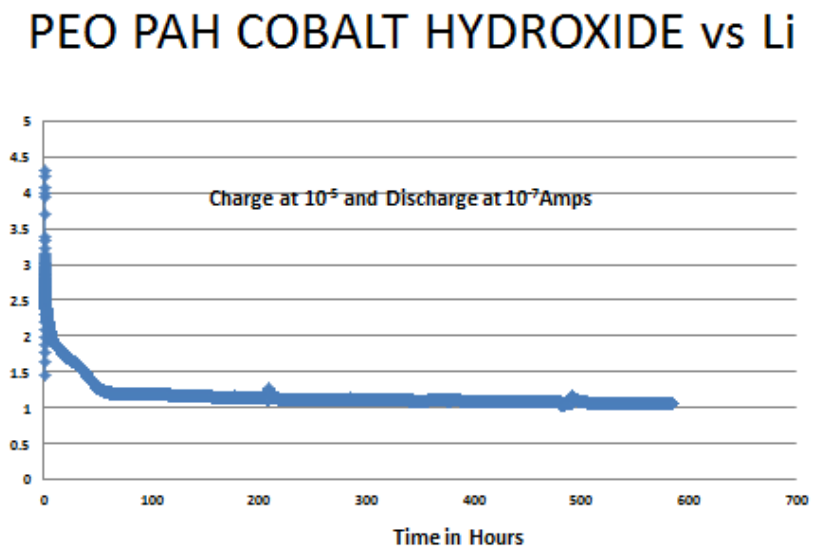

Figure 4.4 Typical corrosion curve; discharge at 10^{-7} Amps

Even though the corrosion takes place against the lithium anode, against the lithiated graphite anode it does not. This is shown schematically in Figure 4.5 schematic 1 below.

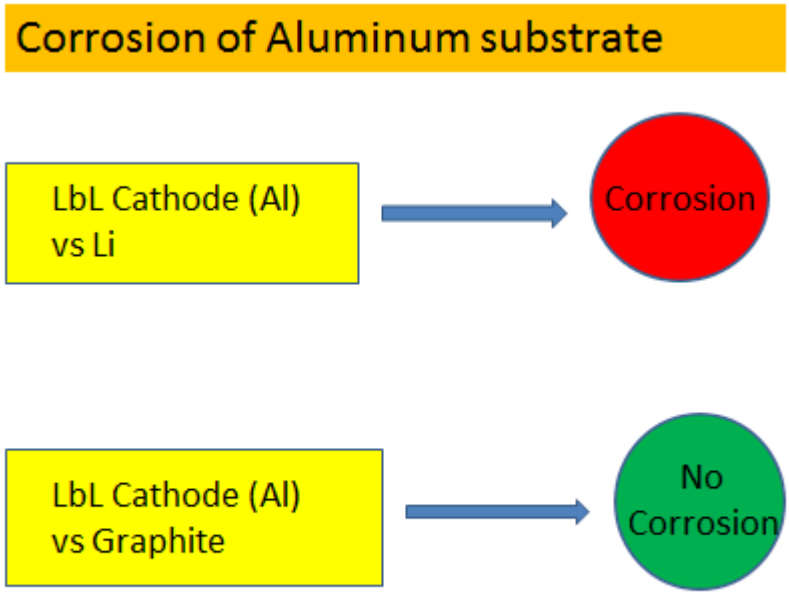

Figure 4.5 Schematic 1

In this research the substrate of the cathode is subject to corrosion too by the lithium anode when present in an organic solvent carrying lithium salts. But when matched against the lithiated graphite anode in the same environment there is little or no corrosion current observed from the aluminum.

The corrosion is visible when the discharge voltage is low, 0.5 to 1.0 Volt. When commercial batteries are discharged to low voltages and at similar low currents they also show corrosion. The value of the current is generally about 10^{-7} Amps. Thus A123 and commercial electrodes show corrosion too.

The testing has been done with both lithium and graphite anodes. As the cut off voltage is 2.0 Volts during discharge, the battery is not under corrosion. Figure 4.6 shows schematically this situation. Hence we adopt this in all our tests. **All cathodes are tested against lithium metal anode and discharged to 2.0 Volts only.** This is indicated in Figure 4.6 below.

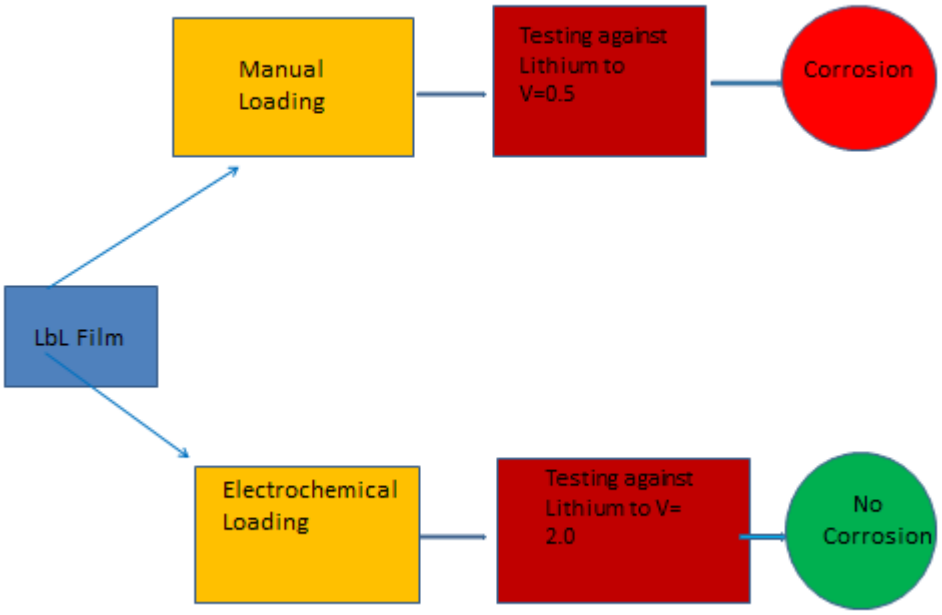

Figure 4.6 Schematic 2

4.2 The Choice of Lithiated Graphite as Counter Electrode

Testing against lithium counter is difficult because of superposition of corrosion and useful currents. The phenomena are more pronounced at lower voltages during discharge. The discharge has to be limited to 2.0 Volts as even then there are possibilities of misinterpretations. A study was undertaken to find an alternative electrode that could serve as a counter electrode.

Use of graphite on the anode reduces the corrosion considerably and the least corrosion seen was with a cathode on stainless steel substrate and anode as graphite. Cells were discharged at $3x10^{-7}$ Amps to 2.0 Volts as shown in Figure 4.7.

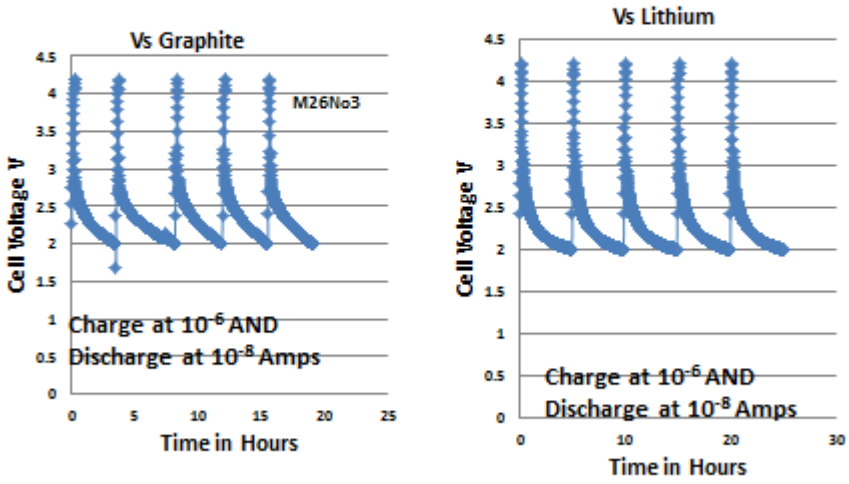

Figure 4.7 Lithium vs. graphite at 10^{-6} Amp charge and 10^{-8} Amp discharge

We see that the above two discharge curves are similar. Figure 4.7 the curve against graphite is similar to that vs. lithium. Hence the two are interchangeable. Also if the discharge voltage cut off is 2 Volts then lithium metal can be used safely for testing purposes. Hence we adopted this approach in our tests.

Chapter 5

Results and Discussion

5.1 Particle size of cobalt hydroxide

As aqueous solutions are involved, this cobalt hydroxide will be in a size matching the ionic radius of Co^{2+}. The size of the Co^{2+} ion is 152pm or 0.152 nm. Thus nano size or lower size particles are entrapped in between each layer of the film. Later when CoOOH is formed by oxidation it should also be similar sized. Sonochemical methods have been used by the Torresi group to prepare $Ni(OH)_2$, $Co(OH)_2$ and a mix of Ni/Co hydroxide nanoparticles[12]. "The appropriate nitrate was mixed with ammonium hydroxide solutions and then sonochemically irradiated for various times. This produced 5nm size NPs." Thus the cobalt oxyhydroxide is expected to be nano sized. The $LiCoO_2$ which is produced during the treatment in the glove box from small sized $Co(OH)_2$ is also expected to be nano in size. This transformation is an electrochemical solid state reaction which is not diffusion controlled (as in martensitic transformations). Sizes are expected to be maintained. Hence both the CoOOH and $LiCoO_2$ produced from $Co(OH)_2$ maintain their size along the lines of the Torresi paper.

Incorporation of cobalt hydroxide [13] in the film

Cobalt hydroxide is used in the nickel electrode for NiCd and NiMH batteries. It is mixed with the active material, $Ni(OH)_2$ in a 1/10 ratio by weight. It is converted electrochemically to cobalt oxyhydroxide (CoOOH). Cobalt oxyhydroxide is easily produced by the oxidation of $Co(OH)_2$. However the CoOOH with a +3 oxidation state is not conducting. It has to be charged at a rate C/5 or better (C is that of $Co(OH)_2$) to be made conductive. When it develops a form with both +3 and +4 oxidation states (a defect structure) it becomes electronically conductive and maintains its conductive state

on discharge till 1.0 V (vs. Cd). If discharged below this voltage it converts to other forms and renders the CoOOH non conducting.

V Pralong, A. Delahyaye-Vidal [13] have detailed the use of cobalt hydroxide in the nickel electrode. For charge rates greater than C/5, relative to the amount of $Co(OH)_2$, the electrochemical oxidation was found to be a solid-state process. This process leads to a nonstoichiometric CoOOH phase having a mosaic structure which enhances the electronic conductivity due to the presence of Co^{+4} ions.

We wanted to prepare CoOOH which would work in a non-aqueous solvent. This solvent is a 50% mix of ethylene carbonate and dimethyl carbonate (EC / DMC). The salt $LiPF_6$ is added and is 1M in concentration. This electrolyte will be used in a much higher voltage range: 0 to 4.5 V in the lithium ion battery. The LbL electrode with CoOOH is produced by oxidation in air while the electrode is drying. Later it is electrochemically converted to a mix of +3 / +4 forms during the first cycle of the battery charging.

Normally the charge current we have used is 10^{-5} Amps in a constant current mode. With respect to $Co(OH)_2$ which has a mass of approximately 15 μgms, the charge rate would be ≈13.6 C for the current chosen. The material, $Co(OH)_2$ has 298 mAhrs/ gm specific capacity. The rate to which $Co(OH)_2$ is subject is much higher than the C/5 required (by extension of the argument presented for nickel electrode in 7N potassium hydroxide). At such high rates (13.6 C) a highly disturbed structure is likely to be produced because of the diffusion limitations in the solid state at high rates of charge and discharge. Hence there is a high likelihood of finding +4 oxidation states along with +3 oxidation state.

The X-Ray test proved the presence of the CoOOH and the battery charge / discharge test indicates the presence of high conductivity. These are indirect evidence of the +4 oxidation state. However XANES or resonant Raman scattering using an energy-dispersive system combined with synchrotron radiation should be used to confirm it.

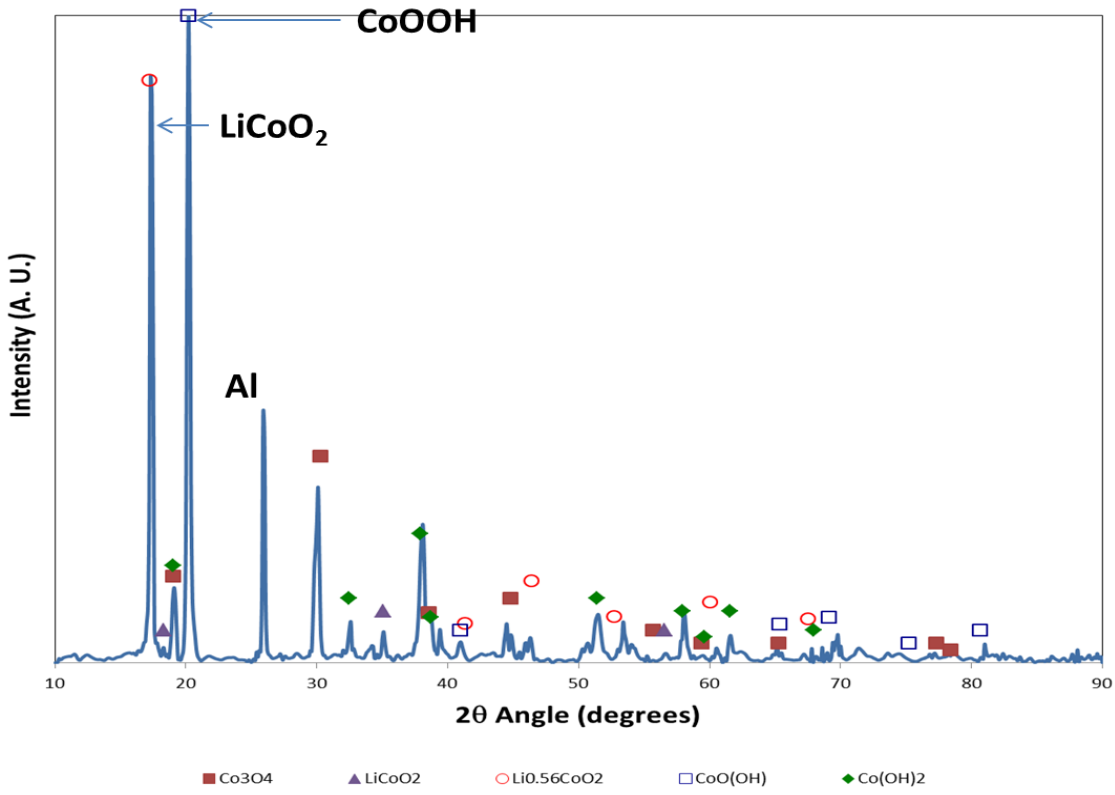

Figure 5.1 XRD shows the presence of $LiCoO_2$ and CoOOH

In the XRD pattern shown above in Figure 5.1 the red circle represents $LiCoO_2$ and the blue rectangle represents the CoOOH.

5.2 Impedance

Compared to the commercial cell the impedance value of the LbL Cathode / Li cell is much higher (570 Ω vs. 3 Ω). However significant improvement has been made compared to cell without cobalt hydroxide in the cathode (570 Ω vs. 40000 Ω). Thus we see how conductivity has changed as a result of the pretreatment.

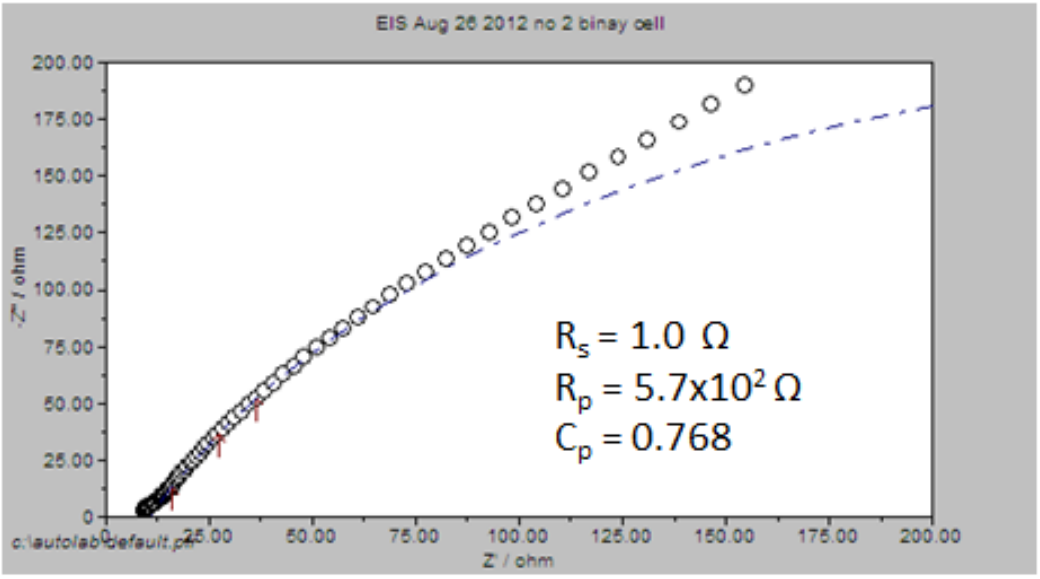

Figure 5.2 The charge transfer resistance value is 570 Ohms of a PEO PAH Cobalt Hydroxide vs. Lithium cell. The measurement is done on the Autolab potentiostat.

Figure 5.2 above is impedance data on a typical LbL cathode.

5.3 Battery Tests and discussions

All newly made batteries are given five formation cycles. Typically this is done at $3.5x10^{-5}$ Amps charge to 4.2 Volts and $3.5x10^{-7}$ Amps discharge to 2.0 Volts with no rest in between. Subsequent to this, batteries are tested as follows:

1) Discharge at $3.5x10^{-5}$ Amps to 0.5 Volts
2) Give a rest for 30 minutes
3) Charge at $3.5x10^{-7}$ Amps to a voltage cut off between 4 and 4.2 Volts
4) Give a small rest say, 5 minutes
5) Do a discharge at $3.5x10^{-7}$ Amps to 2.0 volts. The two volts has been used as a reference stop voltage.
6) The Charge and Discharge can be at $3.5x10^{-5}$, $3.5x10^{-6}$ and $3.5x10^{-7}$ Amps
7) Repeat the 1-5 steps for the number of cycles desired to run.

The charge cut off voltage

The standard electrode potential of the $LiCoO_2$ material is 3.7 Volts. Then we have to allow for the over potential of approximately 0.5 Volts. Thus the charge cut off voltage should be 4.2. The newly made batteries are formed at 10^{-5} Amps to 4.2 Volts during the

charge cycle. Formation is done for five cycles. Later when further work is done on the battery the charge cut off voltage is lowered to 4.0 Volts. This has proven experimentally to be adequate. In fact in a study done by me on all available data has shown that the difference between 4.2 and 4.0 cut off voltage charge cut off makes no real change to the discharge capacity. Shown below are some Figures 5.3 and 5.4 that illustrate this.

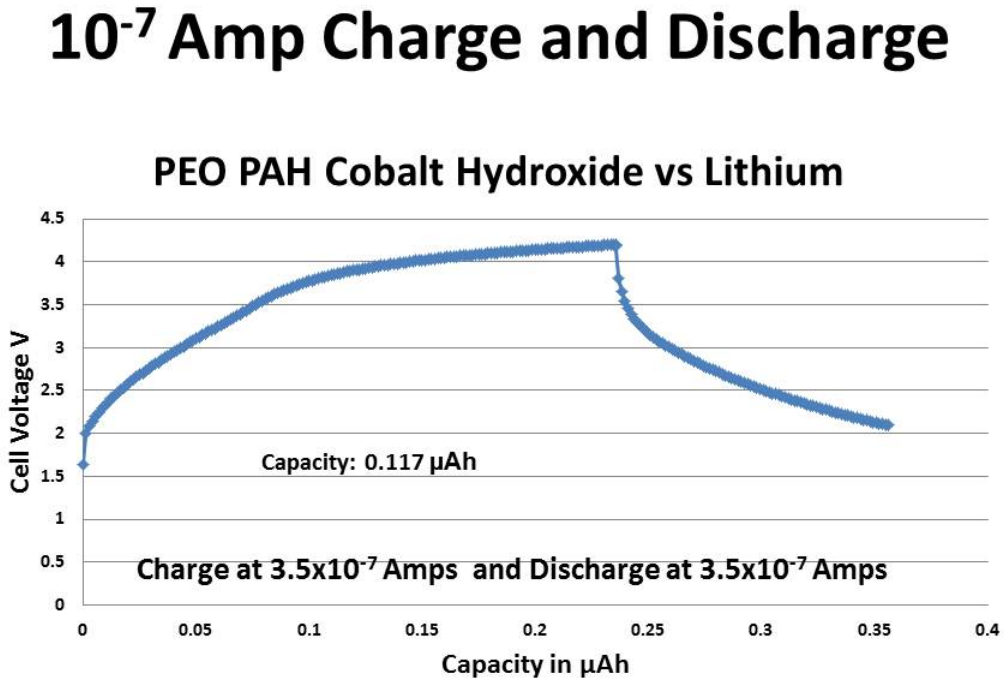

Figure 5.3 Graph shows a cut off voltage of 4.2 during charge

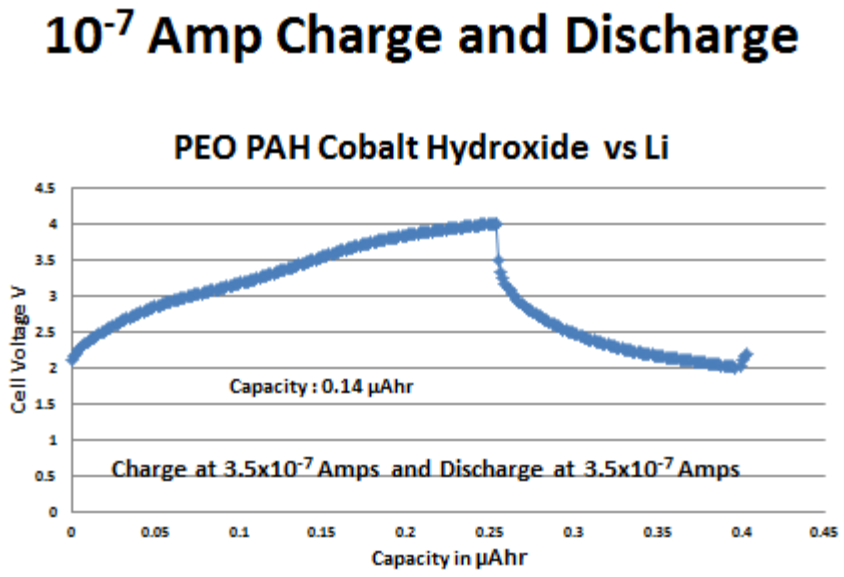

Figure 5.4 Graph shows a cut off voltage of 4.0 during charge. Note the discharge capacity is similar to the figure above' (0.14 vs. 0.117 µAh).

On examining battery charge / discharge data we see that the cells made have high efficiency values. These range from 80 to 90^{+} percent for columbic efficiency. At 0.7C ($3.5x10^{-7}$ Amp) the battery shows 90^{+} efficiency and at 7C ($3.5x10^{-6}$ Amps) it shows about 80% efficiency (Figures 5.8&5. 9). High rate is easily sustained with a large capacity as evidenced by the rate plot (Figure 5.7). **The specific capacity is in excess of the standard value (164 > 137 mAhrs per gram).** This is shown in Table 5.4.

Capacitive contribution

Recent literature is reporting capacitive contribution to the flow of electrons from electrodes that are made of nano particles. Even in my research I have come to this realization. To explain the results, it may be necessary to include the capacitive contributions. In the LbL film made by PEO PAH polymers, there is cobalt hydroxide in each layer. Later when this is converted to CoOOH and $LiCoO_2$ we have presented arguments that the particle size is around 5 nm. Of course particle size determination is

required to be done. **We therefore hypothesize that there is a capacitive contribution coming from these nano particles based on the following:**

1) The behavior of the electrode at $10^{-5}/10^{-7}$ Amp discharge
2) The reported information in literature
3) Determination of mass of active material in the electrode
4) Our CV determination of capacitance in the electrode

We will examine the above four factors to see how a capacitive contribution is likely. Performance behavior of our LbL electrode at the high rate exceeds that at the100 times lower rate. This is indicative of a capacitor. There is evidence available from others' work that capacitance contribution is present. Based on our mass and CV determinations we are able to measure the capacitance contribution. We therefore hypothesize that a capacitance contribution is likely.

Comparison of capacities obtained at 100 times different rates

On a detailed examination of data we find that the capacity found at 10^{-5} Amp rate is more than that at 10^{-7}Amp rate. The ratio of 10^{-5} to 10^{-7} capacities can vary from 17 to 4. As a large number of batteries have been examined there is greater confidence that this ratio will not change considerably. A large surge of electrons are flowing at the high rates in comparison to 100 times lower rate. In a typical battery this ratio should have been much less than one. The Table 5.1 below shows how in our experiments the ratio is more than one.

Table 5.1 Comparison of capacities at 100 times different rates

Sample size	**Ratio of capacity: 10^{-5} / 10^{-7} Amps**
Statistical	17
Eight	8
Fifteen	4

In the above table the ratio should have been much less than 1. If proportionality is maintained it can be 100 times less than 1 at the extreme. In any case the ratio is **not expected to be greater than 1 at all.**

The graph below (Figure 5.5) shows how the battery is at a 70C ($3.5x10^{-5}$ Amp) charge and discharge.

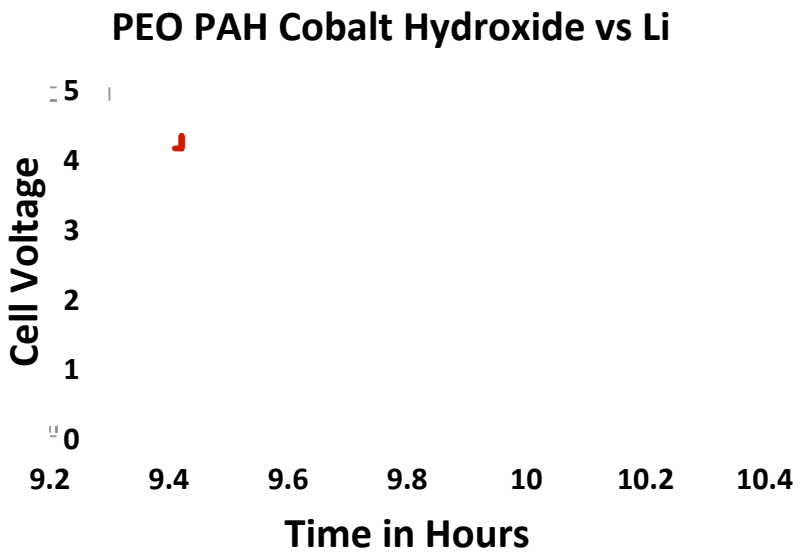

Figure 5.5 Charge and Discharge at 10^{-5} Amps; One cycle charge / discharge shows capacitance in the battery. A fairly large discharge at such high rate is evidence of huge excess of electrons-the contribution coming from capacitive effect.

Figure 5.5 represents a typical situation seen for many batteries at this rate ($3.5x10^{-5}$ Amp charge and discharge). At the70 C rate the battery above runs for 0.25 hrs to 2.0 Volts (also shown in the Table 2 below). On examining the charge discharge plot we find that the columbic efficiency is approximately 37%. It delivers $0.88x10^{-5}$ Ahrs of charge ($3.5x10^{-5}$ x 0.25 Ahrs). But the true C rate of the battery as determined by mass measurements using ICP and XRD is 5.0 $x10^{-7}$ Ahrs. This is the statistically averaged value. Taking the Ahrs as constant (the 1 C value), by comparison of experimental and expected values we find a 17 fold increase in charge ($0.88x10^{-5}$ / 5.0 $x10^{-7}$ = 17). In other words there is a huge surge of electrons at the 70C rate of the battery. The battery is 37% efficient at that high rate. At very high rates, like 70C, the amount of coulombs flowing is

larger than that expected from a battery of this size. Conceding that process variations can cause swings because of high σ values (Table 5.4), still the 70 C discharge will show manifold increase in Ahrs even after corrections. Is there some other phenomena occurring especially at very high rates? This behavior is reminiscent of capacitors. They behave in this manner discharging their high columbic charge at very high rates. Our result is indicative of excellent high rate discharge resembling that of a capacitor. Surprisingly, at 70C the battery has more capacity than at 1C. This is just the opposite of what should happen for a pure battery. A possible contributor can be corrosion current during discharge of the aluminum substrate. Against lithium this (corrosion) generally occurs at a 0.5 Volts [14]. As the discharge cut off is 2.0 Volts, corrosion effect is discounted. One possible explanation for this phenomenon is that the battery we have is not a pure battery. It has significant capacitive contribution which is rate dependent.

Shown below (Figure 5.6) is a hypothetical plot which reveals what could be happening. Charge stored in the capacitor will be different from that in the battery. They are independent of each other. The capacitor here, in the battery contributes in a variable manner: more at higher rates or high currents and less at lower rates. At lower rates the capacitor has less charge because it cannot be charged up quickly enough. We have an electrode on an insulating film of PEO / PAH. In between is CoOOH, which is an electronic conductor. How well it works with respect to rate is unknown. On the other hand the battery behaves as expected. Typically for a pure battery, in an ideal situation, when discharge rates are increased the run time to voltage cut off reduces. The product of discharge current and run time is constant. In other words, ideally Ahrs will be constant. Thus if a 100 Ahr battery produces 1 hr (60 minutes) run when discharged at 100 Amps, it should produce proportionately less run time at higher rates as shown in the Table 5.2. We propose this explanation for the non -typical behavior observed. What we see is the summation of the charges from battery and capacitor at any given rate. The higher the rate, the higher the capacitive contribution and significantly lower the battery contribution. Thus the battery can produce very high Amp-hrs at very high rates (70C) contributed by the capacitor and much lower values at lower rates where there is insignificant capacitor contribution. The battery has a very small amount of $LiCoO_2$ (4.74

µgs). This shows up at the lower rates (0.7C). It is noteworthy to point out that the 70C data is from another battery and the 1C data is a statistical average value based on 10 other cells. However, all electrodes are made and processed exactly the same way but at different times. Due to process limitations we can only process four electrodes at a time in the LbL machine.

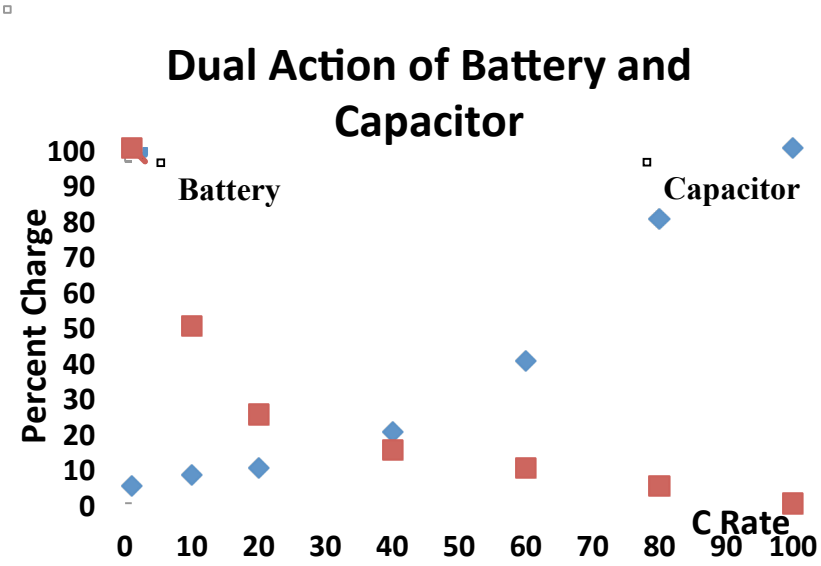

Figure 5.6 Hypothetical Plot explains the observed behavior

From the rate graph (Figure 5.6) we note the difference between 7C and 0.7C values. These two rates are lower than 70C as shown in (Figure 5.7). Here a 10x different rate does not show a 10x different response. Compared to capacity, at 7C ($7.5x\ 10^{-8}$ Ahrs) at 0.7C it is $13.25\ X10^{-8}$ Ahrs. For a 10x different rate there is only a 2x different response. This is another instance of high capacity and high power together in one device! These values suggest that within the films we have been able to provide an environment where high conductivity exists. This is due to the pretreatment done on the LbL electrodes**.** Redox activity of $LiCoO_2$ / Li is also taking place during discharge at many discrete NP centers immobilized within the film. Consequently high efficiency values are seen. Let us recall that there are 20 layers of LbL films with nanoparticles of $LiCoO_2$ and CoOOH present and immobilized in each layer.

From the CV run of the untreated electrode, capacitive contribution to capacity was found. Approximately 30% contribution to capacity is from capacitance behavior and 70% from stoichiometric behavior of $LiCoO_2$. All this translates to a very high rate and very high capacity device. The rate is enhanced and reinforced by capacitance behavior found in our battery. Table 5.2 shows how typically an ideal battery behaves. At higher rates of discharge less run time is obtained and if the battery behaves ideally the product of rate and run time should be constant.

Table 5.2 Ideal Battery Behavior

Number	Rate	Capacity Ahrs	Run time (mins)
1	C/10	100	600
2	C	100	60
3	10C	100	6
4	100C	100	0.6

Experimentally obtained values are shown below in the Table 5.3

Table 5.3 Experimental Values

Number	Rate	Time in Hours to 2.0 Volts	Current Rate Amps
1	70 C	0.25	$3.5x10^{-5}$
2	7 C	7.5	$3.5x10^{-6}$
3	0.7 C	13.25	$3.5x10^{-7}$
4	0.07 C	48	$3.5x10^{-8}$

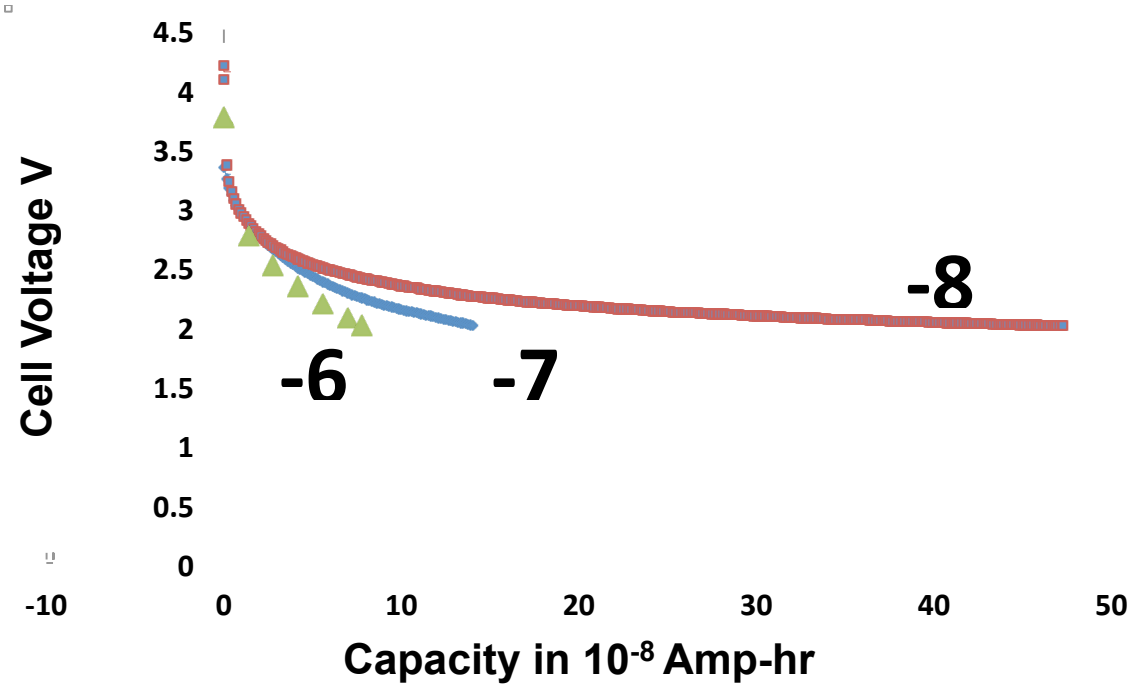

Figure 5.7 PEO PAH Cobalt Hydroxide vs. Lithium. Shown above is battery discharge curves at three different rates. The 10^{-8} , 10^{-7} and 10^{-6} Amp currents are abbreviated as -8,-7, and -6 on the graph and show orders of magnitude.

The following two graphs show the discharge behavior at lower rates. Figure 5.8 is for 10^{-6} Amp discharge and Figure 5.9 for 10^{-7} Amp discharge. They both show high columbic efficiencies.

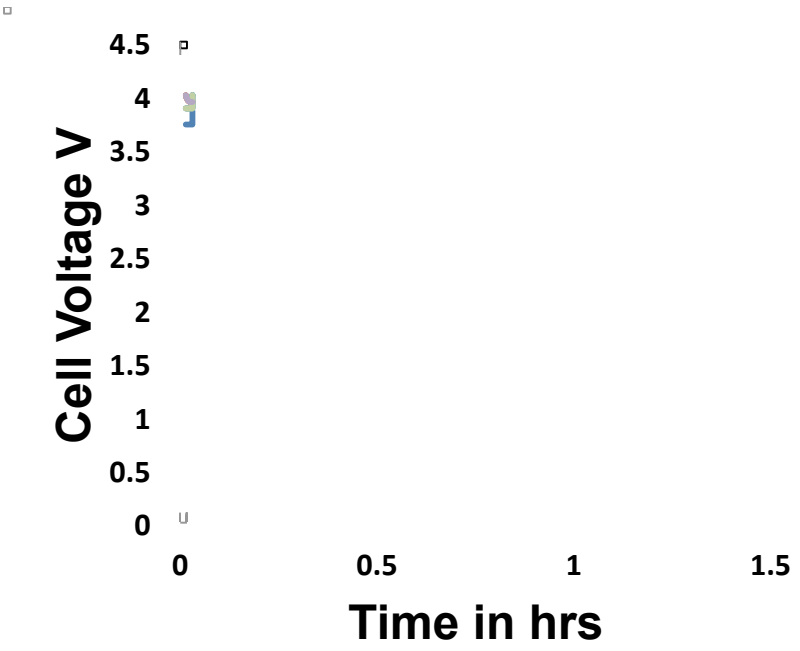

Figure 5.8 PEO PAH Cobalt Hydroxide vs. Lithium at $3.5X10^{-6}$ Amps. Note that the columbic efficiency is approximately 80%.

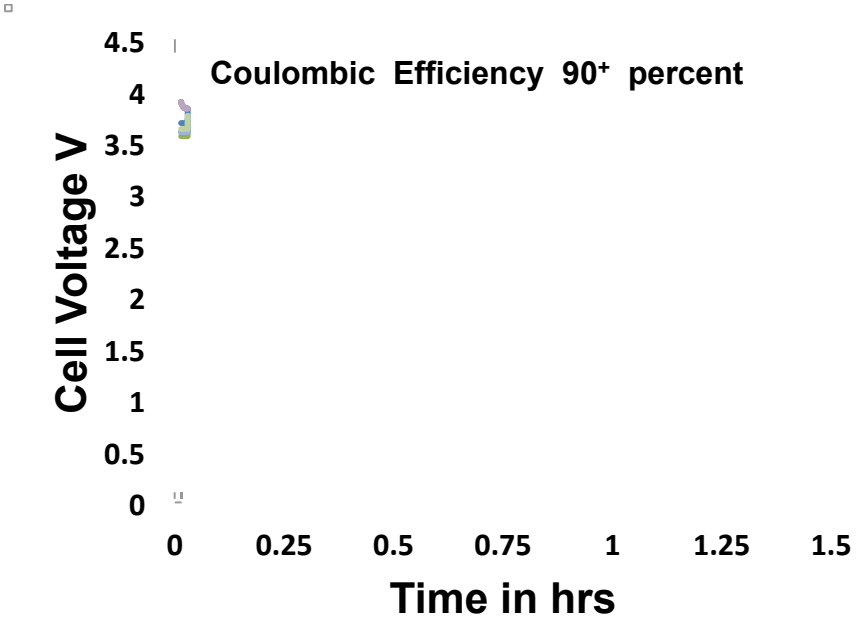

Figure 5.9 PEO PAH Cobalt Hydroxide vs. Lithium at $3.5X\ 10^{-7}$ Amps . At this 10x lower rate the columbic efficiency rises from 80 to 90^{+} %.

5.4 Capacitance contributions reported in literature

There are two major papers that bring to sharp focus the issue of capacitance found in batteries made with nano materials. The first describes the contribution of lithium titanate nano particle to intercalation and capacitive contribution. Nanocrystalline TiO_2 (anatase) was studied [3] over a dimensional regime where both capacitive and lithium intercalation processes contribute to the total stored charge. CV data was analyzed to distinguish between the amount of charge stored by these two processes-capacitive and intercalation. At particle sizes below 10 nm, capacitive contributions became increasingly important, leading to greater amounts of total stored charge (gravimetrically normalized) with decreasing TiO_2 particle size. The capacitive contribution was pseudo capacitive in nature. Moreover, reducing the particle size to the nanoscale regime led to faster charge/discharge rates because the diffusion-controlled lithium ion intercalation process was replaced by faradaic reactions which occur at the surface of the material. The charge storage and kinetics benefits derived from using nanoscale metal oxides provide an interesting direction for materials that offer both power density and energy density. Shown below are Figures 5.10 and 5.11. The first calculates the ratio of intercalation to capacitive behavior of nano particles and the second shows the CV response.

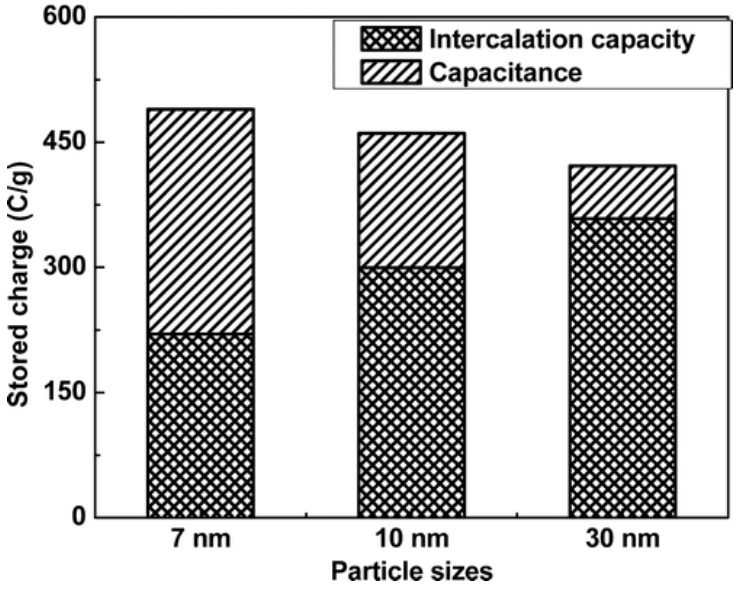

Figure 5.10 Comparison of charge storage for TiO_2 nanoparticle films (0.5 mV/s sweep rate). The total charge is separated into lithium intercalation and capacitive contributions.

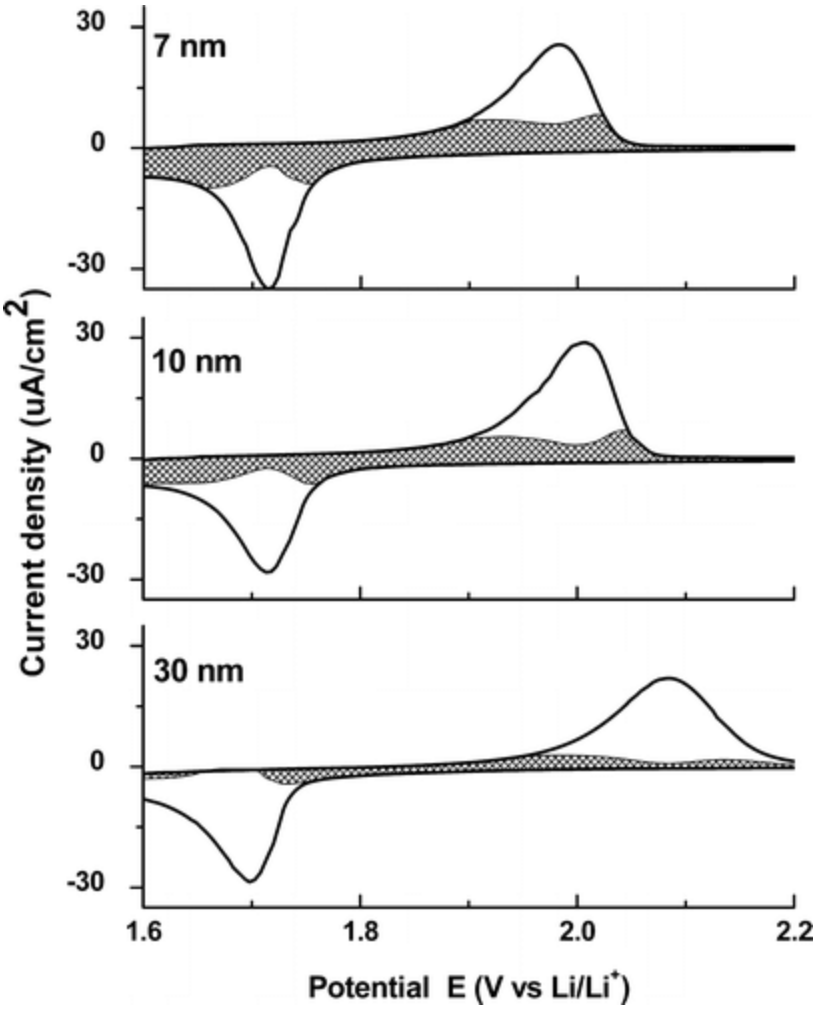

Figure 5.11 Voltammetric response (0.5 mV/s) for the three TiO_2 films. The total current (solid line) is obtained experimentally. The capacitive currents (shaded regions) are determined from the data .

The second paper is the one on nano films [1] of MWCNTs made by LbL process.

Here, is reported an alternative approach based on the redox reactions of functional groups on the surfaces of carbon nanotubes. Layer-by-layer techniques are used to assemble an electrode that consists of additive-free, densely packed and functionalized multi walled carbon nanotubes. The electrode, which is several micrometers thick, can store lithium up to a reversible gravimetric capacity of ~200 mA h $g^{-1}_{electrode}$ while also delivering 100 kW $kg_{electrode}^{-1}$ of power and providing lifetimes in excess of thousands of cycles, both of which are comparable to electrochemical capacitor electrodes.

5.5 Determination of Mass and Specific Capacity

The mass of $LiCoO_2$ produced during the treatment in the glove box on the electrodes is determined using ICP. First, the total amount of cobalt on the electrode surface is determined. Knowing this, the X-Ray diffraction with the help of Jade software, gives the proportion of the compounds with cobalt in it. The weight of $LiCoO_2$ is determined to be 4.74 micrograms. Then the specific capacity is calculated as shown in the Table 5.3 . [See detailed determination in Appendix A]

As noted below, the mean specific capacity found is 164 mAhr per gm . This value is higher than that of Li_xCoO_2 with x=0.5. This value will be 137 mAhr per gm. Also note the large standard deviation, σ = 46.5 mAhrs per gram associated with the mean value of m = 164 mAhrs per gram. This can cause wide variations.

There is excess specific capacity observed. A cyclic voltammetry (CV) plot of the electrode without electrochemical treatment (no $LiCoO_2$) shows sizable capacitance contribution to capacity (54mAhr/gm). (See Figure 5.12)

5.6 Capacitance contribution determination

The capacitance contribution from an LbL electrode has also been shown by others [1]. This contribution is particle size dependent and increases significantly as particle size approaches 10 nm or less [15]. We are seeing a similar contribution in our case (54 mAh/gm). A more detailed study will help reveal the mechanism involved. A CV was obtained with the LbL cathode as working electrode, lithium as counter electrode and platinum as reference electrode. CV was run with several different scan rates but the one reported here is at 50 mVs. The working electrode is the untreated LbL electrode which does not have any $LiCoO_2$. It only has $Co(OH)_2$. The capacity calculated is based on the $Co(OH)_2$ weight determined by us. The capacitance in Farads is obtained by the formula

Capacitance = Area of the CV/ (mass)(scan rate)(voltage window)

Figure 5.12 is a CV used to determine the capacitance value.

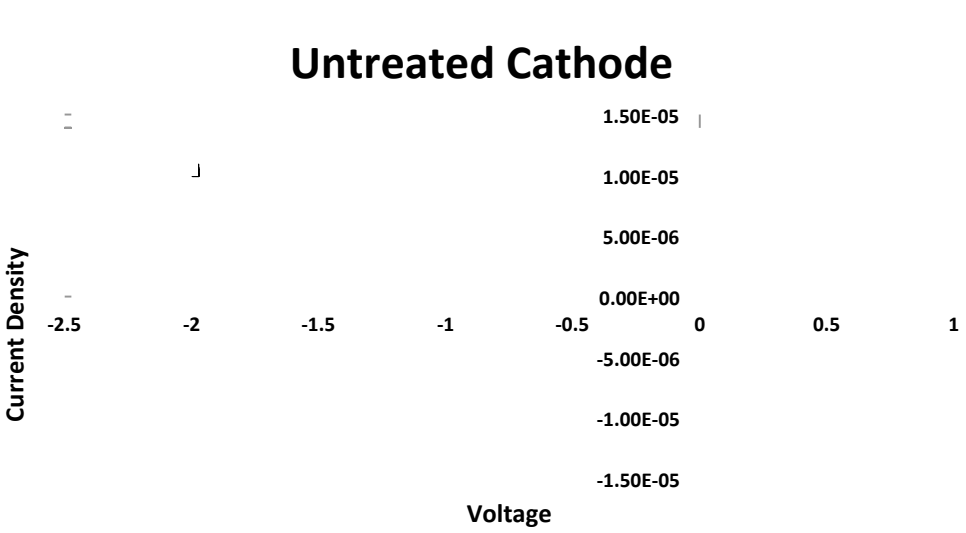

Figure 5.12 CV shows capacitance of the LbL electrode without any $LiCoO_2$. Battery contribution is absent. It is used to determine the capacitive contribution which works out to be 54 mAhrs/g.

Table 5.4 Summarized data. Shows specific capacity values.

Category	Value	Units
Mass	4.74 ± 0.81	µg
Capacity	7.5 ± 2.5	$X10^{-7}$ Ahrs
Specific Capacity	164 ± 46.5	mAhrs / gm
Capacitive Contribution	54	mAhrs / gm
Final Specific Capacity	110	mAhrs / gm

Looking at Table 5.4 we can say that the wide variation of specific capacity can be eliminated or minimized with a larger sample size. Hence it is also possible that the mean value can also be lowered. Thus the final specific capacity of $LiCoO_2$ can be less and fall into place of expected values when taking into account the experimental variation of -46.5 mAhrs/g. Hence the excess capacity can also be explained with this variation on the negative side. But because the 164 ± 46.5 mAhrs/g value has a plus variation, when this is addressed the value becomes 200.5 mAhrs/g and then the value of specific capacity will be in great excess of the maximum standard value of 137 mAhrs per gram. Applying the capacitive contribution of 54 mAhrs/g over on top of this value(200.5 mAhrs/g) can

then bring the final value to 146 mAhrs/g. This is within an easy statistical variation of 137 mAhrs/g. With a larger sample size, even this value can be brought to be less than 137 mAhrs/g. Thus the capacitance contribution explains the excess better, even when imposing the statistical variations.

Impedance of the LbL cathode is approximately 570 Ω. This value is a considerable improvement over 40,000 Ω seen in an LbL cathode without any electronic conductor. However it is 100 times larger than the impedance of the commercial cell tested. This by itself would suggest that the LbL cell would show very poor charge and discharge character. But it does not.

The cells made with this 570 Ω LbL electrode produces more than 100% of specific capacity as shown by ICP+XRD determined mass of the active material, $LiCoO_2$.

Comparing the charge /discharge curves we find greater than 90% columbic efficiency.

At the nano scale is a different mechanism working that allows efficient charge transfer to take place throughout the electrode.

Going into a greater detail helps understand our result. We then understand how a 570 Ω electrode can produce a specific capacity greater than 137 mAh/gm which corresponds to a maximum for x = 0.5 in the compound $Li_x\ CoO_2$.

5.7 Explanation of the phenomena seen

Alkire et al suggest in 1iterature [16] that NPs (nano particles) immobilized between LbL layers is the focus of high research activity. Distinction between faradaic and non-faradaic (double layer) charging is key to understanding how to make all metal centers in NPs redox active. The ability to have charge compensation capability enhanced resides in how NPs are immobilized. The transfer of charge through the film is limited to a small number (30) [16] of layers. Beyond this number the order, as suggested by Decher, it becomes "FUZZY". This prevents charge transfer through the LbL film.

These immobilized NPs will participate in new area of electrochemistry of discrete electro active Nano particles. "These NPs are different from their material counter parts in[16]: (1) the possibility of observing a significant fraction of the redox process for a given NP to originate from interfacial redox sites (which may have intrinsically faster

electrons transfer and ionic compensation processes , (2) the possibility of shorter times required for charge compensating ions to access all of the electro active sites in the NP, (3) The significantly enhanced surface areas of the NPs , which allow for more entry points for these same ions , as well as providing more active sites for cases in which surface structures on the NPs are involved in electro catalytic processes. While the phenomenological observations of faster redox processes for electro active NPs compared to bulk materials and higher electro catalytic activity described above can certainly be explained on the basis of these types of phenomena, much work remains to characterize and more fully exploit these phenomena."

We have two types of nano particles immobilized by the LbL film. One is $LiCoO_2$ and the other CoOOH. The distance between the films is not more than 4 atomic layers. At such a level, charge transfer between redox active particles, namely $LiCoO_2$ occurs in a similar manner as described above. The nature of the LbL structure puts the NPs into close proximity to one another. Thus for cases in which the NPs are electroactive, charge propagation through the films seem most likely to occur by electron exchange, first between the electrode and the layer of NPs closest to the electrode surface and then by electron exchange between the NPs in the film. The CoOOH nano particles provide additional conductivity. The net result is a highly efficient cathode with columbic efficiencies reaching near 90^+ % with a cut off voltage of 2.0 Volts. Higher efficiencies may be realized at lower cut off voltage when the voltage is lowered. A logical cut off can be 1.0 V which is safe distance from the reported corrosion plateau of 0.5 Volts[14] seen during discharge.

Specific capacity values obtained, 164 mAhrs/gm, are also in excess of 137 mAhrs/gm max corresponding to x=0.5 in $Li_X CoO_2$. Generally the value of x does not exceed 0.5. The excess is also explained by the onset of capacitance in the battery. Our hypothesis is that these high values of specific capacity are due to the contribution of nano particles. The capacitive contribution is shown below in Table 5.5.

Table 5.5 Calculation of capacitance and capacity

Capacitance (Farads) : C = Q / V in a capacitor
Capacity is measured in Coulombs or mAhrs
Capacitor Contribution : Capacity : Coulombs = Q_1 = CV
Battery Contribution : Capacity = Coulombs = Q_2 = (Q/t)*t
Total = Q_1 + Q_2 = 164 mAhrs / g Q_1 = 54 mAhrs / g
Hence Q_2 = 110 This is the battery contribution

More work is needed to firmly establish the capacitance derived from the battery as shown in Table 5.5. This will be in the realm of future work.

We have found that the battery made with the LbL cathode has a significant amount of capacitive contribution to the battery capacity. Other researches[1,15] have reported this type of behavior from nano particles. Researchers using Lithium Titanate[15] as cathode vs. Li have noted that the particle size of active materials is critical. The smaller the size in terms of nanometers the more the capacitive contribution. Researchers at MIT have also found very large contribution of capacity derived from pseudo capacitance[1]. They report a 200 mAh capacity coming from functionalized graphite electrodes made by the LbL process.

Prior work (cited)[1,15] has shown capacitive behavior in batteries. We hypothesize that this is also occurring in our system. There is indirect effect and direct effect. The indirect effect is the presence of higher capacity at higher rates of discharge. This manifests itself early in battery testing and suggests to us the possibility of the presence of capacitance The direct effect is the capacitance measured by the CV.

Our objective was to show the feasibility of a LbL cathode with $LiCoO_2$. The observation of capacitive contributions is, at this stage a somewhat speculative aspect, and further work would be needed to confirm this hypothesis. However we have succeeded in showing that, a LbL battery is working and for now, we hypothesize that there is some capacitive contribution.

5.8 Battery charge discharge results

The LbL cathode vs lithium or graphite button cells tested have two sets of polymers PAA/PAH and PEO/PAH. We select PEO/PAH pair for extensive testing. Generally nanocarbon can be added but does not help much. In the presence of the electronic conductor- CoOOH- there is no need to add carbon. In most of the work we have skipped the addition of nano carbon to provide conductivity. The 10^{-7} Amp rate is adopted as the standard. This corresponds to a 0.7C rate. The battery responds to several high and low rates from 0.07 C to 70C rates.

The figure below compares a commercial lithium ion battery with one made in the lab. They both were charged and discharged at similar rates. Essentially they show similar profiles. The commercial cell discharges to 3.5 V and is depleted of all its capacity. On the other hand the LbL electrode discharges more slowly and runs to 2.0 V where it is terminated. This cell discharges in a sloping manner. We have the LbL cell at an impedance at around 1000 ohms. Compare this to commercial cell whose cell impedance is 0.1 to 1 ohm. The LbL cell has a significantly higher impedance and this results in voltage drop at a much higher rate. Thus the discharge profile is sloping. MIT[1] researchers have also found sloping curves due to supercapacitive effects. Their work is on LbL Supercapacitors. As the size of the film is in nano meters range we also found a considerable capacitive contribution to overall capacity. This is approximately 30% in our case. In literature[13] people have also reported 50% supercapacitive contribution (Figure 5.11).

Very noticeable is the absence of a knee in the case of the LbL cell. Because of it's size and the low content of active material the cell is discharged at 10^{-7} Amps. At this value of current the substrate starts corroding producing a steady current. This current is due to electrochemical alloying as reported by A. N. Dey [14] . When the commercial cell is discharged to low voltages and at comparable values of current it also shows an extra long discharge current due to the same phenomena.This is shown in Fig 4.2 in corrosion section.

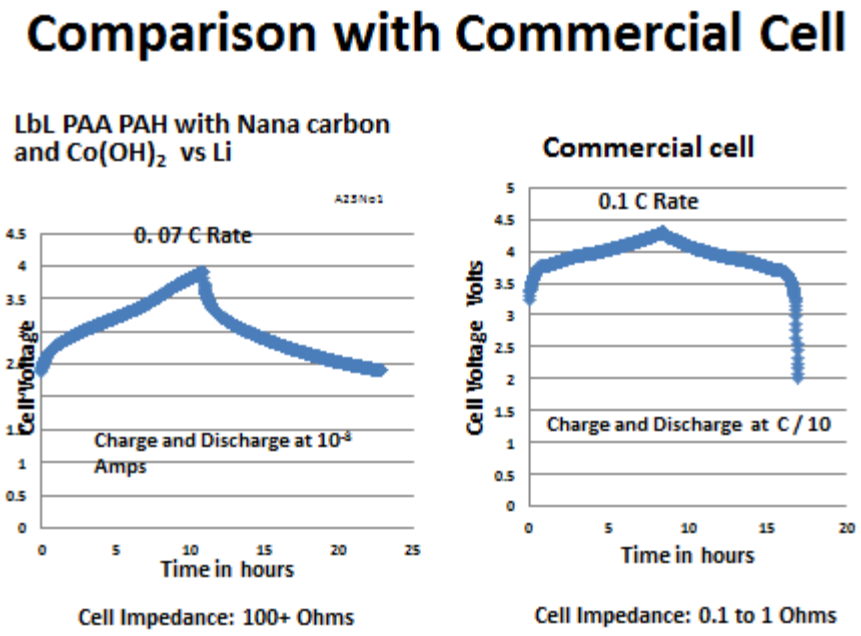

Figure 5.13 Comparison with commercial cell 1

Figure 5.13 compares a commercial cell to a LbL cell with PAA PAH vs. lithium. More or less at similar rates they appear similar. The lower voltages of the experimental cell are explained by the nano size phenomena.

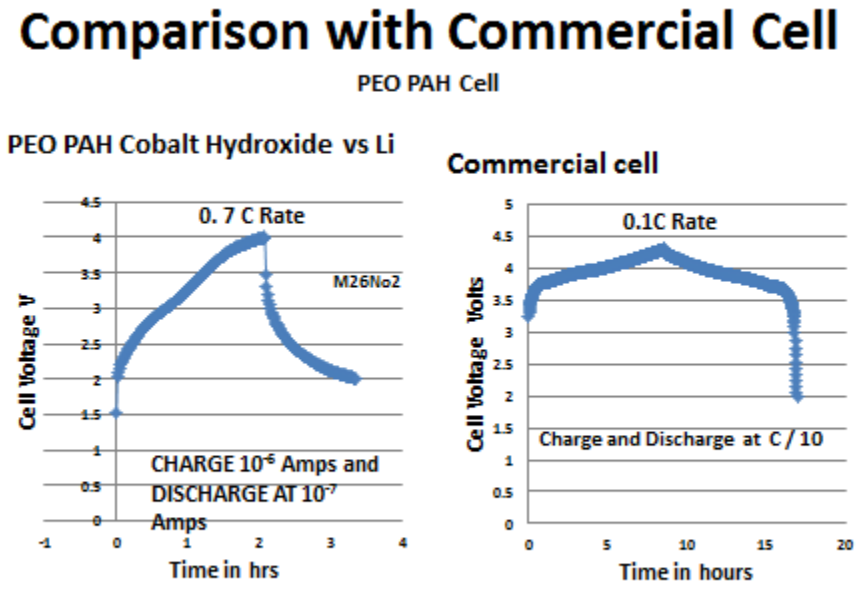

Figure 5.14 Comparison with commercial cell 2

Figure 5.14 compares a commercial cell to a LbL cell with PEO PAH vs. lithium. More or less at similar rates they appear similar. The lower voltages of the experimental cell is explained by the nano size phenomena

Figure 5.15 shows the first five cycles of the LbL battery. It is quite repetitive.

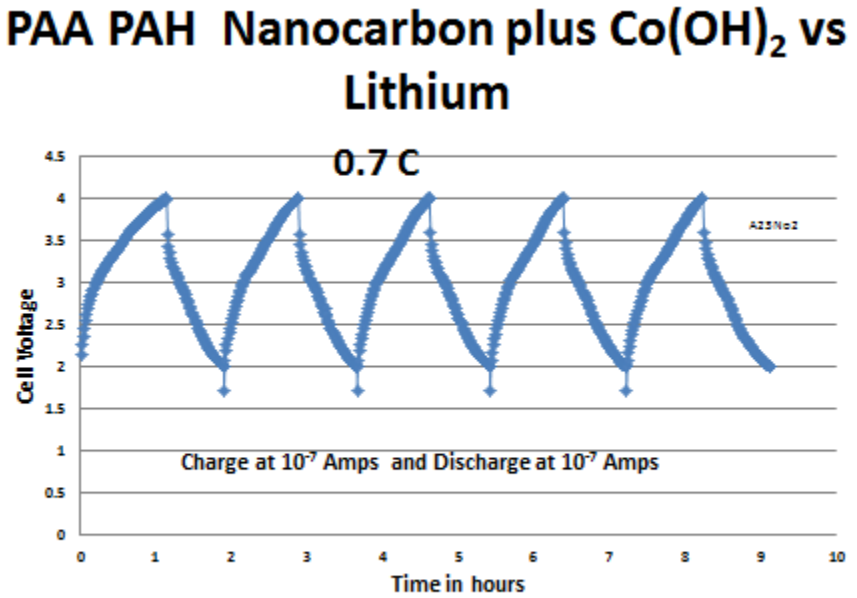

Figure 5.15 5 cycles at 10^{-7} Amp charge and discharge

Definition of the C-rate of a battery

The C-rate of a battery is defined as the rate that produces one hour of discharge time. Rates lower or higher are designated in reference to this C-rate. In our case the C-rate is 5 x 10^{-7} Ahrs. Table 5.6 shows how rates are calculated in terms of the C rate.

Table 5.6 Battery Rate Capability

Discharge Current	C rate capacity	Rate
3.5x10^{-5} Amps	5X10^{-7} Ahrs	70 C
3.5x10^{-6} Amps	5X10^{-7} Ahrs	7 C
3.5x10^{-7} Amps	5X10^{-7} Ahrs	0.7 C

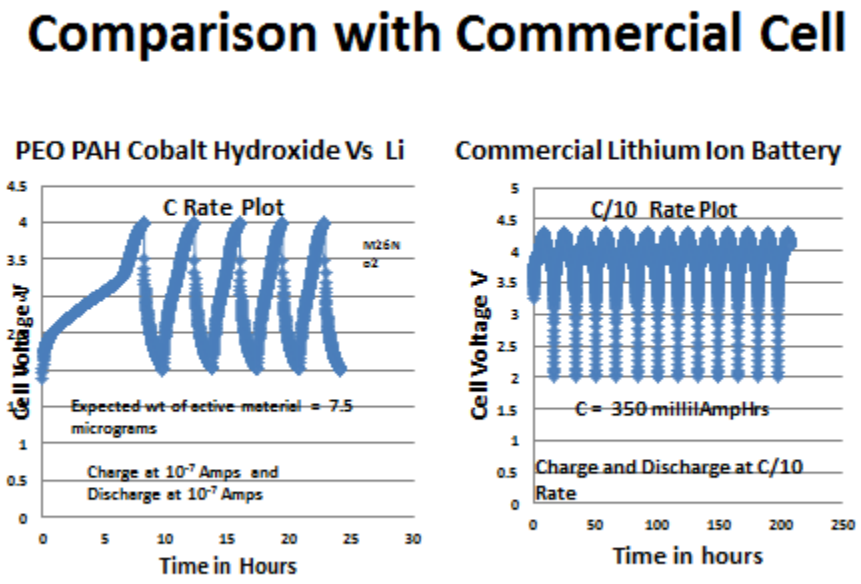

Figure 5.16 Comparison with commercial cell 3

Figure 5.16 compares the cycle life phenomena of a commercial cell to the experimental cell.

Various curves from Figure 5.13 to 5.16 show how batteries with two polymer pairs PAA/PAH and PEO/PAH are performing. Charge discharge at different rates show typical battery responses. Even large number of run cycles with only slight fade is

demonstrated. **This establishes the feasibility of the LbL process for making viable lithium ion batteries**.

5.9 Conclusion on Statistical Analysis

The numbers obtained by the experiments were analyzed statistically [See Appendix B]. Software called the R statistics was used to calculate the mean expected value of specific capacity. Non parametric statistics was applied to determine the type of distributions of capacity and mass. This approach is independent of the distribution and gives results by a non- parametric analysis.

The results obtained give an accurate value of the expected specific capacity. Using this approach we get the mean values of mass, capacity and specific capacity. Along with capacitance determined by CV we are able to estimate the true specific capacity to be 110 mAhrs/ gm which falls in the region of the expected value, 137 mAhrs/ gm. A 54 mAhs/gm of capacitive contribution is found which accounts for approximately 30 % of the specific capacity.

5.10 Summary of the Research

We have shown how using polymer films, a high performance lithium ion battery is made. Nano particles are deposited within the films and later treated. Thus we were able to produce a LbL cathode, which demonstrates a very high efficiency, high specific capacity and possibly high capacitance. The capacitor in the battery contributes to coulombs or additional current especially at the very high rates. This is all due to the pretreatment done to the electrode prior to constructing the battery. Hence we show that the pretreatment is crucial to developing an electrode showing high capacity and high rate capability. It holds promise of very high energy density and very high power density co-existing in one device. It heralds the beginning of a very important area of investigation and also a direction for future efforts.

It also expands the application of materials and techniques to other areas of electrochemistry. For instance the electronically conducting CoOOH can be used in other non- aqueous electrochemical systems for sensors, catalytic and energy producing

devices, including lithium ion cathodes of mixed oxides ($LiNi1_{/3}Mn_{1/3}Co_{1/3}$ O_2, etc.) and $LiFePO_4$. The in situ method of production of nanoparticles of lithium cobalt oxide can be extended to other lithium cathode systems and other places for deposition of nano particles. Appearance of capacitive contribution to capacity by nano particles can be useful in all areas of energy production. It may very well double or triple energy and power densities in various battery systems made with the LbL process.

5.11 Future Work

The capacitive aspect of the LbL electrode needs a careful inquiry in much greater detail. A very large run with hundreds of electrodes made by the LbL process and treated to produce the $LiCoO_2$ and CoOOH should be done**.** Through this work we intend to answer three questions:

(1) What is the origin of the capacitance and how much is its magnitude?

(2) At 100 times higher rate of charge and discharge how much is the 10^{-5} Amp capacity greater than that of 10^{-7} Amp capacity? Why is it larger?

(3) What is the particle size of the $LiCoO_2$ and CoOOH?

As a follow up the following can be done:

1) Examine Functionalized Graphite LbL cathode with active materials
   It will be interesting to realize the impact of putting $LiCoO_2$ and CoOOH within the layers of functionalized Graphite LbL electrodes. The expectations is the large improvement of power and energy density in one device
2) All LbL Cell: Anode and Cathode both made by LbL method
   How will an all LbL Cell work?
3) Finally a battery may be found that produces both very high Energy and Power densities. Attempts can then be made to increase $LiCoO_2$ loading.

Appendices

Appendix A

Mass and Specific Capacity Determinations

A.1 Introduction

We want to determine the weight of $LiCoO_2$ formed within the film. This determination becomes difficult as there is no standard method available. The weight is in the micro gram range. The ICP method can determine very small quantities of ions in solution. If we dissolve all that is in the film, we can measure a specific metal present like lithium or cobalt. The total amount of any metal ion can be ascertained by ICP. For instance total cobalt determination can be done on the electrode surface. This cobalt later converts to the chemicals-$LiCoO_2$,CoOOH and $Co(OH)_2$. XRD can then determine the presence and their relative proportion. Finding these, we can determine the weight of $LiCoO_2$ present on an electrode. We have performed these measurements and have determined the weight of $LiCoO_2$. Here in we describe in detail the technique used.

A.2 XRD: Background information [1]

It has been known that diffraction, as of visible light, by a ruled grating occurs whenever wave motion encounters a set of regularly spaced scattering objects, provided that the wave length of motion is of the same order of magnitude as the repeat distance between the scatting centers. Crystals or atoms are 1 to 2 Angstroms apart. X-rays are also 1-2 Angstroms in wavelength. Hence X-rays can diffract when passing through periodic lattice arrangements of crystals.

Diffraction is essentially due to certain phase differences between two or more waves. The differences of path length travelled by X-rays before and after diffraction lead to differences of phases. The introduction of phase differences produces a change in amplitude. Two rays that are completely in phase whenever their path lengths differ

either by zero or by a whole number of wavelengths are additive in intensity. Diffraction itself is essentially a scattering phenomenon. A diffracted beam may be defined as a beam composed of a large number of scattered rays mutually reinforcing one another.

Braggs Law

$$2d\text{Sin}\Theta = n\lambda$$

It states the essential conditions that must be met if diffraction is to occur. The integer n is called the order of reflection; it may take integral values consistent with sin$\boldsymbol{\Theta}$ not exceeding unity and is equal to the number of wavelengths in the path difference between rays scattered by adjacent planes. The rays scattered from planes with n=1, 2, 3, 4, and in agreement with Braggs Law are completely in phase and reinforce one another. This is constructive interference and rays form a diffracted beam in one direction. The diffracted beam is rather strong compared with the sum of all the rays scattered, in the same direction, simply because of the reinforcement that occurs. The diffracted beam is extremely weak compared to the incident beam since the atoms in the crystal scatter only a small fraction of the energy incident on them. It is worthwhile to remember the incident beam, the normal to the reflecting plane and the diffracted beam are always coplanar. The angle between the diffracted beam and the transmitted beam is 2$\boldsymbol{\Theta}$**.** This is known as the diffraction angle, and it is this angle, rather than $\boldsymbol{\Theta}$, which is usually measured experimentally.

A.2.1 Quantitative Analysis for Multiphase Case using XRD

Quantitative analysis by diffraction is based on the fact that the intensity of the diffraction pattern of a particular phase in a mixture of phases depends on the concentration of that phase in the mixture. The relationship between intensity and concentration is not generally linear, because the diffracted intensity depends markedly on the absorption coefficient of the mixture and this itself varies with concentration.

To find the relationship between diffracted intensity and concentration, we must use the basic equation of intensity diffracted by a powder specimen. The exact expression for intensity of a diffracted beam by a single phase powder specimen in a diffractometer is

$$I = \left(\frac{I_0 A \lambda^3}{32\pi r}\right)\left[\left(\frac{\mu_0}{4\pi}\right)^2 \frac{e^4}{m^2}\right]\left(\frac{1}{v^2}\right)\left[|F|^2 p \left(\frac{1 + \cos^2 2\theta}{\sin^2 \theta \cos \theta}\right)\right]\left(\frac{e^{-2M}}{2\mu}\right).$$

We can simplify this equation considerably for special cases. As it stands it applies only to a pure substance. But suppose we wish to analyze a mixture of two phases α and β. Then we can concentrate on a particular line of the α phase and rewrite in terms of that phase alone. The intensity, I now becomes I_α, the intensity of the selected line of the alpha phase. The right side of the equation must be multiplied by C_α the volume fraction of alpha in the mixture; to allow for the fact that the diffracting volume of alpha in the mixture is what it would be if the specimen were pure alpha. Finally we must substitute μ_m in place μ where μ_m is the linear absorption coefficient of the mixture. In this case all factors are constant and independent of concentration of alpha except C_α and μ_m.
We can write

$$\mathbf{I_\alpha = K_1 C_\alpha / \mu_m}$$

K_1 is a constant. The value of K_1 is unknown because I_0 is generally unknown. However K_1 will cancel out if we measure **the ratio of I_α to the intensity of some standard reference line.** The concentration of α can be found from this ratio.

There are three main methods of analysis that differ in what is used as a reference line: (1) External Standard Method (a line from pure α), (2) Direct Comparison Method (a line from another phase in the mixture), and (3) Internal standard method (a line from a foreign material mixed with specimen)

We will experimentally determine values using the Direct Comparison Method.

A.3 ICP: Background [2]

This is a technique used to accurately determine the concentrations of different metal ions in a given solution. We are interested in determining the cobalt ion concentration in a solution containing the Co^+ that has been prepared by dissolving all cobalt in a group of electrodes in nitric acid. The cobalt in the plate can come from 3 different sources, $Co(OH)_2$, $LiCoO_2$, and CoOOH. The ICP can give an accurate estimate of the total

cobalt on the electrode body. Using this number and knowing the proportions of the 3 compounds, we can find the weight of $LiCoO_2$ present in an electrode.

A.3.1 Operation of the ICP for the determination of metal ions concentration in solution

Procedure:

A.3.1.1 Introduction

Inductively Coupled Plasma Optical Emission Spectrometry (ICP-OES) is a type of emission spectroscopy that uses plasma (i.e. inductively coupled plasma) to produce excited atoms that emit electromagnetic radiation at a wavelength characteristic of a particular element. The intensity of this emission is indicative of the concentration of the element within the sample. This technique is also referred to as ICP-AES (Inductively coupled plasma atomic emission spectroscopy).

The following procedure will describe the process of preparing the sample, making the standards, and running the ICP instrument.

A.3.1.2 Securing Materials

In order to run the ICP, we will need several materials, which are listed in Table A1.

Table A.1 Materials for running the ICP

Materials
Argon - Refrigerated Liquid “210”
Distilled Water (1 gal)
Metal Standard Solutions
Aqua Regia
Plastic Test Tubes
50 mL Tubes
Test Tube Rack
Standard Solution Rack

The metal standard solutions are located under the hood in the Dow lab. We currently have standards for the following metals: Pt, Pd, Cu, Ni, Co, Li ,Fe, Sn, C, Mo, Ru, Zn, Au, Ti, Al, S, and W.

Dissolve the sample in aqua regia if it isn't water-soluble or a liquid already. Aqua regia is a mixture of one part nitric acid to three parts hydrochloric acid. Use the concentrated acid solutions found in the acid cabinet under the hood. The standard solutions should be prepared in big 50 mL test tubes, found in a cabinet under a bench (the ones with the orange caps).

A.3.1.3 Sample Preparation

For each sample that we are going to run, we need about 30 mg of material. Figure 1 shows the scheme. Weigh out 15 mg of material into two plastic test tubes. We recommend weighing the empty tube, the sample by itself, and the sample in the test tube as a check.

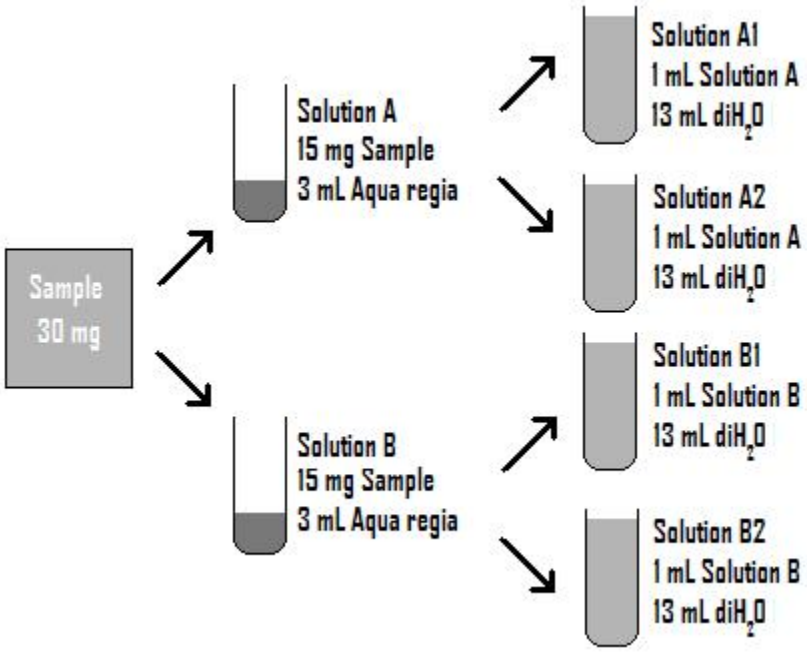

Figure A.1 ICP Dilution Scheme

Next, we need to dissolve the sample. The aqua regia reacts to form chlorine gas, which is toxic, so let the sample sit in the hood and dissolve overnight. The next day, we need to dilute the sample solution in deionized water, one mL sample solution in 13 mL diH_2O. For each sample four test tubes are needed. That is, we dissolve 15 mg of sample in two test tubes, and from each of those tubes we will make two dilutions - so four replicates in all. This takes extra work, but it will really help with your statistical analysis. First, use the 5 mL micropipette to add 13 mL diH_2O to each test tube. Next, use the 1 mL micropipette to add 1 mL of sample solution to the appropriate tube. When finished, cover all the tubes with parafilm to prevent evaporation.

A.3.1.4 Making the Standards

In order to quantitatively measure the amount of a certain element in our sample, the ICP needs to have a reference to compare the sample against. This section describes the process for preparing the reference standards for our run.

First we need to estimate the concentrations of the different elements in our sample, and then we need to determine the concentrations of our standard solutions. Prepare six tubes: one blank, and five standards of varying concentrations.

Suppose that we have a catalyst which contains 4 weight percent platinum supported on molybdenum carbide (4% Pt/Mo_2C). We estimate the concentration of platinum in the diluted solution as follows:

Table A.2 Calculation of concentration

Catalyst (mg)	Wt% Pt	Mass Pt (mg)	Diluted Concentration (mg/L)
15.00	4.00	0.60	14.29

Now we design the six standard solutions to encompass a range of concentrations within which lies the estimated Diluted Concentration. The first tube is pure dilute H_2O. The next five tubes cover a range of concentrations.

Table A.3 Concentrations in standard solutions

Standard Tube #	0	1	2	3	4	5
Percent of Estimated Concentration	0%	33%	66%	100%	133%	166%
Pt Concentration (mg/L)	0.00	4.76	9.52	14.29	19.05	23.81

A.4 Calculation of Specific Capacity

The estimated weight of active material is needed before these calculations can be done. The expected weight of the active material is in the low microgram range. Its determination presents a special challenge. We have adopted and modified a process wherein ICP (Inductive Coupled Plasma) and X-Ray diffraction are used together. The ICP determines the total cobalt content on the electrode and the XRD the proportion of cobalt in the materials, as weight % $LiCoO_2$. Thus the ICP and XRD do the following:

(1) ICP Test
This test is done by dissolving 20 samples of the electrode in dilute nitric acid (25%) and later running the instrument to detect the quantity of Co on the electrode.

(2) XRD Test
80 electrodes are used by scraping off material from them. The XRD plot identifies the phases present and their relative amounts.

When the two tests are performed on the electrode material, the amount and proportion of $LiCoO_2$ is determined. $LiCoO_2$ is the battery active material.

Experimental Determination of Active Material Mass (ICP)

The amount of $LiCoO_2$ on the film after the electrochemical treatment is a critical parameter to be determined accurately. The strategy used first was to determine the amount of total lithium on the electrode by ICP. It was tried but reliable values were not obtained. The treatment is done in a solution containing lithium. Excess unconverted lithium is left behind. This is hard to remove by any method which will not also remove the $LiCoO_2$ on the film.

Determining Li^+ did not work. Another approach is to determine the total cobalt content on the electrode. This will pick up cobalt from three possible sources, namely $LiCoO_2$,

CoOOH and $Co(OH)_2$. If we can determine the proportion of the three compounds then weights can be assigned to each one of them. That XRD is capable of doing.

The table below shows the calculations of the total weight of cobalt on the film. 20 electrodes were dissolved in a known volume of dilute nitric acid. The ICP procedure gives the details of how the test was conducted. The value of total cobalt is shown in the Table A.4

Table A.4 Calculation of weight of $LiCoO_2$

Item	**Calculation**	**Total**	**unit**
Total volume of test solution	**15**	**15**	**cc**
ICP determined concentration	**15.23**	**15.23**	**µg/cc**
Cobalt wt of 20 electrode	**15.23x15**	**228.45**	**µg**
Cobalt wt of 1 electrode	**228.45 / 20**	**11.43**	**µg**
Wt of L*iCoO_2 assuming only $LiCoO_2$ is produced	**11.43*98/59**	**18.98**	**µg**
Wt of $Co(OH)_2$ assuming only $Co(OH)_2$ is produced	**18.98*93/98**	**18.01**	**µg**
At 19% $LiCoO_2$ Conversion	**18.98*0.19**	**3.61**	**µg**
At 25% $LiCoO_2$ Conversion	**18.98*0.25**	**4.75**	**µg**
At 32% $LiCoO_2$ Conversion	**18.98*0.32**	**6.07**	**µg**

The conversion proportion is obtained from X-Ray diffraction by taking the most likely fit value which is 75/25 where 25% relates to the $LiCoO_2$ conversion. This determination is described below.

X-Ray adapted to get weight of phases in a mixture: Basis

In here we outline the principle behind the determination of relative weights of phases in a mixture containing $LiCoO_2$, $Co(OH)_2$ and CoOOH.

1) Line Intensity is: $$I = \left(\frac{I_0 A \lambda^3}{32\pi r}\right)\left[\left(\frac{\mu_0}{4\pi}\right)^2 \frac{e^4}{m^2}\right]\left(\frac{1}{v^2}\right)\left[|F|^2 p \left(\frac{1+\cos^2 2\theta}{\sin^2\theta\cos\theta}\right)\right]\left(\frac{e^{-2M}}{2\mu}\right).$$

2) Intensity of a diffraction line $I = km/\mu$ where μ is the mass absorption coefficient, k is a machine related constant and m is mass.

3) Intensity ratio in a mixture is the ratio of masses present: $I_1 / I_2 = m_1 / m_2$

4) Representative intensity is the weighted sum of the available peaks: $I_j = \Sigma w_i I_{ij}$ and $I_r = \Sigma w_h I_{hr}$ summed over i= 1 and h=1 to n_1 and n_2 respectively where n_1 and n_2 are the number of related peaks

5) W_i and W_h are the corresponding weights

6) Unfortunately no quantitative instructions can be given and weighting is largely based on heuristic judgments

7) Greater weightage should be given to the well resolved and strong peaks less susceptible to preferred orientation and to fluctuations in the number of reflecting crystallites.

8) To simplify, putting w_j and $w_h = 1$ we have $I_j = \Sigma w_i I_{ij}$ and $I_r = \Sigma w_h I_{hr}$ becoming : $I_j = \Sigma I_{ij}$ and $I_r = \Sigma I_{hr}$

9) Individual intensity lines can be summed for each phase separately.

10) A ratio of intensity lines of two phases will be in the ratio of their masses present in the X-Ray samples

11) Thus $\Sigma I_{Co(OH)2} / \Sigma I_{LiCoO2} = mass_{Co(OH)2} / mass_{LiCoO2}$

    Using the above procedure we will sum up the intensities of different phases. The ratio of the sums will give the ratio of their masses.

A.4.1 Details of XRD Calculations

From the XRD pictures we have to determine the best fit and then using ICP values get the proportion of various chemicals seen. The first XRD pattern is taken and intensities belonging to a particular phase are summed up. This can be done manually from the plot or the computer software can perform this task. We used the Jade software to give proportions of various compounds seen in the XRD plot. Multiple answers will be seen because there are many possibilities of the pattern chosen from the data bank. For instance $LiCoO_2$ has at least 10 or more possibilities. So does $Co(OH)_2$ and CoOOH. There are several possible combinations of the three compounds. This results in many possibilities. An analysis of deviations of lines from standard is performed. This gives the most likely fits which show the least deviation. Examples are provided below. In Figure A2. XRD is the run showing all possible fits for the compounds observed. Note that the $Co(OH)_2$ shows a large presence, followed by $LiCoO_2$. The presence of CoOOH is small and can be excluded without any loss in accuracy. Hence we will try to find the proportion of $LiCoO_2$ and $Co(OH)_2$.

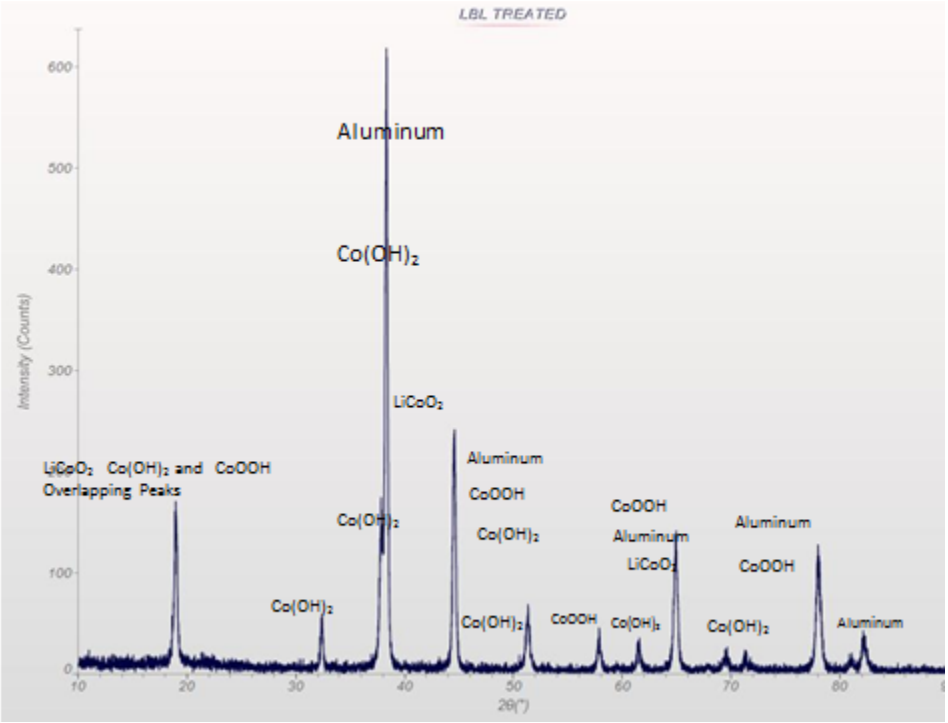

Figure A.2 Map of phases detected by intensity lines

The following three XRDs Figures A.3-5 show the proportions of $LiCoO_2$ and $Co(OH)_2$

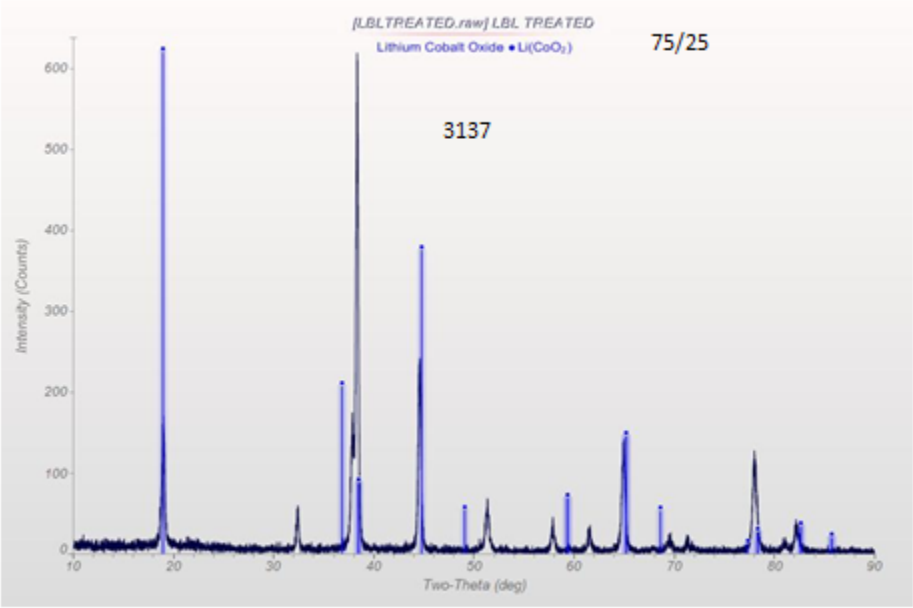

Figure A.3 XRD of 75/25 distribution of $LiCoO_2$ and $Co(OH)_2$

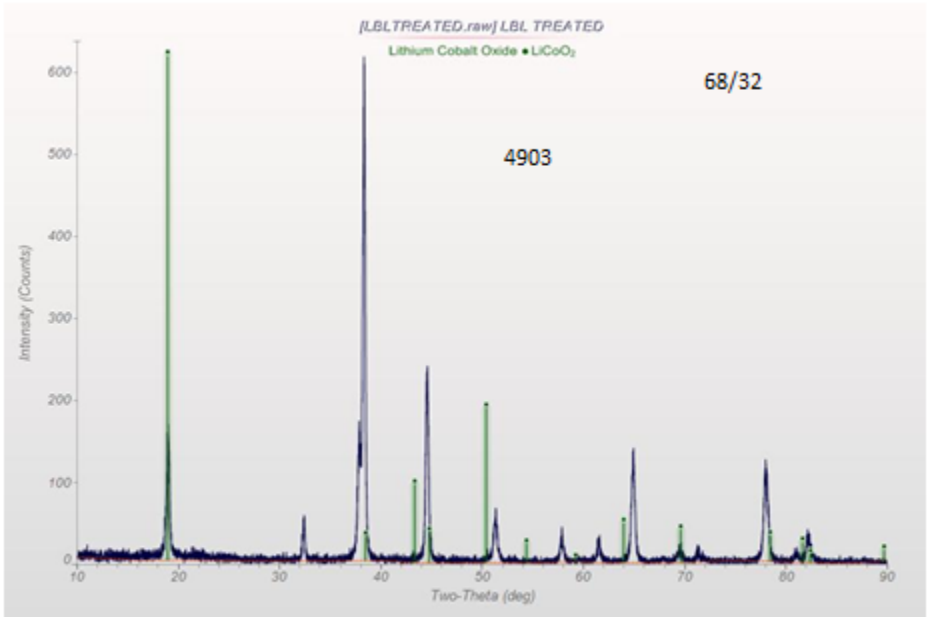

Figure A.4 XRD of 68/32 distribution of $LiCoO_2$ and $Co(OH)_2$

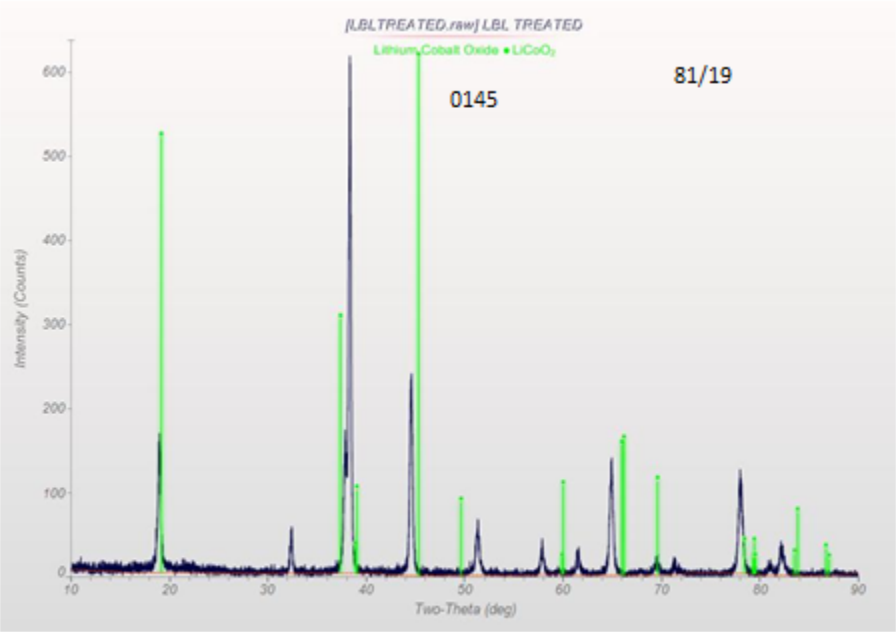

Figure A.5 XRD of 81/19 distribution of $LiCoO_2$ and $Co(OH)_2$

Once we find the possible proportions we have to select the best fit. This is done by estimating deviations as in Table A5. The one with the least deviation is the best fit.

Table A.5 Error Estimation: XRD.
Based on 4 most intense lines.

$LiCoO_2$ %	**Deviation verses $LiCoO_2$**	**Deviation verses $Co(OH)_2$**	**Rank**
32	**6.17**	**0.5**	**3**
25	**3.5**	**0.2**	**1 (Best)**
19	**4.5**	**1.3**	**2**

From the above we see that 25% $LiCoO_2$ showing the least error will be adopted.

A.4.1.1 Statistical Calculations: Expected values of Capacity, Weight and Specific Capacity

The definition of expected value of a discrete random variable is given below. Expected value of x is $E(x) = \sum xp(x)$ where x is the variable and p(x) is its probability density function. This is one of the most important concepts in probability theory. When the probability of x is all equal, E(x) simplifies to the arithmetic mean. The variability of x is given by σ the standard deviation. It denotes the variation of x at a confidence level of 68% when $\sigma = 1$ and 95% when $\sigma = 2$. The square root of variance is equal to σ.
We have the values of x for capacity and mass. With these, we will run a simulation using R, common statistical software.
The equation E (Specific Capacity) = E (Capacity) / E (Mass) is used with the following assumptions:

1) Factors affecting Capacity: (1)Processing Conditions (2)Mechanical Fit (3) Electrochemical conditions
2) Factors affecting Mass: (1) ICP Test Variation (2) ICP Solution Variations (3) XRD Proportion Variations
3) Capacity and mass are treated independent of each other i.e. the covariance between them is zero.

Table A6 below gives the probability of x as observed in the experiment. A manual determination is done. The histogram figure shows independently the results of the simulation. The two results are very closely matched.

Data analysis

Statistical program called R has been used to analyze the data. To calculate the expected value of capacity, 10 data points of cells actually run have been included. For mass determination it has been assumed that the best fit obtained using Jade software in X-Ray Diffraction is the applicable one. The best fit was obtained for the 25% $LiCoO_2$ group. The ICP test was run with 8 samples at 10 different wave lengths. Only the 3 most likely wave lengths were used in calculations. These are: (1) 238.892 nm (2) 230.786 nm (3) 237.863 nm . Expected value of mass is run with a sample size of 24.

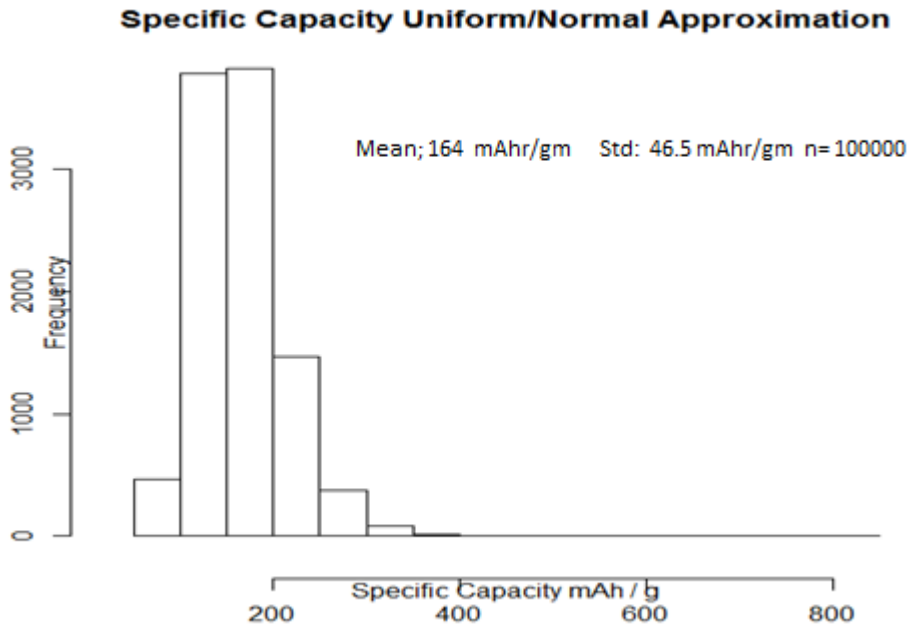

Figure A.6 Histogram showing mean and standard deviation of specific capacity

Table A.6 Expected Values Calculations

		Mass		
	x	p	xp	E(Mass) Sum (xp)
Mean + sigma	5.56	0.12	0.67	
Mean	4.75	0.81	3.85	4.84 µg
Mean - sigma	3.94	0.08	0.32	
		Capacity		
	x	p	xp	E(Capacity) Sum (xp)
Mean + sigma	10	0.16	1.6	
Mean	7.5	0.8	6	7.8x10-7 Ahrs
Mean - sigma	5	0.04	0.2	

Table A7 has been developed on the assumption that the proportion of $Co(OH)_2$/ LiCoO2 is 75 / 25 by weight. It calculates expected mass and expected capacity. Then taking the ratio E (Specific Capacity) = E (Capacity) / E (Mass) obtained from Table A.6, it finally calculates the expected specific capacity. That works out to be 4.84 µg / 7.8x10-7 Ahrs = 161 mAhr / gm which is very close to 164 mAhr / gm obtained by the simulation and shown in the histogram of Figure A.6.

A summary of the results are given in the Table A.7 . It gives at a glance all the calculated results.

Table A.7 Summary table

Category	Value	Units
Mass	4.74 ± 0.81	µg
Capacity	7.5 ± 2.5	$X10^{-7}$ Ahrs
Specific Capacity	164 ± 46.5	mAhrs / gm
Capacitive Contribution from CV	54	mAhrs / gm
Final Specific Capacity	110	mAhrs / gm

There is a capacitance contribution to capacity. This has been added to the Table A.7 above. The battery has two sources of energy. One comes from the active material, $LiCoO_2$ and the other is supercapacitor effect. This additional energy comes from a change of charge with respect to voltage which also is defined as the supercapacitor effect. It manifests itself when dimensions of particles approach nano sizes. It is determined as explained below.

Run a CV of untreated LbL cathode vs. lithium and a reference (Pt). **The untreated electrode used has only $Co(OH)_2$ and no $LiCoO_2$.** The generated graph provides the capacitance value of the $Co(OH)_2$. Several cycles were run, 50 to be exact. The last 50 mV scan is used for capacitance calculations. Other scan rates were tried and produced similar results.

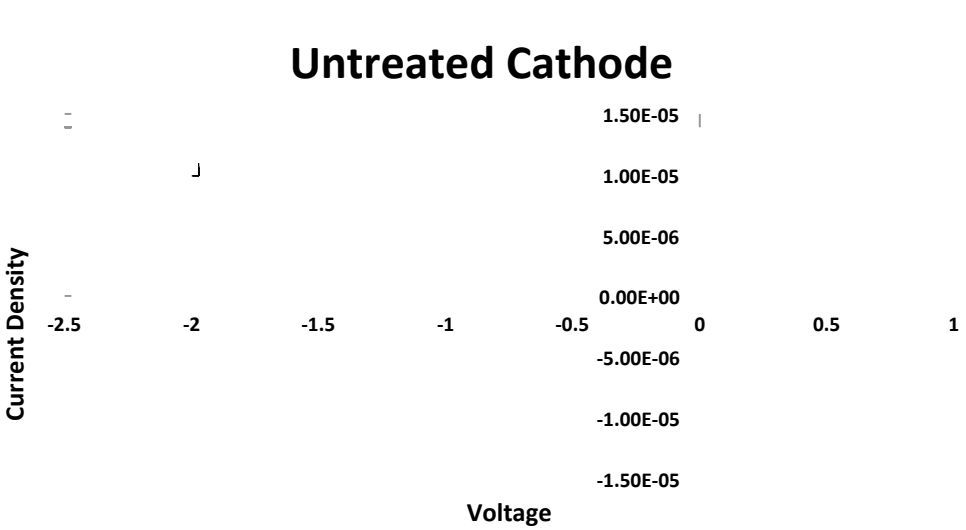

Figure A.7 Voltammogram showing capacitance from the untreated LbL electrode. This value works out to be 54mAhr/g.

The area of the curve in A.7 has been obtained from a program that integrates small elemental rectangles of a voltage step x current. The Area / (scan rate x voltage window of CV x mass) gives the charge Q. Finally mAhrs / gm is obtained by (Q/Sec) x3600/mass of $Co(OH)_2$ .This gives the contribution of the LbL film and cobalt hydroxide towards capacitance. **Note the film has not been through the electrochemical treatment and does not have any $LiCoO_2$.** All capacitance obtained is from fast redox reaction and not from the redox activity of the active chemical, $LiCoO_2$. Approximately 30% of the total capacity observed came from pseudo capacitance or supercapacitance.

Errors

By comparing the XRD experimental values to those obtained from the Jade software the best fit is the 25% $LiCoO_2$ proportion amount. But there are errors in finding this fit. In addition to these effects, there are other errors possible as explained below. These determine the variations depicted by the standard deviation values.

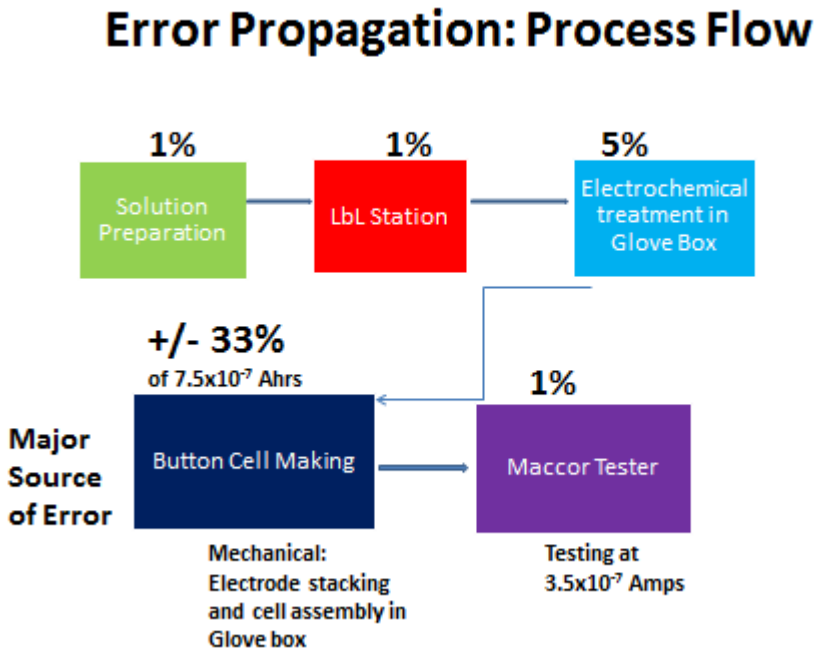

Figure A.8 Variation in the process of electrode making

As seen in Figure A.8 there are small errors that are introduced at various steps of the process. Major variation occurs during cell assembly. This is taken into account in the Statistical Analysis performed

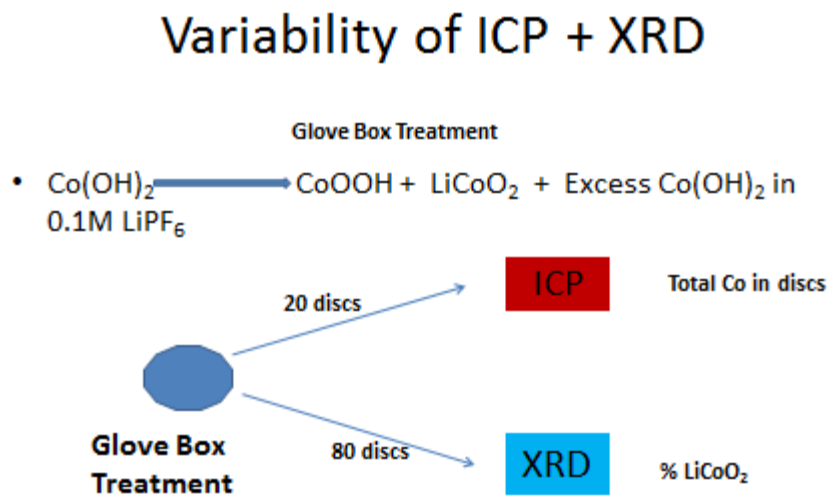

Figure A.9 Electrodes required for the test

The above Figure A.9 is a flow diagram and explains the process and the requirement of samples.

References

1) Quantitative X-Ray Diffractometer by Lev S Zevin and Giora Kimmel pg 137-139.

2) ICP Standard Operating Procedure

Appendix B

Statistical Analysis

The data accumulated throughout the work was analyzed. The Statistical Analysis uses 24 data points from ICP test. Using the expected values of mass and capacity it calculates mean mass of the $LiCoO_2$ on one electrode and variations.

B.1.1 Some definitions in statistics [1,2]

In order to reduce a mass of data to an understandable form which can be grasped, a frequency table has to be constructed. This gives a frequency histogram or curve. It is useful to simplify the presentation further by defining certain measures which describe important features of the distribution.

Definition: Any measure indicating a center of distribution is called *a measure of central tendency***.**

Definition: A numerical value indicating the amount of scatter about a central point is called a *measure of dispersion.*

Measures of central tendency

The Mean (or Arithmetic Mean)

Definition: For a set of N numbers $X_1, X_2, \ldots\ldots X_N$ the mean or arithmetic mean is defined as

$M = (X_1+X_2+\ldots\ldots X_N)/N = \sum X_i / N$

Example: Find the mean for the numbers 11, 14, 17, 20, 16, 10

$$m = (11+14+17+20+16+10) / 6 = 14.67$$

It will be observed that the arithmetic mean is what is frequently called the average. However the term "average" is also used for other measures of central tendency.
If the data are presented in a frequency table, we do not know the exact value of the variates but only the classes in which they lie. However it seems reasonable to assume that the data within a class are uniformly distributed about the class middle point, so for the purposes of calculating the mean we shall assume that all data within a class actually occur at the midpoint, which results in the following definition.

Definition:

If a frequency table has h classes and the class middle points are $X_1, X_2 \ldots\ldots X_h$ and the respective frequencies are $f_1, f_2, \ldots f_h$ then the mean is defined as

$$m = X_1f_1+X_2f_2+\ldots\ldots\ldots X_hf_h / f_1+f_2+\ldots..f_h = \sum X_if_i / \sum f_i$$

Theorem

If a set of N_1 variates has a mean m_1 and another set N_2 has mean m_2 then the mean of the set of N_1+N_2 variates obtained by combining these two sets is given by

$m = m_1N_1+m_2N_2 / N_1+N_2$. This can be generalizes d to the case of combining more than two sets of data.

Example:

A class is divided into two sections, both of which are given the same test. Section1 (41 students) has a mean score of 62 and sect ion 2 (52 students) has a mean score of 58. Find the mean of the whole class.

Since $N_1 = 41$ $m_1 = 62$; $N_2 = 52$ $m_2 = 68$

We find $m = 69(41)+68(52) / 93 = 65.35$

The Median

The median of a set of N numbers arranged in order of ascending or descending magnitude is the middle number of the set if N is odd, and the mean of the two middle numbers if N is even.

The Mode

The class or classes for which the frequency is the greatest is called the modal class (or modal classes)

The geometric mean

For a set of N non negative numbers X1, X_2, …….X_N the geometric mean is defined as $Ma = [X_1.X_2.X_3……X_N]^{1/N}$ It is convenient to express it in logarithmic form. It is applied to data for which the ratio of any two consecutive numbers is either constant or nearly constant. This occurs for example in data representing the size of a population at consecutive time intervals or the value of a sum of money which is increasing at a compounding rate.

The harmonic mean

This is another measure of central tendency.

Definition:

For a set of N numbers $X_1,X_2……X_N$ the harmonic mean denoted by M_h is defined as

$M_h = N / (1/X_1+1/X_2+ ……..X_3) = N/\sum 1/X_i$

Relative Merits of Mean, Median and Mode

The most frequently used measure of central tendency is the arithmetic mean. It is easy to compute, easy to define, takes all measurements into consideration, and is well designed for algebraic manipulations. From the arithmetic means of different sets of data, the mean of the combined group can easily be calculated. One of the chief advantages of the mean is its reliability in sampling. If we regard a set of data as being a sample from the same population, the means of two samples will in general show closer agreement than will two medians, i.e. ., generally speaking the mean is more stable than the median. For these reasons the mean is the most widely used measure of central tendency in statistics.

The median, although not easy to calculate and easy to define, is not influenced by extreme measurements, which for certain circumstances may prove to be advantageous. In economic statistics it is often desirable to disregard extreme variates, which may be due to unusual circumstances. The median is particularly useful when the magnitude of the extreme data is not given, but when their number is known. In this case the mean cannot be calculated.

The mode is even less important than the median because of its ambiguity. It is possible that two non-adjacent classes will have the same maximum frequency, thereby yielding two modal values, which may be purely accidental because of the particular choice of the class interval. On the other hand the mode like the median, is easy to understand and is not greatly influenced by extreme cases.

Measures of dispersion

Although the arithmetic mean is a satisfactory measure of central tendency, it does not in itself give a clear picture of a set of variates or their distribution. We need therefore some measure of their spread or dispersion of a set of variates about their mean. The first measure of that might occur to us is the difference between their largest and their smallest value. This is known as the range.

Definition: For a set of numbers the range is the difference between the largest and the smallest numbers. Although the range does give some indication of the spread of the data about the mean, it depends solely on the extreme values, which may be purely accidental, and tells us nothing about the distribute ion of the variates between these two extremes or the concentration of the variates about the center.

A second measure which immediately suggests itself is the sum of the deviations in a set of variates from their mean. Since for the purposes of describing this dispersion it is immaterial whether a variate is at a certain distance above or below the mean, the sign of the deviation can be ignored. The average of deviations, all taken as positive, therefore measures the dispersion of the data about the mean, is called the *mean deviation*. Its definition involves the concept of absolute value.

Definition:

For a set of N numbers, $X_1, X_2, X_3, \ldots\ldots X_N$ whose mean is m, the mean deviation denoted by M.D. is defined as

$$\text{M.D.} = \sum' (X_i - m) / N$$

More accurately this measure should be called the mean absolute deviation.

The Variance or the Standard Deviation

A method of converting positive and negative quantities, which are all positive, is the process of squaring. The average of the squared deviation from the mean, called the *variance* is used as a measure of dispersion.

Definition:

For a set of N numbers, $X_1, X_2, X_3, \ldots\ldots X_N$ whose mean is m, the variance is denoted by σ^2 is defined as

$$\sigma^2 = \sum(X_i - m)^2 / N$$

Variance is a widely used measure of dispersion in statistic al analysis. It is expressed in units which are squares of the original units. For many pure purposes it is desirable that a measure of dispersion be expressed in the same units as the original variates and their mean. Such a measure of dispersion is the standard deviation, which is obtained by taking the square root of the variance.

Definition: The square root of the variance is called the standard deviation and is defined as

$$\sigma = [\sum(X_i - m)^2 / N]^{1/2}$$

It is not as easy to grasp the meaning of standard deviation in comparison to the mean deviation, since the standard deviation is not the mean of a set of deviations. On the other hand, the standard deviation has the very remarkable property that in many frequency distributions, in so called normal distribution, approximately two thirds of the variates fall in between $m - \sigma$ and $m + \sigma$. The variance and the standard deviation have all the advantages of the mean deviation, and in addition are suitable for algebraic work. The variance and the standard deviation are therefore by far the most frequently used measure of dispersion.

Expected value[2]

One of the most important concepts in probability theory is that of expectations of a random variable. If X is a discrete random variable having a probability mass function p(x) the expectation or expected value of x is denoted by E(X) , is defined by

$$E(X) = \sum xp(x)$$

In other words the expected value of X is a weighted average of possible values that X can take on, each being weighted by the probability that X assumes it. For instance if the probability mass function of X is given by $p(0) = ½ = p(1)$

$E(X) = 0(1/2) + 1(1/2) = ½$ is just the ordinary average of the two possible values 0 and 1 that X can assume. On the other hand, if $p(0) = 1/3$ and $p(1) = 2/3$

Then E(X) = 0(1/3) + 1(2/3) = 2/3 is a weighted average of the two possible values 0 and 1 , where the value 1 is given twice as much weight as the value 0, since p(1) = 2p(0) The concept of expectation is analogous to the physical concept of the center of gravity of a distribution of mass. When in an experiment X is the outcome with all X values being equally probable, then the expected value of X is the arithmetic mean.

Let X = 1,2,3,4,5 with p(1) = p(2) =p(3) =p(4) p(5) = 0.2
E(X) = 1(0.2)+2(0.2)+3(0.2)+4(0.2)+5(0.2) = (1+2+3+4+5)0.2 = 1+2+3+4+5 /5 = arithmetic mean

Variance

Given a random variable X with its distribution function F, it will be extremely useful if we were able to summarize the essential properties of F by certain suitably defined measures. One such measure would be E(X), The expected value of X. However although E(X) yields the same weighted average of possible values of X, it does not tell us anything about the variation, or spread, of these values. As we expect X to take on values around its mean E(X) it would appear that a reasonable way of measuring the possible variations of X would be to look at how far X would be from its mean on the average. One possible way to measure this would be to consider the quantity E(X-m) where m = E(X). However this turn out to be mathematically inconvenient. We therefore use a more tractable quantity, namely the expectation of the square of the difference between X and its mean.

Definition: The variance of X is defined as Var (X) = E[$(X-m)^2$]
It turns out that Var (X) = E[$X]^2$ –($E[X])^2$

Covariance, variance of sums, and correlations

Propositions: (1) The expectation of a product of independent random variables is equal to the product of their expectations
E[g(X)h(Y)] = E[g(X)]E[h(Y)]
Propositions: (2) The covariance between X and Y, denoted by Cov(X,Y) is defined by
Cov(X,Y) = E[(X- E[X])(Y- E[Y])]
Propositions: (3)

- $\mathrm{Cov}(X, Y) = \mathrm{Cov}(Y, X)$
- $\mathrm{Cov}(X, X) = \mathrm{Var}(X)\ \mathrm{Cov}(aX, Y) = a\,\mathrm{Cov}(X, Y)$
- $\mathrm{Cov}(\sum X_i \sum Y_i) = \sum\sum(\mathrm{Cov}(X_i, Y_i))$

The expected frequency of occurrence of r heads in tossing n coins follows a binomial distribution. If the number of trials n is large the calculations of frequency and probability by means of binomial theorem becomes tedious. There is a more rapid method available. The normal distribution is one of the most important continuous probability distribution. Statistics Theory is based on this. We can instead use this method.

Theorem: In the binomial distribution for N samples of n trials each where the probability of success in a single trial is p, if the value of n is increased, the histogram approaches a curve, called the *normal curve,* whose equation is

$$\text{Frequency of occurrence of } X = Y = N[e^{-(X-m)2/2\sigma 2}]/\sigma(2\pi)^{1/2}$$

The standard normal probability curve is: $y = (e^{-z2/2})/(2\pi)^{1/2}$

Random Sample:

Sampling is one of the most important concepts in the study of statistics. It is basic to statistical theory and to applications of the statistical theory in all fields of physical, biological, and social sciences, in economics, in medicine, in agriculture, and in business and industry. Fundamental ideas of population and samples need to be defined.

Definition: A population (or universe) is the totality of measurements or count obtainable from all objects possessing some common specified characteristics.

In the statistical sense, therefore a population is never a set of objects, but always a set of measurements or counts. A population may consist of finitely or infinitely variates. For example, in a study of size of a particular variety of fruit at some specified stage of development we may be interested only in the fruits on a certain limb of a tree; the sizes of these fruits, then constitutes a population. Or we may wish to study all the fruits on all the trees of a particular orchard; in this case the population consists of the sizes of all the fruits in the orchard. Frequent , we wish to extend the applicability of our conclusion s beyond such finite populations , to encompass ,say, all the fruits in a particular state of development on all such trees, which now exist , or will exist in the future. In this

population the number of measurements of size may be inexhaustible, and this constitutes an infinite population. Since we can rarely investigate a whole population, we are obliged to formulate conclusions regarding a population one of the most important problem in statistical theory or practice. Good estimates concerning a population necessitate good sampling. Securing good samples is not easy, but generally it can be done. A precise definition of a good sample, so called random sample, follows.

Definition: A random sample is a sample in which any one individual measurement in the population is representative of the population

Definition: A biased sample is a sample in which certain individual measurement has a greater chance to be included than others.

Definition: A numerical characteristic of a population, such as its mean or standard deviation, called a population parameter or simply a parameter.

Definition: A quantity calculated from a sample, such as its mean or standard deviation, is called a simple statistics, or simply a statistic.

Non Parametric Statistics

The sample mean satisfies a normal distribution only if the population is normally distributed. In general the distributions of sample statistics depend upon the type of distribution which is satisfied by the population. Since in many cases little or no knowledge is available about the distribution of the population, it becomes desirable to employ methods which make no assumptions regarding the distribution and the parameter of the population.

Definition: Statistical analyses which do not depend upon the knowledge of the distribution and parameters of the population are called *non parametric or distribution free methods*.

In 1945 Frank Wilcoxon proposed a test now referred to as the Wilcoxon 2-sample test which is distinguished both by its simplicity and very excellent results it gives in cases where the distribution is known to be normal. For these reasons the use of non-parametric techniques has become very widespread.

The Wilcoxon Test

Assume that two samples of n_1 and n_2 variates are given and we have to test the hypothesis of equal means. Then the two samples together have $n = n_1 + n_2$ variates. In Wilcox on test, these n variates are graded according to increasing size, that is, we substitute the scores (ranks) 1,2,3,,,,,,n for the actual data. If there is no difference between the sample means, then the total of the ranks corresponding to the first and those corresponding to the second sample should be about the same. If , however, the total of the ranks for one sample is appreciably lower than that of the other, we calculate –under the hypothesis of equal population means- the probability of obtaining by chance alone a sum of ranks less than or equal to that obtained in the given experiment. If this probability is less than the significance level, we reject the hypothesis, otherwise , we accept it.

Wilcoxon test is also possible to use when there are repeat variates. Then an average rank is assigned replacing repeat value ranks. The test can also be applied when the two sample sizes are not the same.

In our experiment we have taken samples of two quantities. To calculate specific capacity, mass and capacity values are required. Experimentally for mass there are 24 points and for capacity 10. These are considered random samples. The following work using statistical simulation using R software is based entirely on the concept of random numbers.

B.1.2 Statistics by Yashvir Prasad

I got help from Mr. Yashvir Prasad in interpreting the data. He suggested that this type of data can only be properly analyzed using non parametric statistics. Statistical analyses which do not depend upon the knowledge of the distribution and parameters of the population are called **non parametric or distribution free methods**.

Regular statistics is founded on the concept of normal or bell shaped outcomes. It is customary to use statistical software like the one used here. Using “R” Statistical package the checks were performed for distribution of capacity and mass data. It was

found that capacity distribution is not a normal distribution. It is called a uniform distribution in statistics.

Data for Capacity and mass

E(Specific Capacity) = E(Capacity) / E(Mass)

```
capacity=c(10.5,6.125,5.25,8.75,7,9.75,12.25,5.25,5.6,5.6)

Mass<-c(21.412,14.3844,13.7994,14.0553,12.9896,
16.4155,13.9165,13.0042,22,14.9869,14.4866,13.7046,17.3632,
14.7879,13.8586,13.8586,21.9363,14.7383,14.1819,14.45,13.3436,
14.2716,14.2716,13.3661)

###Converting the Mass###
Mass<-Mass*(15/20)*(98/59)*.25
```

B.1.2.1 Assumptions

4) Factors affecting Capacity: (1)Processing Conditions (2)Mechanical Fit (3) Electrochemical conditions
5) Factors affecting Mass: (1) ICP Test Variation (2) ICP Solution Variations (3) XRD Proportion Variations
6) Capacity and mass are treated independent of each other i.e. The covariance between them is zero

B.1.2.2 Simulation

7) Calculates using E(Specific Capacity) = E(Capacity) / E(Mass)
8) Uses 10 data points for capacity and 24 data points for mass
9) Run with n= 100,000

B.1.2.3 The Detailed Programming Used

```
######Reading  in the Capacity and Mass Data###################

capacity=c(10.5,6.125,5.25,8.75,7,9.75,12.25,5.25,5.6,5.6)
length(capacity)
Mass<-c(21.412,14.3844,13.7994,14.0553,12.9896,
16.4155,13.9165,13.0042,22,14.9869,14.4866,13.7046,17.3632,
14.7879,13.8586,13.8586,21.9363,14.7383,14.1819,14.45,13.3436,
14.2716,14.2716,13.3661)

###Converting the Mass###
Mass<-Mass*(15/20)*(98/59)*.25

###############Calculating the Mean and Std. Dev. of Capacity and Mass Data#########

hist(capacity, type='l')
summary(capacity)
SDcap<-sd(capacity)
MeanCap<-mean(capacity)

hist(Mass)
summary(Mass)
SDmass<-sd(Mass)
Meanmass<-mean(Mass)

###############Run Diagnostics to check if a Normal Distribution Would Work for mass, and uniform for Capacity#######
probplot(capacity,qdist=qunif,xlab='Capacity 10^-7 Ah')
probplot(Mass, qdist=qnorm, xlab='Mass')


#######  Simulating the Mass and Capacity Data individually,
assuming that mass and Capacity Data are Normal and unif(5,10) respectively############

capacitance<-rnorm(10000,MeanCap,SDcap)
capacitance1<-runif(10000,min=5, max=10)
mass<-rnorm(10000,Meanmass,SDmass)

######Diagnostics  & Quantities of interest Of the Simulation information regarding Specific energy#########

####Specific  Energy Mean and SD Under Simulation#########
mean(100*capacitance1/mass)
sd(100*capacitance1/mass)
hist(100*capacitance1/mass, main='Specific Capacity Uniform/Normal Approximation',xlab='Specific Capacity mAh / g', line=TRUE)
summary(x<-100*capacitance1/mass)
```

Table B.1 Summary of mass, capacity and specific capacity data determined by ICP and X-Ray Diffraction

Category	Value	Units
Mass	4.74 ± 0.81	µg
Capacity	7.5 ± 2.5	$X10^{-7}$ Ahrs
Specific Capacity	162 ± 46.5	mAhrs / gm
Capacitive Contribution	54	mAhrs / gm
Final Specific Capacity	110	mAhrs / gm

Table B.1 is the summary of results obtained in the research.

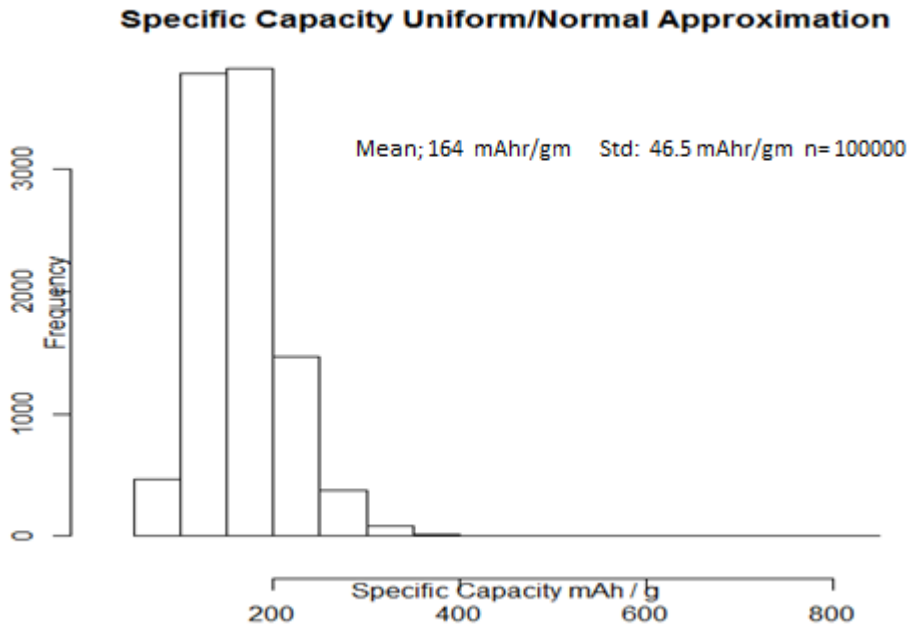

Figure B.1 This histogram gives the mean and standard distribution of the specific capacity data

Using the above histogram, Figure B.1 we get the mean value to be 164 mAhr/gm. This number obtained by using simulation in R statistical package agrees very well with 162 mAhr/gm obtained by manual determination and shown in the table above.

We calculate E(Specific Capacity) using two distributions, one for the numerator E(Capacity) and another for the denominator E(Mass) in the equation:

E(Specific Capacity) = E(Capacity) / E(Mass)

The two distributions have to be tested using the statistical package for normal distribution to see if they both are indeed normal distributions. As is seen from the next two plots, B2 and B3 the distribution for capacity does not look normal. It resembles what is called as uniform distribution. The distribution for mass turns out to be a normal distribution.

The linear fit done on these distributions shows that mass gives a better fit than capacity. The bar chart developed using these for the specific capacity is shown above

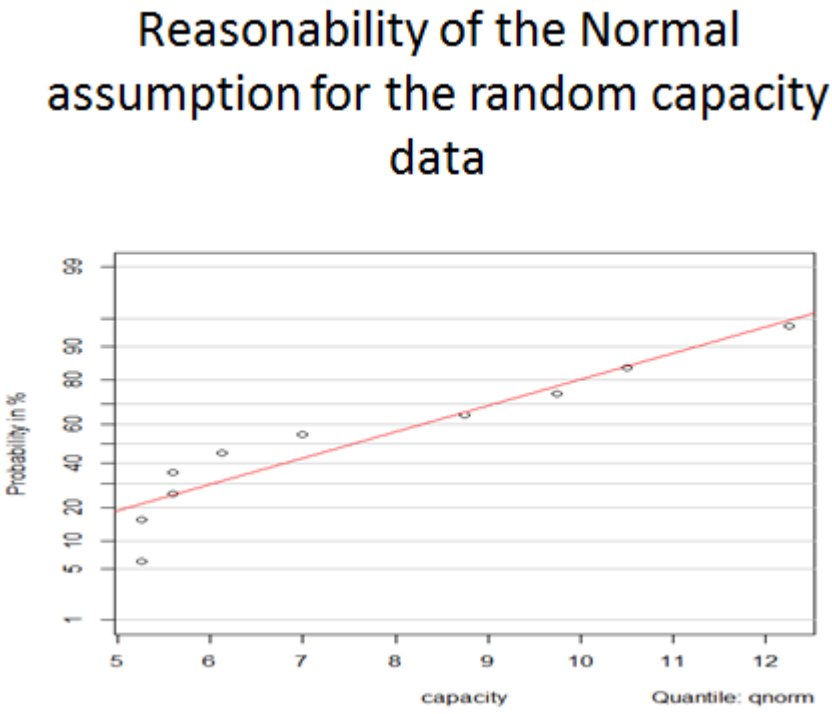

Figure B.2 The fit does not show a good normal distribution. It resembles what is called as uniform distribution.

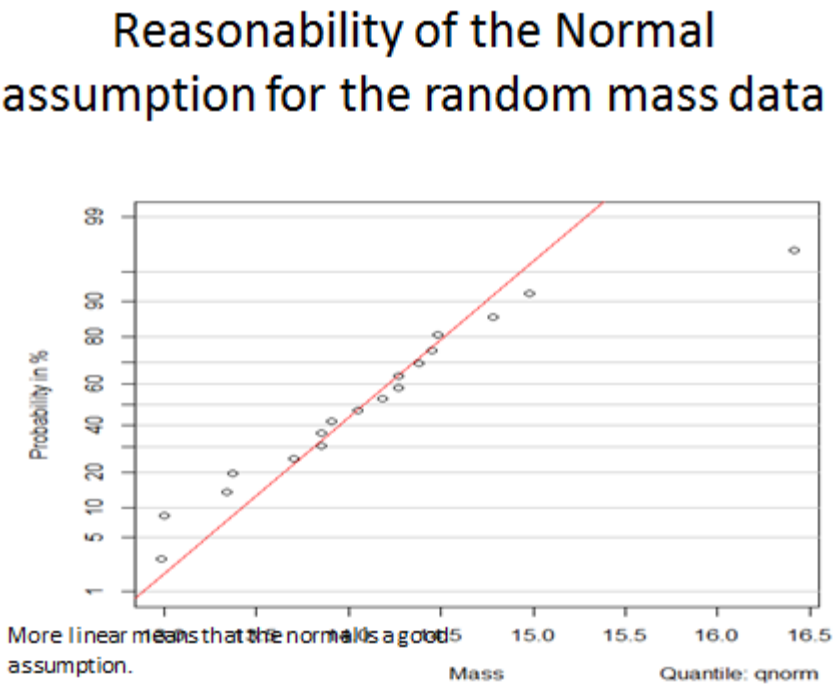

Figure B.3 The linear fit shows that normal distribution assumptuion for mass data is good

B.2 Conclusion on Statistical Analysis

The numbers obtained by the experiments were analyzed statistically. Software called the R statistics was used to calculate the mean expected value of specific capacity. Non parametric statistics was applied to determine the type of distributions of capacity and mass. This approach is independent of the distribution and gives results by a non - parametric analysis.

The results obtained give an accurate value of the expected specific capacity. Using this approach we get the mean values of mass, capacity and specific capacity. Along with capacitance determined by CV we are able to estimate the true specific capacity to be 110 mAhrs/ gm which falls in the region of the expected value, 137 mAhrs/ gm. A 54 mAhs/gm of capacitive contribution is found which accounts for approximately 30 % of the specific capacity.

References

(1) Introduction to probability and statistics by H.L. Adler and E.B.Roessler

(2) A first course in Probability by Sheldon Ross

References

1. Lee, Seung Woo, Naoaki Yabuuchi, Betar M. Gallant, Shuo Chen, Byeong-Su Kim,and Paula T. Hammond. "High-Power Lithium Batteries from Functionalized Carbon-Nanotube Electrodes." *Nature Nanotechnology* 5 (2010): 531–537. © 2010
2. Advances in Electrochemical Science and Engineering Vol 11 Chemically Modified Electrodes. Edited by Richard C Alkire, Deiter M Kolb , Jasep Lipkowski and Philip N Ross
3. Raimondi, F., Scherer, G.G., Koetz, R. and Wokaun, A. (2005) Angewandte Chemie-International Edison, 44, 2190.
4. Wieckowski, A. (2003) Electrochemistry (Tokyo, Japan), 71, 206
5. Daniel, M.C. and Astruc, D. (2004) Chemical Reviews, 104, 293.
6. Riley, D.J. (2002) Current opinion in Colloid and interfacial science, 7, 186.
7. Murray,R.W. (2008) Chemical Reviews 108, 2688.
8. Bard, A.J., Ding Z. and Myung, N. (2005) Structure and Bonding Springer (Berlin, Germany), Semiconductor Nanocrystals and Silicate Nano Particles, vol 118, 1.
9. Chen, S.W. (2007) Journal of Materials Chemistry, 17, 4115.
10. Guyot-Sionnest, P. (2008) Microchimica Acta 160, 309.
11. Gero Decher, Fuzzy Nanoassemblies, Science 277 , 5330 1232-1237, Aug 1997
12. Vidotti, M., Silva, M.R., Salvador, R.P., Cordoba, De Torresi, S.I. and Dall'antonia, L.H. (2008) Electrochimica, Acta, 53, 4030.
13. V Pralong, A. Delahyaye-Vidal, B. Beaudoin, J-B Leriche, and J.M. Tarascon, Journal of the Electrochemical Society, 147 (4) 1306-1313 (2000).
14. A.N. Dey, Electrochemical Alloying of Lithium in Organic Electrolytes, Journal of the Electrochemical Society, October 1971, 1547-1549.
15. John Wang; Julien Polleux; James Lim; Bruce Dunn; *J. Phys. Chem. C* **2007,** 111, 14925-14931
16. Alkire, Kold, Lipkowski, Ross (Eds.); Chemically modified Electrodes, chapter 4: Electrochemistry of Electroactive surface-mobilized Nanoparticle pages 169 to 193
17. R. Lakes, Nature 361, 511 (1993)
18. K.B. Blodgett, J. Am. Chem. Sco. 56, 495 (1934)
19. – and I. Langmuir, Phys. Rev. 51, 964 (1937)

20. H.K. uhn and D. Mobius, Agnew. Chem. Int. Ed. Engl. 10, 620 (1971).
21. O. Inacker, H. Kuhn, D. Mobius, G. Deuch, Z. Phys. , Neue Foldge 101, 337, (1976)
22. L. Netzer AND j. Sagiv, J. Am Chem. Soc. 105, 674 (1983)
23. G. Cao, H.-G. Hong, T.E.Mallouk, Acc. Chem. Res. 25, 420 (1992).
24. G. Decher and J-D Hong, Makro. Chem. Macromol. Symp. 46, 321 (1991)
25. – J. Schmitt, Thin Solid Films 210-211, 831 (1992).
26. G. Decher in Templating, Self –Assembly and Self Organization, vol 9 of Comprehensive Supramolecular Chemistry, J-P. Sauvage and M.W. Hoseini, Eds. 507-528.
27. W. Knoll, Curr. Opin, Colloid Interface Scince. 1, 137 (1996).
28. M.A.C. Stuart, G.J. Fleer, J. Lyklema, W. Norde, J.M.H.M. Scheutjens, Adv Colloid Interface Sci. 34, 477 (1991).
29. I. Haller, J. Am. Cem. Soc. 100, 8050 (1978).
30. T. Afsharad, A. U. Bailey, P.F. Luckham, W. Macnaughton, D. Chapman, Colloids Surf. 25, 263 (1987)
31. P. Berndt, K. Kurihara, T. Kunitake, Langmuir 8, 2486 (1992).
32. C-G. Golander, H. Arwin, J.C. Eeiksson, I. Lundstrom, R. Larsson, Colloids Surf. 5, 1 (1982).
33. R.K. LLer, J. Colloid Interface Sci. 21 569 (1966).
34. R. Fromherz, in Electron Microscopy at Molecular Dimensions, W. Baumister and W. Vogell, Eds 338349.
35. H.E.Reis and B.L. Meyers, J. A. Polymer Sci. 15, 2023, (19710.
36. R. Aksberg and A.L. Oldgen, Nord. Pulp Pap Res. J. 5,168 (1990).
37. S.S. Shiratori and M.F. Rubner pH –Dependent thickness behavior of sequentially adsorbed layers of Weak Polyelectrolytes, Macromolecules 2000, 33, 4213-4219
38. Mendelsohn, J.D.., Barrett , C.J., Mayes, A.M., Rubner, M. F. Langmuir,
39. Michaels, A.S., Miekka, R.G., J. Phys. CChem. 1961, 65, 1765
40. Fleer, G.J., Cohen Stuart,M.A., Scheutjens, J.MH.M., Cosgrove, T., Vincent, B. Polymers at Interfaces; Chapman and Hall; London,1993
41. Souheng, W. Polymer Interfaces and Adhesion; Mackrel Dekker, New York, 1982.
42. Lvov, Y.M. and Decher, G. Crystallogr. Rep. 1994, 39, 628.
43. Vermeer, A.W.P.; Leermakers, F.A.M.;Koopal, L.K. Langmuir,1997, 13, 4413.
44. Wu, A.; Yoo D. Lee, J. –K .; Rubner, M.F. J. Am. Chem. Soc. 1992, 121, 4883.
45. Joly, S.; kane, R.; Radzilowski, L.; Wang, T.; Wu A.; Cohen, R.E.; Thomas, E.L. Rubner, M.F. Langmuir 2000, 16,1354.
46. Mendelsohn, J.D.;Barrett, C.J.;Chan, V.V.;Pal, A.J.;Mayes, A.M.; Rubner, M.F. Langmuir

47. K.Ozawa, Solid State Ionics, 69,212 (1994).
48. M. Doyle, T. F. Fuller, and J Newman. J . Electrochemical . Soc., 140, 1526 (1993).
49. T. F. Fuller, M. Doyle, and J Newman. J . Electrochemical . Soc., 141, 1 (1994).
50. T. F. Fuller, M. Doyle, and J Newman. J . Electrochemical . Soc., 141, 982 (1994).
51. M. Doyle, J Newman. A. S.Gozdz, C.N.Schmutz and J.M. Tarascon J . Electrochemical . Soc., 143,18 90 (1996).
52. C.Ho, I.D.Raistrick and R.A.Huggins, J. Electrochemical . Soc., 127, 343 (1980).
53. M. G. S. R. Thomas, P. G. Bruce, and J. B. Goodenough. J . Electrochemical . Soc., 132, 1521 (1985).
54. B. V. Ratnakumar, C. Di. Stefano, and G. Nagasubsuramanian, and C. P. Bankston, . J . Electrochemical . Soc., 136, 6 (1989).
55. B. V. Ratnakumar, C. Di. Stefano, and C. P. Bankston, . J . Appl. Electrochem., 19, 813 (1989).
56. J. Farcy, R. Messina, and J. Pericon. J . Electrochemical . Soc., 137, 1337 (1990).
57. G. Pistoia, L. Li, and G. Wang, Electrochim. Acta, 37, 63 (1992).
58. Cl. Bohnke, O. Bohnke, and B. Vuillemin, Electrochim. Acta, 38, 1935 (1993).
59. F. C. Laman, M. W. Matsen, and J. A. R. Stiles, J . Electrochemical . Soc., 134, 2441 (1986).
60. B. D. Cahan, M. L. Daroux and E. B. Yeager, J . Electrochemical . Soc., 136, 1585 (1989).
61. C. Gabrielli, in Physical Electrochemisrty, Chap. 6. I. Rubenstein, Editor. Marcel Dekker , Inc. New York (1995); Impedance Spectroscopy: Emphasizing Solid Materials and Systems. J. R. Macdonalds, Editor. John Wiley and Sons, Inc. New York (1987) .
62. S. D. Bhakta, D. D. Macdonald, B. G. Pound, and M. Urquidi-Macdonald. J . Electrochemical . Soc., 138, 1353 (1991).
63. D. D. Macdonald, M. Urquidi-Macdonald, S. D. Bhakta, , B. G. Pound, J . Electrochemical . Soc., 138, 1359 (1991).
64. D. C. Grahame. J . Electrochemical . Soc., 99, 390C (1952).
65. M. E. Orazem, P. Agarwal, and L. H. Garcia-Rubio, . J . Electroanal. Chem., 378, 51 (1994).
66. Allen J. Bard and Larry R. Faulkner in Electrochemical Methods Fundamentals and Applications, second edition, John Wiley & Sons Inc.
67. K. B. Prater, ibid., Chap 8
68. D. Britz, “Digital Simulations in Electrochemistry,” Springer-Verlag, Berlin, 1988.
69. K. B. Prater and A. J. Bard, J. Electrochem. Soc., 117, 207 (1970).
70. K. B. Prater and A. J. Bard, J. Electrochem. Soc., 117, 335, 1517 (1970).

71. V. J. Puglisi and A. J. Bard, J. Electrochem. Soc., 119, 833 (1972).
72. L. S. R. Yeh and A. J. Bard, J. Electrochem. Soc., 124, 189 (1977).
73. J. Margarit and M. Levy, J. Electroanal. Chem., 49,369 (1974)
74. J. Margarit, G. Dabosi and M. Levy, Bull. Soc. Chim . France, 1975,1509
75. MacDIARMID, ALAN G. High Capacity Polyaniline electrodes; US Patent number , 4,940,640
76. Evgenij Barsukov and J Ross Macdonalds Impedance Spectroscopy Theory and Experiment, and Applications page 17